Mass balance and related topics of the Greenland ice sheet

Report of the 5th workshop

Friedrich Obleitner and
Ole B. Olesen (editors)

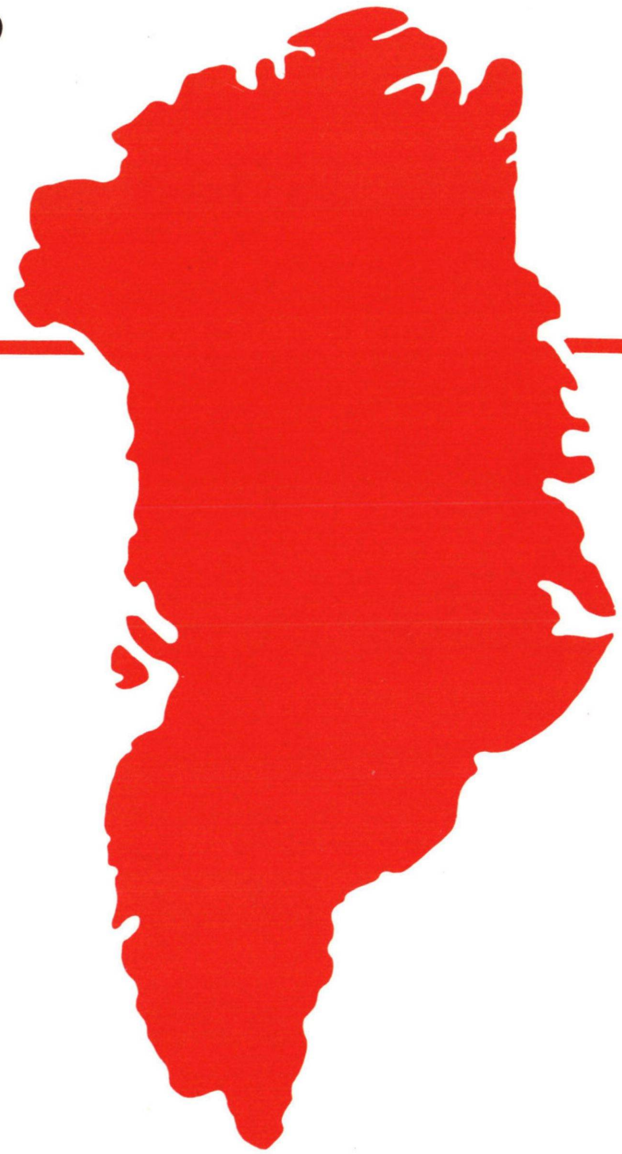

Open File Series 95/5

March 1995

GRØNLANDS GEOLOGISKE UNDERSØGELSE
Ujarassiortut Kalaallit Nunaanni Misissuisoqarfiat
GEOLOGICAL SURVEY OF GREENLAND

GRØNLANDS GEOLOGISKE UNDERSØGELSE
Ujarassiortut Kalaallit Nunaanni Misissuisoqarfiat
GEOLOGICAL SURVEY OF GREENLAND
Øster Voldgade 10, DK-1350 Copenhagen K, Denmark

The Geological Survey of Greenland (GGU) is a research institute affiliated to the Mineral Resources Administration for Greenland (MRA) within the Danish Ministry of Environment and Energy. As with all other activities involving mineral resources in Greenland, GGU's investigations are carried out within the framework of the policies decided jointly by the Greenland Home Rule Authority and the Danish State.

Open File Series

The Open File Series consists of unedited reports and maps that are made available quickly in limited numbers to the public. They are a non-permanent form of publication that may be cited as sources of information. Certain reports may be replaced later by edited versions.

Citation form

Open File Series Grønlands Geologiske Undersøgelse

conveniently abbreviated to:

Open File Ser. Grønlands geol. Unders.

GGU's Open File Series består af uredigerede rapporter og kort, som publiceres hurtigt og i et begrænset antal. Disse publikationer er midlertidige og kan anvendes som kildemateriale. Visse af rapporterne vil evt. senere blive erstattet af redigerede udgaver.

ISSN 0903-7322

GRØNLANDS GEOLOGISKE UNDERSØGELSE
Open File Series 95/5

Report of the

5th Workshop on

Mass balance and related topics of the Greenland ice sheet

Friedrich Obleitner and Ole B. Olesen

(editors)

held at

Institut für Meteorologie und Geophysik

University of Innsbruck, Austria

28th–29th November 1994

March 1995

Contents

Introduction

On November 28th and 29th 1994 the 'Fifth Workshop on Mass Balance and Related Topics of the Greenland Ice Sheet' was held at the Institute für Meteorologie und Geophysik of the University of Innsbruck, Austria. The workshop was attended by 16 participants presenting papers, and some guests.

The workshops were originally initiated as a forum for discussing recent plans, experiences and results on mass and energy balance studies carried out in Greenland which, in the context of climatic changes, developed into a prospective field of interest. Some other workshops dealing with similar topics unfortunately happened to be held within the same time frame this year, resulting in a decreased number of participants when compared with the last workshop. In spite of this it was generally felt that the original spirit is still alive and well within our scientific community.

The presentations succeeded in covering the most actual topics within the framework of the workshop focusing on experimental and modelling approaches towards understanding and predicting the mass and/or energy budget of the Greenland ice cap. Exchange of information about ongoing and planned projects was stimulated by the presentations and it was generally agreed, that the informal nature experienced during this workshop should also be maintained in the future.

Like the earlier workshops this one gave a strong impression of ongoing progress within the various fields of interest which is likely to positively affect the next meeting. It was agreed to hold the forthcoming 'Sixth Workshop on Mass Balance and Related Topics of the Greenland Ice Sheet' in Copenhagen, January 1996.

F. Obleitner / O. B. Olesen

Participants and adresses

W. Ambach
Inst. für Medizinische Physik
Müllerstrasse 44
A-6020 Innsbruck
Austria
Tel. (int.+43) 512 507 3550
Fax (int.+43) 512 507 2860

Carl Bøggild
Grønlands Geologiske Undersøgelse
Øster Voldgade 10
DK-1350 Copenhagen K
Denmark
Tel. (int.+45) 33 11 88 66
Fax (int.+45) 33 93 53 52
e-mail boeggild@vx1.ggu.min.dk

Marcel Haefliger
ETH Zürich
Geograhisches Institut
Wintherthurerstr. 190
CH-8057 Zürich
Schweiz
Tel. (int.+41) 1 257 5226
Fax (int.+41) 1 362 5197

E.A.C. Henneken
Vrije Universiteit Amsterdam
Faculty of Earth Sciences
De Boelelaan 1085
NL-1081 HV Amsterdam
The Netherlands
Tel. (int.+31) 20 548 5772
Fax (int.+31) 20 646 2457

Friedrich Jung-Rothenhäusler
Alfred-Wegener-Institut für Polar- und Meeresforschung
Postfach 120161
D-2850 Bremerhaven
Germany
Tel. (int.+49) 471 483 1347
FAX (int.+49) 471 483 1149

Kristian Keller
Niels Bohr Institutet for
Astronomi, Fysik og Geofysik
Geofysisk Afdeling
Haraldsgade 6
DK-2200 Copenhagen
Denmark
Tel (int. +45) 35 32 05 86
FAX (int. +45) 35 82 25 65
e-mail kk@gfy.ku.dk

Wouter Knap
IMAU
Princetonplein 5
3484 CC Utrecht
The Netherlands
Tel. (int.+31) 30 934 780
Fax (int.+31) 30 543 163
e-mail knap@fys.ruu.nl

M. Kuhn
Universität Innsbruck
Inst. für Meteorologie u. Geophysik
Innrain 52
A-6020 Innsbruck
Austria
Tel. (int.+43) 512 507 5451
Fax (int.+43) 512 507 2924

Anton G. C. A. Meesters
Vrije Universiteit Amsterdam
Faculty of Earth Sciences
De Boelelaan 1085
NL-1081 HV Amsterdam
The Netherlands
Tel. (int.+31) 20 548 5311
Fax (int.+31) 20 646 2457

Heinz Miller
Alfred-Wegener-Intitute für Polar und Meeresforschung
Postfach 120161
D-2850 Bremerhaven
Germany
Tel. (int.+49) 471 483 1210
Fax (int.+49) 471 483 1149

Friedrich Obleitner
Universität Innsbruck
Institut für Geophysik und Meteorologie
Innrain 52
A-6020 Innsbruck
Austria
Tel. (int.+43) 512 507 5451
Fax (int.+43) 512 507 2924
e-mail C70799@subz-nov.uibk.ac.at

Hans Oerlemans
Utrecht University
Inst. for Marine and Atmospheric research
Princetonplein 5
NL-3584 Utrecht
The Netherlands
Tel. (int.+31) 30 533 272
Fax (int.+31) 30 543 163
e-mail oerlemns@fys.ruu.nl

Hans Oerter
Alfred-Wegener-Intitut für Polar- und Meeresforschung
Postfach 120161
D-2850 Bremerhaven
Germany
Tel. (int.+49) 471 483 1347
FAX (int.+49) 471 483 1149
e-mail hoerter@awi-bremerhaven.de

Atsumu Ohmura
ETH
Geograhisches Institut
Winthertuhrerstr. 190
CH-8057 Zürich
Schweiz
Tel. (int.+41) 1 257 5220
Fax (int.+41) 1 362 5197

Ole B. Olesen
Geological Survey of Greenland
Øster Voldgade 10
DK-1350 Copenhagen
Denmark
Tel.: (int.+45) 33 11 88 66
Fax.: (int.+45) 33 93 53 52
e-mail oleseno@ggu.min.dk

Manfred Stober
FH f. Technik Stuttgart
Fachber. Vermessung
Postfach 101452
D-70013 Stuttgart
Germany
Tel. (Int.+49) 711 121 2563
Fax (Int.+49) 711 121 2666

H. F. Vugts
Vrije Universiteit Amsterdam
Institute of Earth Sciences
De Boelelaan 1085
NL-1081 HV Amsterdam
The Netherlands
Tel. (Int.+31) 20 548 4151
Fax. (Int.+31) 20 646 2457

HORIZONTAL AND VERTICAL ICE MOVEMENTS 1990-1994 AT THE ETH-CAMP

Manfred **Stober**

Fachhochschule für Technik Stuttgart,
Stuttgart, FRG

1. The geodetic program

In continuation of earlier campaigns (1990, 1991) a geodetic program was performed from 23.05. to 23.06.1994 at the ETH-camp, which is now run by the University of Colorado at Boulder. The main purpose was the investigation of refraction in trigonometric leveling, but another important topic was the evaluation of ice movements and deformations. According to calculations of OHMURA the station was expected to be situated at the equilibrium line. It is a main glaciological interest to test this statement and to determine velocity parameters for this part of the Greenland ice sheet.

In this paper only the ice movements will be discussed. The measuring program 1994 was:

- Attachement of the ETH-Camp by GPS to Jakobshavn (19.06.1994),
- Remeasurement of the deformation figure (terrestrial + GPS),
- Reconstruction of old positions from 1990 and 1991 in terrain,
- Remeasurement of old positions 1990 and 1991 in terrain,
- strategraphy in snow pits at 4 places .

As GPS-receicers only instruments operating with high resolution on two frequencies were used:

1990 + 1991	: Wild-Magnavox WM 102,
1994	: Leica GPS-System 200.

The displacement is calculated from repeated GPS-positionings. Point C3 was measured in three periods (1990, 1991 and 1994). Another point (A2) was first established in 1991 and remeasured in 1994. All positions have been fixed to the same reference point JAKOBSHAVN by direct simultaneous baselines in 1991 and 1994, but only indirectly by JAKOBSHAVN - CONSTABLE-PYNT - CAMP in 1990.

2. Horizontal ice movements

2.1 Flow vector by GPS-measurements

As we see from **table 1**, azimuth and flow velocity of point C3 (nearby the camp) are not exactly agreeing in the periods 90-91 and 91-94, probably due to the weak positioning in 1990. As best values we have to consider the period average 91 - 94, which is long enough and derived from homogeneous GPS-measurements. The same horizontal displacement is resulting at point A2 (**table 2**). There is a very good agreement in the velocity, but the azimuth is little different (1°). On the whole, the general flow vector shows into direction of the Jakobshavn glacier.

date	time interval	horizontal displacement at C3		
		value	velocity	azimuth
	days	m	m / Tag	° ' "
13.07.90 27.07.91 20.08.91 19.06.94	379 24 1031	121.71 7.97 320.49	0.3211 0.3321 0.3109	236 01 32 232 08 05 234 31 24
13.07.90 19.06.94	1434	450.14	0.3139	234 53 21
average 91 19.06.94	**1043**	**324.49**	**0.3111**	**234 28 59** =260,54 gon

Table 1: Horizontal displacement at CU/ETH-Camp (C3) 90 - 94

date	time interval (days)	horizontal displacement at A2		
		value (m)	velocity (m/day)	azimuth
average 91 19.06.94	1043	326.68	0.3132	233°35'17" =259,54 gon

Table 2: Horizontal displacement at CU/ETH-Camp (A2) 91-94

2.2 Deformations in a terrestrial network

It was possible to find all 4 points from the network 1991 and remeasure the deformation network by GPS and terrestrial methods as well. The ranges of the network are in the order of 1 km (**fig. 1**). By transformation and calculation in the same local coordinate system, we obtain displacement vectors for all 4 points (**table 3**).

Conclusions:

- the average displacement 324,67 m (corresponding to 0,3196 m/day) is very good agreeing with the results from GPS.

- velocities and flow azimuthes are not completely homogeneous. Each point has individual values, so local effects (surface topography and/or bedrock topography) may have great influence.

- the differences are significant, because the measuring accuracy is much better (order of 1 cm) in relation to the big displacements.

point	displacement of point from 1991 to 1994		discrepancies average - individual	
	range (m)	azimuth (gon)	range (m)	azimuth (gon)
A2	326,56	259,4983	-1,89	+0,1037
B2	321,87	258,9277	+2,80	+0,6743
C2	324,64	260,1933	+0,03	-0,5913
D	325,60	259,7888	-0,93	-0,1868
average	324,67	259,6020		

Table 3 : Horizontal displacements 1991 - 1994 in a terrestrial network

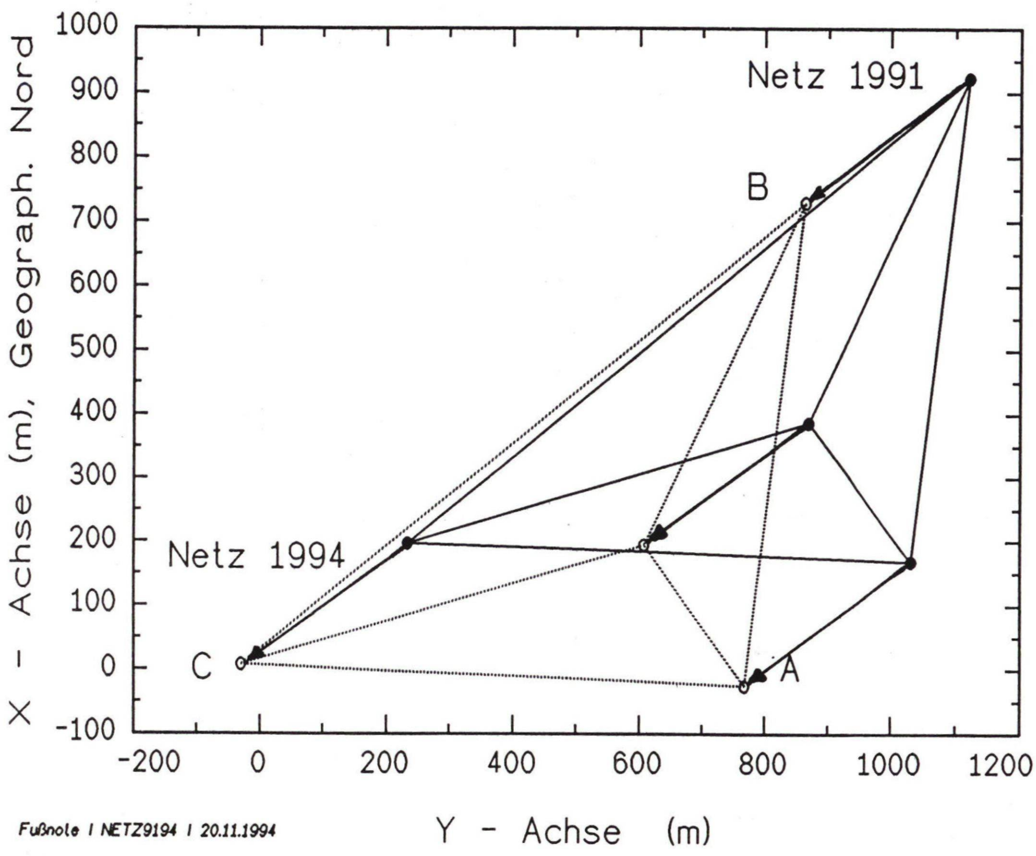

Figure 1 : Deformation figure and horizontal displacements 1991 - 1994

Comparing the changes of length in the deformation network, we also find individual distortions of ranges **(table 4)**. The flow azimuth coincides approximately with direction B-C, but the distortions along and across this azimuth are almost equal. On the other hand, lines in about the same azimuth (C-B, C-D) do not show the same distortion, all the distortions are individual ones. There are even some ranges (D-C and A-C) remaining unchanged. Due to this inhomogeneous behavior no strain rates were calculated.

From	To	length 91	lenght 94	change of lenght 94-91		
		(m)	(m)	(m)	ppm	ppm/day
C2	A2	798,012	797,860	-0,152	- 190	-0,19
C2	B2	1146,762	1148,848	+2,086	+1816	+1,79
B2	A2	760,262	761,592	+1,330	+1746	+1,72
D	A2	271,768	272,372	+0,604	+2118	+2,08
D	B2	592,613	593,846	+1,233	+2076	+2,04
D	C2	663,490	663,468	-0,022	- 33	-0,03

Table 4: Distortions in the network 1991 - 1994

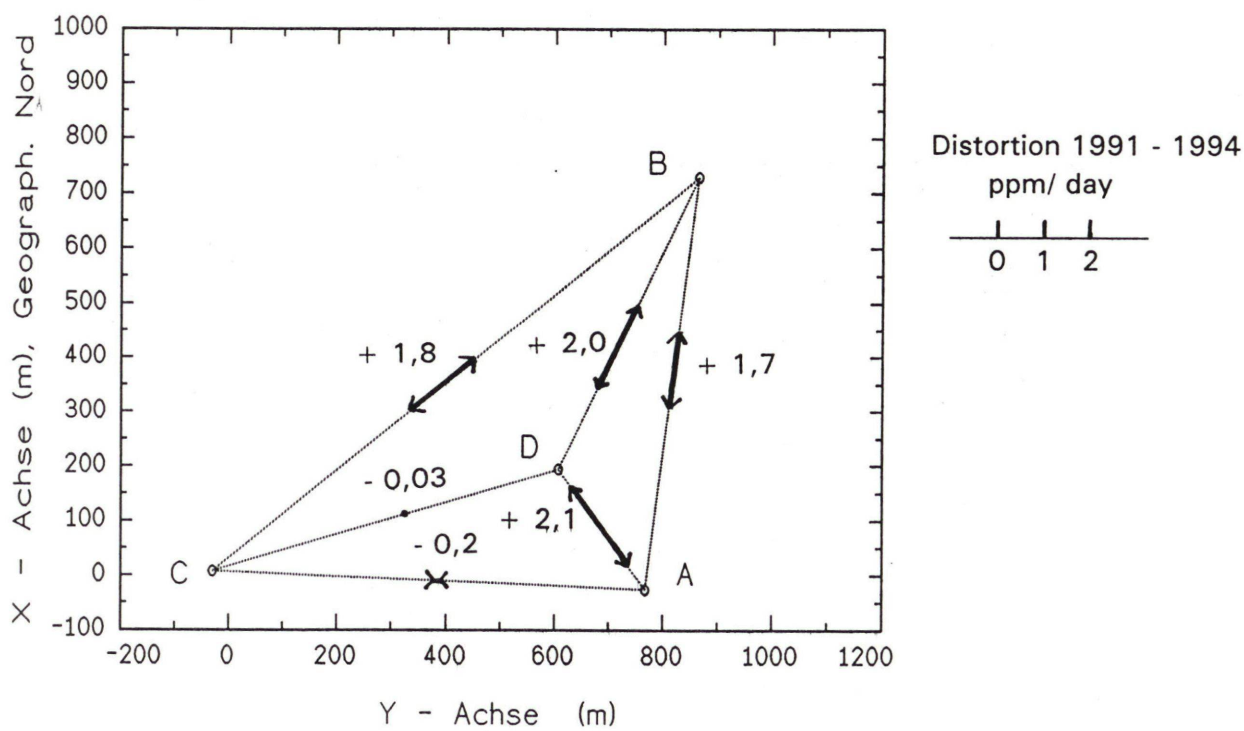

Figure 2: Distortions in the network 1991 - 1994

3. Vertical ice movements

3.1 Height changes at the same place

For all questions concerning the mass balance the change of height at the same position is most important. For this purpose the old positions from 1990 and 1991 of point C3 were reconstructed in the field . This was only possible by using previous values of the deformation rate and azimuth. Only now, after evaluation of the actual displacement vector, we are able to define the true old positions. In order to correct the previous heights, a topographic map was determined arround the supposed area, from which the exact heights could be found by interpolation.

In order to determine the snow accumulation, snow pits were dug at 4 positions: C2(94), C2(91), A2(94) and D(94). At positions C2 and D the original wooden stick was found, so the old snow horizon was well known. The strategraphy is shown in **figure 3**.

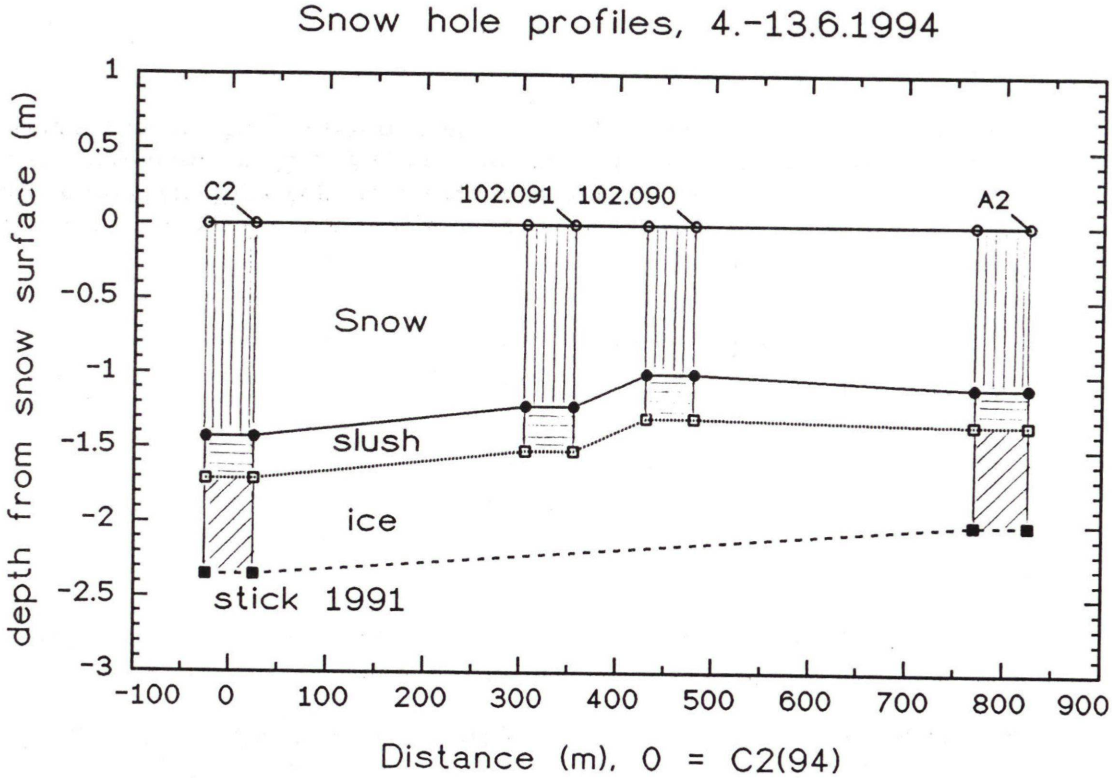

Figure 3: Strategraphy of snow pits 1994

Combining the GPS-heights at the snow surface and the data of snow pits we are able to give absolute heights of all snow and ice horizons. For this presentation all the heights are related to Jakobshavn with ellipsoidal height JAV = 52.093 m, what is not the true ellipsoidal height, but a fix value for all height comparisons.

The results are shown in **table 5**. The most important value is the ice horizon, because the snow surface might be disturbed by local and seasonal effects. From 1990 to 1994 the ice height was decreasing -2,68 m, in the period 1990 to 1991 -0,59 m, corresponding -0,67 respectively -0,20 m/year. The big difference between the two periods is probably effected by the bad height determination in 1990 (indirectly via Constable Pynt). But in 91 and 94 we had homogeneous and short GPS baselines with good results , so we can really suppose a height diminuation in the last 3 years of -0,20 m/year. This result is in good accordance with those from the EGIG-line (KOCK 1993), but contradicts the results from satellite altimetry with increasing ice +0,3 m/year (ZWALLY 1989).

position of C3 at date	height changes (m)				vertical velocity of ice =change of height per year (m / year)	
	94 - 90		94 - 91			
	snow	ice	snow	ice	94 - 90	94 - 91
average 91			+0,09	-0,59		-0,20
7/90	-1,58	-2,68			-0,67	

Table 5: Height changes of snow and ice at the same position

3.2 Vertical ice flow

The vertical component of ice flow is derived by observation of the moving wooden stakes, which were found at the two points C2 and A2 from 1991. In 1991 they had been established in surface horizon, and in 1994 they had been found 0,65 m below the actual ice horizon. All heights (in relation to fix point JAV = 52.093 m) of the moving stakes are shown in **figures 4 and 5**.

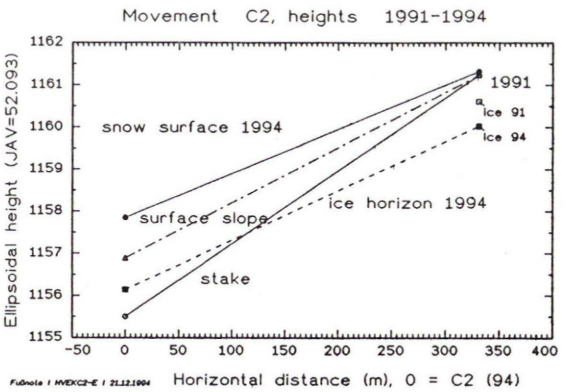

Figure 4: Height changes 1991 - 1994 of point C2/C3

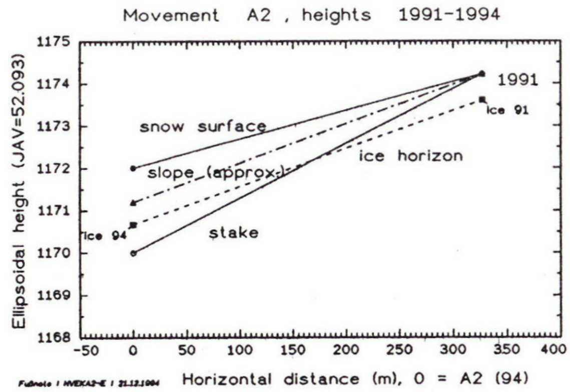

Figure 5: Height changes 1991 - 1994 of point A2

Vertical ice flow at point 1991 - 1994	C2/C3	A2
Height difference of stick in flow direction Surface slope inclination (measured/approx.)	- 5,73 m - 4,34 m	- 4,22 m - 3,0 m
Vertical movement, free from inclination	- 1,39 m	- 1,22 m

Table 6: Vertical ice flow 1991 - 1994

We obtain the results (**table 6**): At both places (A,C) the vertical movement of the stake is greater than the height change effected by slope. So the flow vector has a downward trend and the model of rising ice layers, such as postulated by some scientists, cannot be confirmed for this part of the Greenland ice sheet. Together with the big accumulation of snow and new ice over the old stakes we also see, that the ETH/CU-camp is not situated at the equilibrium line, contraryly to the expectations of OHMURA 1991.

4. REFERENCES

KOCK, H.: Height determination along the EGIG line and in the GRIP area. Mass balance and related topics of the Greenland ice sheet, 3rd workshop dec. 1992, GGU Open File Series 93/5, April 1993.

OHMURA, A. et al.: ETH Greenland Expedition, Progress Report No. 1, Department of Geography, ETH Zurich, March 1991.

SECKEL, H.: Höhenänderungen im Grönländischen Inlandeis zwischen 1959 und 1968. Medd. om Gronland, Bd. 187, Nr.4, Kopenhagen 1977.

STOBER, M.: The Geodetic Programme 1990/1991. ETH Greenland Expedition, Progress Report No. 2, Department of Geography, ETH Zürich, 1992.

ZWALLY, H.J: Growth of the Greenland Ice Sheet: Measurement/Interpretation. Science,Vol. 246, 1989.

THE ICE DEFORMATION AND MASS BALANCE AT THE SUMMIT OF GREENLAND AS DETERMINED BY GPS AND GRAVITY MEASUREMENTS

Kristian Keller, Niels Gundestrup, Dorthe Dahl-Jensen and Carl Christian Tscherning
Geophysical Department, University of Copenhagen,
&
René Forsberg and Simon Ekholm
National Survey and Cadastre (KMS), Denmark.

Introduction.

During the Greenland Ice Core Project (GRIP) field seasons of 1991-1994, extensive gravity and geodetic surveying were performed on the summit of the ice sheet, using gravimeters and the Global Positioning System (GPS). The GPS data provided the background for the computation of a elevation model of the summit, covering an area of approx. 100 x 100 km. In the same area a gravity anomaly model was computed (Ekholm & Keller, 1993). In addition, the collected data are used as ground-truth control for the Greenland Aero-geophysics Project (Brozena, 1991), where airborne altimetry and gravimetry were collected, and for the validation of satellite altimetry (Tscherning et al. 1992; Ekholm et al. 1993).

The strain net.

At eleven points, poles were put up (whereof three were established by the University of Washington) as a strain net for measuring ice movements. A main reference marker was established 400 m Southwest of the GRIP camp area and was fixed 80 m down into the ice sheet. Repeated observations of these poles around GRIP (25-60 km distance from the camp site) have provided information about ice movements on the top of the ice sheet. Data from 1991 and 1992 were considered of insufficient accuracy and thus left out. In 1991, the observation time was too short and the high ionospheric activity corrupted the data. In 1992, the data was disturbed by a nearby placed STD-C telex transmitter. Furthermore, the instruments were replaced by new and improved models in 1993. Figure 1 shows the changes in position from 1993 to 1994. A regular pattern with the large velocities are seen in eastern and western direction, where the surface slope is steepest, and small velocities along the North-South ice divide, where the slope is more shallow.

Using the above mentioned velocities and a ice model by Reeh (1989), it is possible to determine the centre of the ice sheet. At each velocity point, the curvature and ice thickness were determined from figure 1. Furthermore, the accumulation rate was also calculated (Bolzan & Strobel, 1994) at each point. These data were then used, according to the elliptical ice flow model by Reeh, in a least squares determination of the ice centre. In the calculation, it is assumed that the flow line is along a straight line from the centre, e.g. the point is placed on the axis of an approximated ellipsoid (for further details see Reeh, 1989). According to this calculation, the centre is 1.4 km East of and 5.7 km North of the reference pole. This result is not satisfactory, but is probably due to the simplified flow model.

The reference marker.

The local gravity and GPS measurements are tied to the reference marker fixed at a depth of 80 m. This reference marker, in turn, is referenced to the global network using a reference benchmark (No.61388) in Kangerlussuaq (Søndre Strømfjord). This marker is both a precise gravity station tied to the Greenland absolute network, and a precise 3-dimensional benchmark established by KMS as well.

Even though all processing is not yet completed, the results (for this baseline of considerable length; 796 km) are quite satisfactory (using precise ephemerides and GPSurvey software).

In table 1, the GPS-measurements indicate that the reference marker at GRIP is sinking and is moving somewhat in the northwest direction, according to the present accumulation of 23 cm of ice, corresponding to an annual layer thickness of 25 cm at a depth of 80 m (S. Johnsen, Geophys. Dept, pers. comm.). This also confirms that the ice sheet is stable within the estimated accuracy of the GPS observations (15 cm).

	Annual Change in Position		
Year	Latitude	Longitude	Ell. Height
1992-1993	+ 7 cm N	+ 18 cm W	- 33 cm
1993-1994	+ 11 cm N	+ 23 cm W	- 17 cm
Mean	+ 9 cm N	+ 20 cm W	- 25 cm

Table 1: Movement of the top of the reference marker at GRIP, 1992-1993-1994. Point 61338 in Kangerlussuaq is used as fixed reference: 67° 00' 21.5426" N; 50° 42' 11.5802" W; h(ellip) = 67.056 m (W.B. Krabill, NASA/Wallops Flight Facility, pers. comm.) This leads to following position for the reference pole at GRIP (No. 47913): 72° 34' 31.2049'' N; 37° 38' 31.2049'' W; h(ellip) = 3280.5 m. The antenna height is 2.20 m and the geoid undulation is 48.2 m according to latest geoid model (GEOID93B) by R.Forsberg. Hence, the GRIP elevation above sea level is estimated to be 3230.1 m.

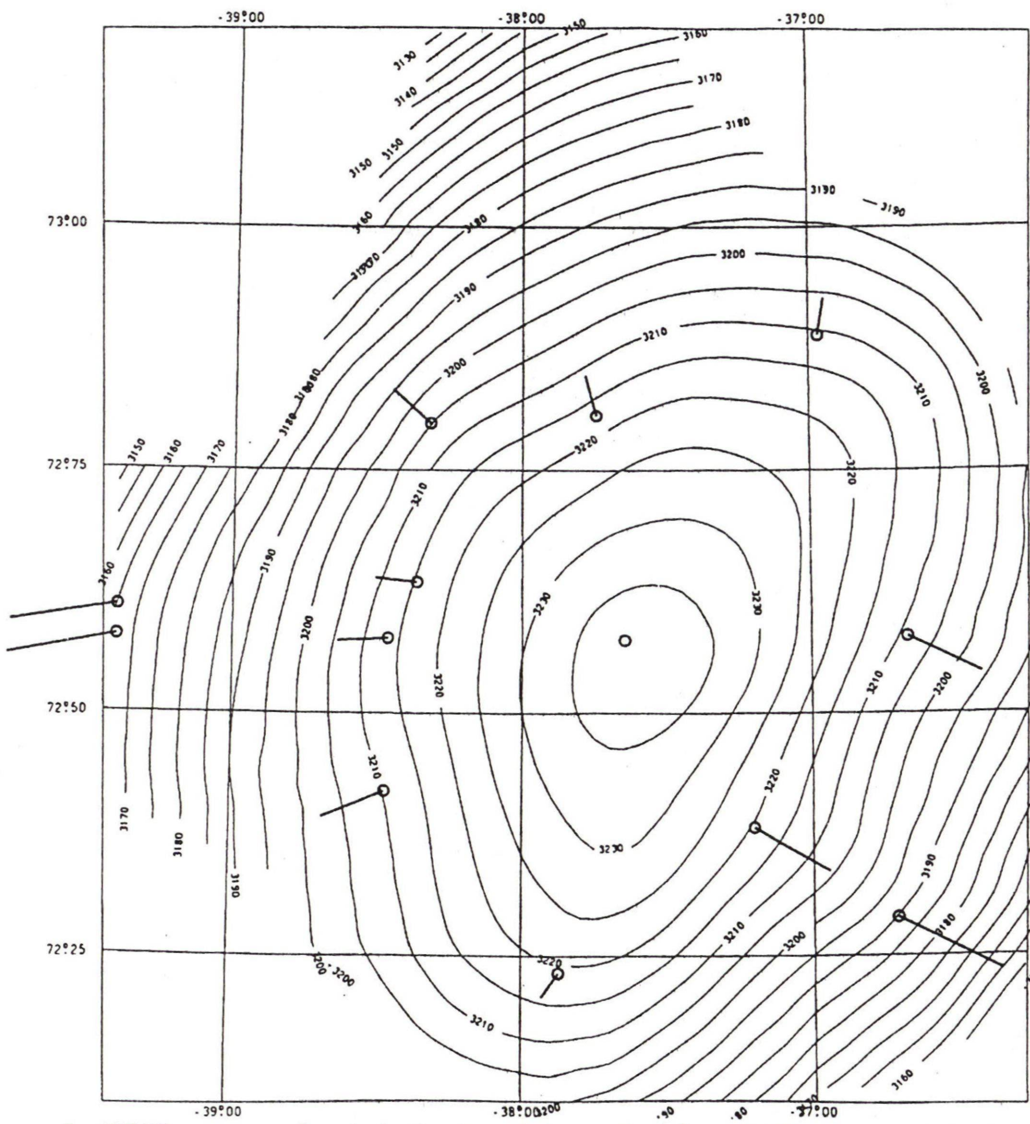

Figure 1: GRIP topography (c.i. 5 m) and ice velocities (1993-1994). Velocities are indicated by the vectors. 1 cm = 2 meters/year.

The Gravity tie.

From measurements of gravity at the top of the reference marker in successive seasons, the vertical movement of the ice at a depth of 80 m can in principle be observed. The expected annual sinking rate of the pole is 25 cm, sufficiently in order to be observed in the gravity measurements under ideal conditions.

During the project (1992-1994) two LaCoste & Romberg gravimeters were used each year, altogether there were four different gravimeters used in the survey. Each gravimeter has it's own individual scale and scaling factor. The scaling factors are estimated from an adjustment including only the ties between the absolute gravity stations in Copenhagen, Søndre Strømfjord and Jakobshavn, thus making the procedures of the gravity adjustment more complex than normal. This fact plus the rough transportation are the likely reasons for a rather low accuracy (approx. 100μGal). Figure 2 presents the gravity at the top of the reference marker at GRIP.

In spite of the rather noisy data, we observed a signal of gravity increase of approx. 72 μgal in the data adjustment, equivalent to 23 cm descent of elevation, using the free-air gravity gradient of 0.3086 mgal/m.

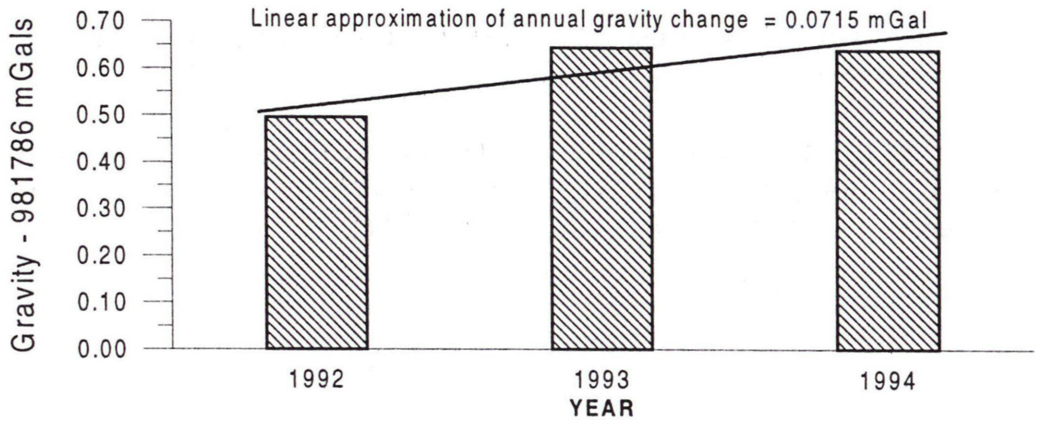

Figure 2. Gravity at the top of the reference pole at GRIP in the years 1992, 1993, and 1994

Conclusion.

Local gravity and surface topography were measured in a 50 km network around GRIP. The accuracy of the surface topography model is comparable to the height of a sastruga (30cm).

Repeated GPS observations at the eleven pole strain net 50 km around GRIP has provided surface velocities in the area. The estimated error of the velocity is approx. 10 cm/year.

Long GPS baselines from GRIP to Kangerlussuaq has indicated an ice sinking rate in agreement with the present accumulation, which shows that the ice sheet is stable within the observation accuracy.

This has also been confirmed by means of repeated gravity measurements.

Further measurements in 1995, and in the future, will provide a considerable accuracy improvement.

More advanced ice models will be applied in future calculations of the ice centre.

Acknowledgements.

This work is a contribution to the Greenland Ice Core Project (GRIP), a European Science Foundation Programme with eight nations collaborating to drill through the central Greenland ice sheet.

References.

Bolzan, J.F. & M. Strobel: 'Accumulation Rate Variations around Summit, Greenland.' Journal of Glaciology, Vol. 40, No. 134, p.56-66, 1994.

Brozena, J.M.: 'The Greenland Aerogeophysics Project: Airborne Gravity, Topographic and Magnetic Mapping of an Entire Continent.' IUGG General Assembly, Vienna, August 1991.

Ekholm, S., R. Forsberg, J.M. Brozena: 'Accuracy of Satellite Altimeter Elevations over the Greenland Ice Sheet.' Journal of Geophysical Research, in press.

Ekholm, S. & K. Keller: 'Gravity and GPS Survey on the Summit of the Greenland Ice Sheet 1991-1992.' National Survey and Cadastre, Geodetic Division, Technical Report no. 6, 1993.

Reeh, N.:'The Age-depth Profile in the Upper Part of a Steady-state Ice Sheet.' Vol. 35, No.121, p.406-418, 1989.

Tscherning, C.C. P. Knudsen, S. Ekholm & O. Baltazar Andersen: 'An Analysis of the Gravity Field in the Norwegian Sea and Mapping of the Ice Cap of Greenland using ERS-1 Altimeter Measurements.' ERS-1 Symposium, Cannes, 1992.

THE SURFACE ALBEDO OF THE GREENLAND ICE SHEET: AVHRR-DERIVED MEASUREMENTS IN THE SØNDRE STRØMFJORD AREA (CENTRAL WEST GREENLAND) DURING THE 1991 MELT SEASON

Wouter **Knap** & Hans **Oerlemans**
Institute for Marine and Atmospheric research Utrecht
Utrecht University, The Netherlands

Introduction

This paper presents the satellite derived albedo of the Greenland ice sheet in the area east of Søndre Strømfjord (central west Greenland) in the 1991 melt season. We will focus on an area of 200 x 200 km^2 centred on the GIMEX transect (approximately 67° N; figure 1). Radiances were measured by the Advanced Very High Resolution Radiometer (AVHRR) during day passes of the NOAA-11 satellite. The instrument measures in five distinct spectral intervals of which channel 1 (560 - 680 nm) and channel 2 (730 - 1100 nm) provide the visible and near-infrared radiances that formed the basic input for the calculation of the surface albedo.

Method

We corrected for the interaction between radiation and the atmosphere by a linear relationship between planetary albedo (α_t) and surface albedo (α_s).

$$\alpha_s = a + b\,\alpha_t$$

The coefficients a and b, usually determined by radiative transfer modelling (e.g. Koepke 1992 or Koelemeijer and others 1993), were obtained by the measured planetary allbedo and ground truth of the surface albedo in homogeneous areas of dry snow and sea (both outside the study area). The dry snow surface albedo was assumed to be 0.85. The surface albedo of sea was calculated as a function of the actual solar zenith angle and ranged from 0.09 to 0.16. This method has two major advantages above modelling of the atmosphere: (1) there is no need for information on the actual physical characteristics of the atmosphere, (2) sensor drift (degradation of the AVHRR sensitivity) is included in the obtained constants. In order to use this equation, the AVHRR channel radiances were integrated over the entire solar spectrum by a linear relationship. The anisotropy of the reflected radiation field is ignored.

Results

In total we processed 18 scenes in the 1991 melt season. In figure 2 we present two images, obtained on June 15th and July 25th, showing some interesting features. The right side of the figure shows the albedo along the GIMEX transect. The situation of June 15th shows that high albedo values are dominant, implying that most of the surface is still covered by the previous winter's snow pack. On 25th July we see that the albedo has decreased tremendously. Most striking is the albedo decrease in the first 40 km distance from the ice edge. This decrease, with increasing altitude, is opposite to what is usually found on glaciers. In situ measurements during GIMEX-91 revealed the same feature (Oerlemans and Vugts, 1993). A possible explanation for the low albedo values is the abundance of meltwater accumulating at the surface. As the ice is cold, an effective internal drainage system cannot develop and most of the meltwater has to drain supraglacially. This drainage is counteracted by a small surface slope. The grey-tone image of July 25th shows a distinct zonation roughly parallel to the ice edge. This zonation is projected on the GIMEX transect in the right panel of figure 2. Zone (II) could be representative for a zone of "wet" ice. Closer to the ice margin, meltwater is effectively drained by a system of moulins and crevasses. Moreover, the relatively large surface slope facilitates run-off. Zone (I), therefore, is a zone of "dry" ice. The lower boundary of zone (III) coincides with the mean equilibrium line altitude (1420 m a.s.l.). This could indicate that the surprisingly constant albedo of the zone is caused by a uniform area of superimposed ice. The sudden increase in albedo at 110 km distance from the ice edge is likely to be caused by the transition ice/snow. Zone (IV), therefore, refers to the snow zone.

AVHRR albedo values proved to differ substantially (up to 0.1) from the GIMEX surface measurements. However, temporal variation in the AVHRR albedo is consistent with the GIMEX albedo. Two explanations for systematic differences can be given: (1) shortcomings in the retrieval method, (2) different spatial coverage of the space-born and surface sensor. Ongoing research and field experiments will give more insight in the errors that are introduced by the retrieval method.

References

Koelemeijer, R., J. Oerlemans, S. Tjemkes (1993). Surface reflectance of Hintereisferner, Austria, from Landsat 5 TM imagery. *Annals of glaciology* **17**, 17-22.

Koepke, P. (1989). Removal of atmospheric effects from AVHRR albedos. *Journal of applied meteorology* **28**, 1341-1348.

Oerlemans, J., H. F. Vugts (1993). A Meteorological Experiment in the Melting Zone of the Greenland Ice Sheet. *Bulletin of the American Meteorological Society* **74** (3), 355-365.

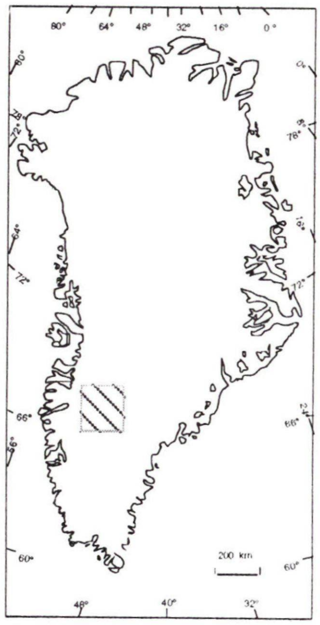

Figure 1: the hatched area represents the study area on the Greenland ice sheet. The area is centred on the GIMEX transect at about 67° N and measures roughly 200 x 200 km^2.

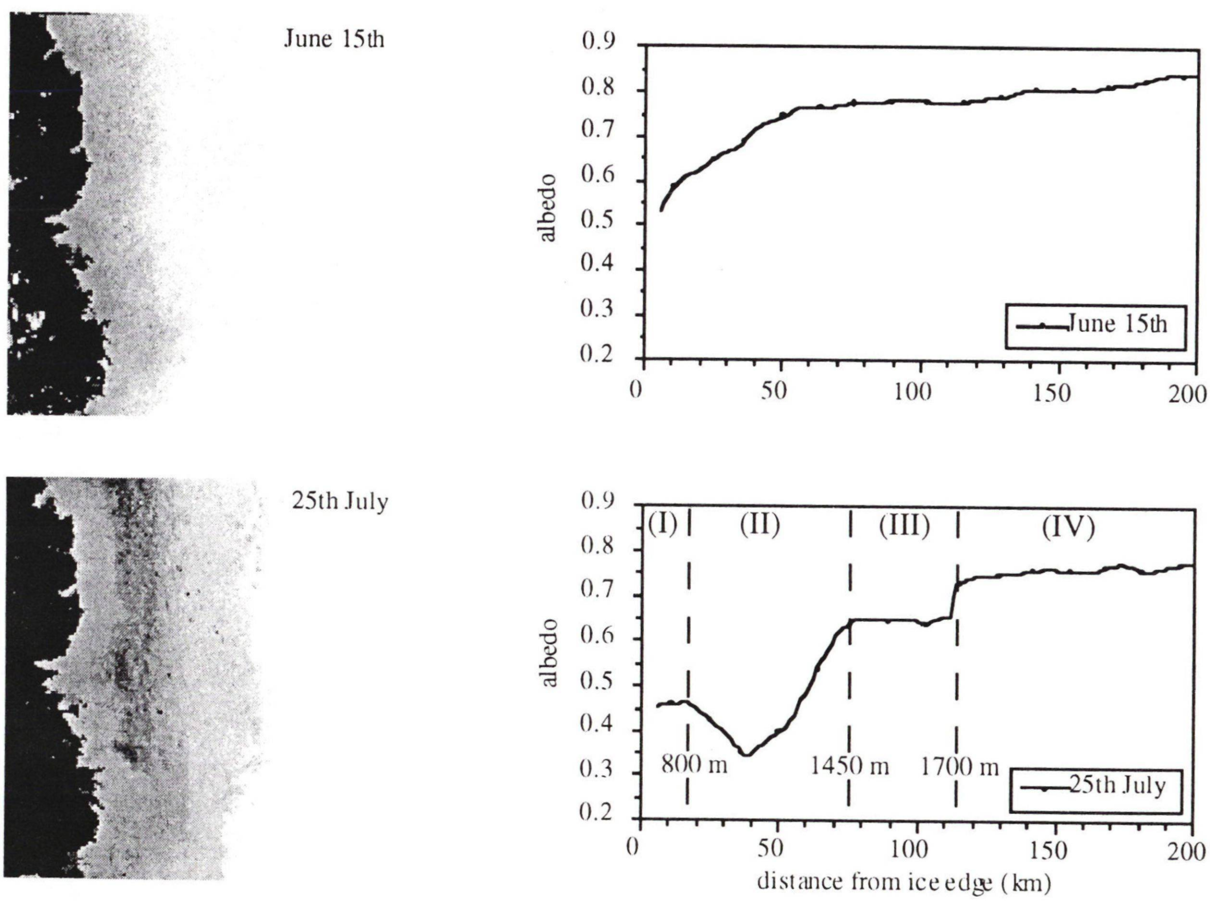

Figure 2: the left panel shows grey-tone pictures of the albedo distribution in the Søndre Strømfjord area. Black represents an albedo of 0.20 or less and white represents an albedo of 0.90 or more. See figure 1 for the study area. The low albedos on the left (black) represent the tundra. The ice edge is found at the stepwise increase in the albedo. The right panel shows the albedo along the GIMEX transect as a function of distance from the ice edge. The Roman numerals are explained in the text. The altitudes are given in m a.s.l..

RADIATION BALANCE OVER THE GREENLAND ICE SHEET DERIVED BY NOAA AVHRR SATELLITE DATA AND IN SITU OBSERVATIONS

Marcel **Haefliger**
Department of Geography
Swiss Federal Institute of Technology
Zürich, Switzerland

A method is presented which determines the clear sky radiation balance of Greenland using NOAA Advanced Very High Resolution Radiometer (AVHRR) satellite data. An important data set are the radiation measurements, radiosonde ascents and synoptic observations carried out during the summer months of 1990 and 1991 near the equilibrium line altitude at 1155 m a.s.l. in the western part of the Greenland Ice Sheet (ETH Camp, 69° 34' N, 49° 17' W; Ohmura et al., 1991, 1992).

Three radiative transfer models were evaluated, using 122 clear sky (up to 3/8 clouds) radiosonde profiles from ETH Camp. LOWTRAN7 (Kneizys et al., 1988) and STREAMER (Key, 1994) were used for modeling and comparing longwave irradiances and radiances, STREAMER and 6S (Second Simulation of Satellite Signal in the Solar Spectrum, Deuze et al., 1994) for shortwave irradiances. All models performed similarly. Incoming longwave irradiances are underestimated by about 7 to 8 Wm^{-2} compared to clear sky measurements at ETH Camp. Global radiation can be modeled with an accuracy better than 10 Wm^{-2}. Problematic seems to be the computation of diffuse radiation. The calculated values are overestimated by 6 to 9 Wm^{-2} and the differences between calculated and measured values increase with decreasing solar altitude. Also taking into account the radiosonde error in retrieval of temperature and humidity profiles results in an error of 4.5 Wm^{-2}.

An ice surface temperature retrieval algorithm is developped by regressing thermal infrared data from 10.8 μm (AVHRR channel 4) and 12.0 μm (AVHRR channel 5) channels against measured ice surface temperatures at the ETH Camp (Haefliger et al., 1993). The satellite sensor radiances were simulated using LOWTRAN7 and the 122 clear sky radiosonde profiles. The ice surface temperatures at ETH Camp were converted from outgoing longwave radiation measurements according to Stefan-Boltzmann. Modeled directional snow emissivities (Wiscombe and Warren, 1980), which are different in the two channels, are used. Sensor scan angle is included. Coefficients that correct for atmospheric attenuation are given for NOAA 11 and 12. The RMS error in the estimated ice surface temperature is less than 0.3 K.

Also based on channels 4 and 5 is a rough estimation of total water path. The RMS error in the estimated total water path is less than 1.5 kgm^{-2}. Precipitable water vapor can be converted from the total water path.

A simple linear regression was found to determine incoming longwave radiation, based on ice surface temperature and precipitable water vapor amount. The RMS error is 7.3 Wm^{-2}.

Albedo is retrieved using an algorithm based on NOAA AVHRR channels 1 and 2 (Koepke, 1989). The calibration of the two channels has to be done very careful in order to take into account the satellite sensor drift. Global radiation is determined with a parameterization based on radiative transfer model results (Bird and Hulstrom, 1981a, 1981b).

Figure 1 presents the method of retrieving the net radiation in form of a flowchart. Thick boxes present algorithms which are based on radiative transfer calculations. Gray boxes present existing data sets.

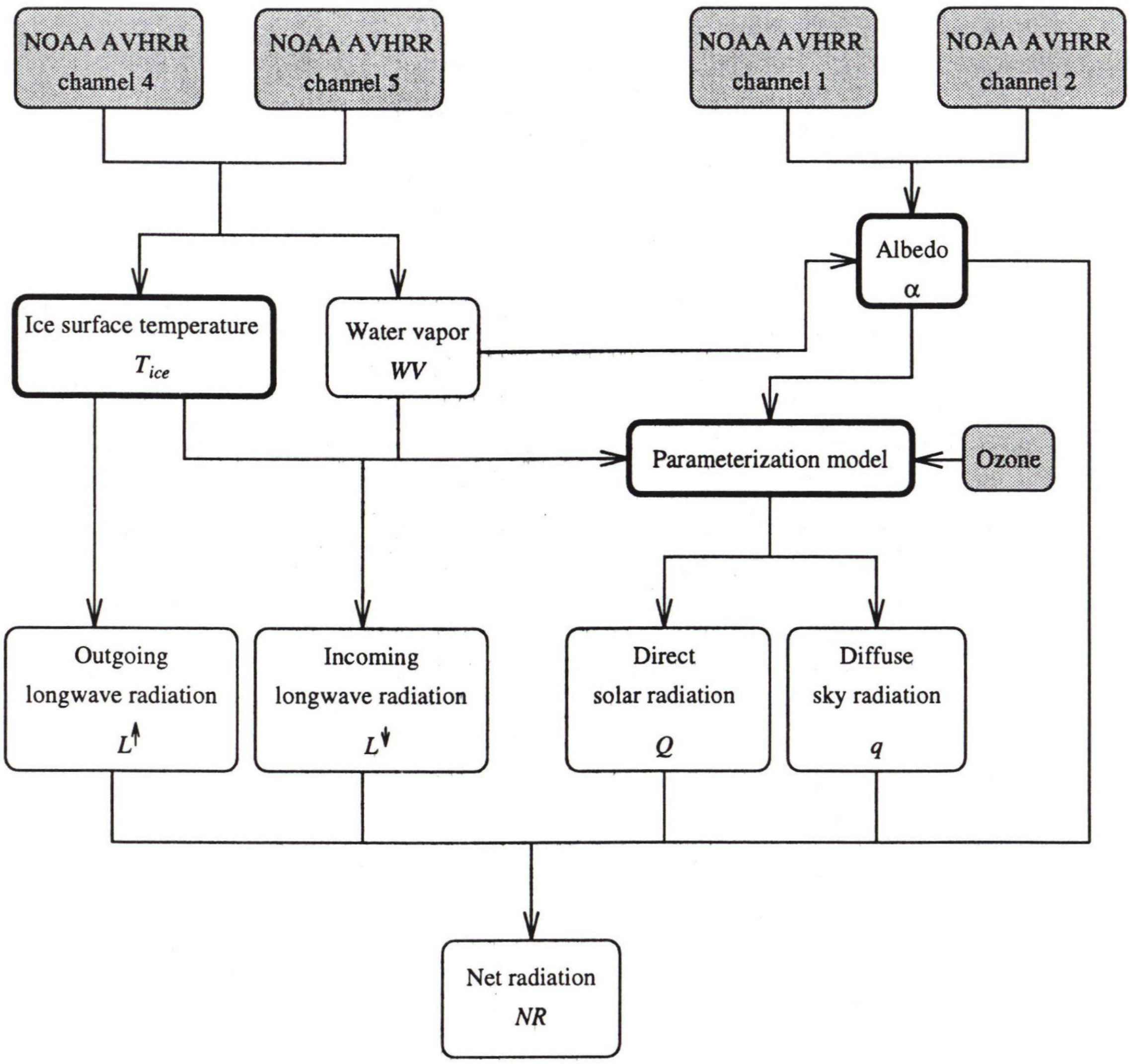

FIGURE 1: *The retrieval of the radiation balance presented in form of a flowchart. Filled boxes present data sets, thick line boxes present algorithms which are based on radiative transfer calculations. The results are presented in thin line boxes.*

Applying the algorithms to 14 AVHRR LAC (1 km resolution) and 54 GAC (4 km resolution) images has shown an overall good performance. Whereas longwave irradiances can be determined within measurement accuracy, the shortwave irradiance parameterizations do not perform as well. The mean difference between calculated and measured net radiation is about 10 Wm^{-2}. The error in the albedo retrieval is not small enough to determine the net radiation with an accuracy better than 5%.

NOAA AVHRR images are found to be useful for studies of the entire Greenland Ice Sheet. The 1 km resolution images (LAC) allow accurate studies of mesoscale areas. The 4 km resolution images (GAC) are useful for studies of the entire ice sheet. Accurate information of the clear sky radiation balance on the ice sheet can be retrieved. In order to complete the studies cloudy sky situations have to be included for future work.

Acknowledgements

The work was financed by the Swiss Federal Institute of Technology (ETH), Zürich (Grant Nos. 0-20-004-90, 0-40-040-90, 0-15-003-90, 0-15-080-90, 0-15-150-90, 0-43-018-91) and the Swiss National Science Foundation (Grant Nos. 21-27449.89, 20-32649-91).

References

Bird, R. and R. L. Hulstrom, 1981a: Direct insolation models. *Trans. ASME J. Sol Energy Eng. 103*, 182–192.

Bird, R. E. and R. L. Hulstrom, 1981b: A simplified clear sky model for direct and diffuse insolation on horizontal surfaces. SERI/TR-642-761. *Solar Energy Research Institute, Golden, Colorado.*

Deuze, J. L., M. Herman, J. J. Morcrette, D. Tanré, and E. Vermote, 1994: Second Simulation of Satellite Signal in the Solar Spectrum (6S) Technical report, Laboratoire d'optique atmosphérique, université des sciences et techniques de Lille.

Haefliger, M., K. Steffen, and C. Fowler, 1993: AVHRR surface temperatures and narrowband albedo comparison with ground measurements for the Greenland ice sheet. *Annals of Glaciology 17*, 49–54.

Key, J., 1994: *Streamers User's Guide.* Cooperative Institute for Research in Environmental Sciences.

Kneizys, F. X., E. P. Shettle, L. W. Abreu, G. P. Anderson, J. H. Chetwynd, W. O. Gallery, J. E. A. Selby, and S. A. Clough, 1988: *User's Guide to LOWTRAN 7.* AFGL-TR-088-0177.

Koepke, P., 1989: Removal of Atmospheric Effects from AVHRR Albedos. *Journal of Applied Meteorology 28*, 1341–1348.

Ohmura, A., K. Steffen, H. Blatter, W. Greuell, M. Rotach, T. Konzelmann, J. Forrer, A. Abe-Ouchi, D. Steiger, M. Stober, and G. Niederbäumer, 1992: Energy and mass balance during the melt season at the equilibrium line altitude, Paakitsoq, Greenland Ice Sheet, ETH Greenland Expedition Progress Report No. 2. *Dept. of Geogr., Swiss Fed. Inst. of Technol., Zürich*, 108.

Ohmura, A., K. Steffen, H. Blatter, W. Greuell, M. Rotach, T. Konzelmann, M. Laternser, A. Abe-Ouchi, and D. Steiger, 1991: Energy and Mass balance during the melt season at the equilibrium line altitude, Paakitsoq, Greenland Ice Sheet, ETH Greenland Expedition Progress Report No. 1. *Dept. of Geogr., Swiss Fed. Inst. of Technol., Zürich*, 108.

Wiscombe, W. J. and S. G. Warren, 1980: A Model for the Spectral Albedo of Snow. I: Pure Snow. *Journal of the Atmospheric Sciences 37*(12), 2712–2733.

MICROCLIMATE, SPECTRAL REFLECTANCE AND ENERGY-BALANCE ON THE STORSTRØMMEN GLACIER

Carl Egede Bøggild[1], Hans Oerter[2], Niels Reeh[1], Friedrich Jung-Rothenhäusler[2]

[1]*The Geological Survey of Greenland, Øster Voldgade 10, DK-1350 Copenhagen K, Denmark*
[2]*Alfred-Wegener-Institut für Polar- und Meeresforschung, Bremerhaven, Germany*

During the summer of 1994 a total of 5 automatic climate recording stations were installed on selected stakes along the stakeline on the Storstrømmen glacier 77 °N on the eastcoast, where the location is described in detail by Bøggild et al (1994a). The aim of making detailed microclimatic studies on the Storstrømmen glacier is to study and to quantify the parameters which determine the highly "noisy" ablation pattern which charactrize glaciers in Northgreenland (Bøggild et al., 1994b).

Station	Location	Logger-type	Sensors	Type
Station 29	NE2993	Campbell BDR 320	Ventilated-air temp. Anemometer	Vector T302 RISØ
Station 11	NE1189	Campbell BDR 320	Ventilated-air temp. Anemometer	Vector T302 RISØ
Station 8 A	NE08.1A89	Ryan Inst - RTM 2000	Air temp. Wind-way	PT100 Lambrecht 1440
Station 7	NE0789	Campbell BDR 320	Air temp./ humidity Anemometer Pyranometer	Vaisala-HMP310FA Vector A102R Kipp and Zonen-CM7
Station 6	NE0689	Ryan Inst.- RTM 2000	Air temp. Wind-way	PT100 Lambrecht 1440

Table 1. Climate stations and sensors on the Storstrømmen glacier in 1994.

The 5 data loggers involved in this experiment were operating in a period of one month between July 12 and August 10, at which time the participants carried out fieldwork on the more northerly location in Kronprins Christian Land (Oerter et al., 1994). Three loggers of the brand Campbell Scientific BDR 320 has been purchased for this project with financial aid from the Commision for Scientific Research in Greenland. Two of the Campbells were mounted with anemometers kindly lend by the research institute RISØ. Table 1 show the loggers and sensor configuration as they were installed on Storstrømmen during the experiment. The remoteness and very high logistical cost associated with operating in North-East Greenland calls for small and light climate stations, which can be mounted on the existing network of ablation stakes. Ventilated as well as unventilated temperature sensors has been applied in the project. The advantage of obtaining air temperatures from a ventilated sensor is to avoid the effect of radiational heating of the sensor during conditions with little wind and clear sky. Such conditions usually measure too high temperature values when the sensor is not ventilated. Additionally at station 7 global radiation and albedo (integrated surface reflectance) was measured automatically with a Kipp and Zonen CM7 pyranometer. Also relative humidity was measured, providing a data set from Station 7 which is sufficient for making energy-balance calculations of heat fluxes determining the observed melt rates.

When the ablation stakes were visited, additional measurement were carried out with a Spectron Ingineering type SE 590 handheld spectrometer. This instrument can determine the surface reflectance in 252 discrete bands, with a spectrum from the ultraviolet wavelengths to the near infrared wavelengths (from 300 to 1100 nm). The spectrometer was operated and controlled through a portable PC, where also the digital data were stored. The spectometer was rented from the Norwegian Hydrotechnical Laboratory and was applied on both Storstrømmen and at the icemargin off Kronprins Christian Land. Fig 1 shows the an example of spectral characteristics of the surface reflectance at station 6 for different types of ice surfaces. The wide distribution of spectral surface reflectance values are common for the glacier surfaces in Northgreenland.

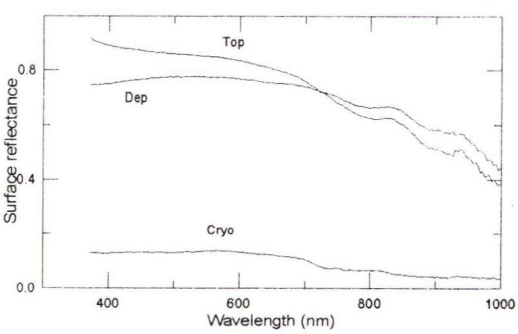

Fig. 1. Measured surface reflectance at Storstrømmen. Wavelength is in nm. Top, dep and cryo refer to crest, depression and cryoconite.

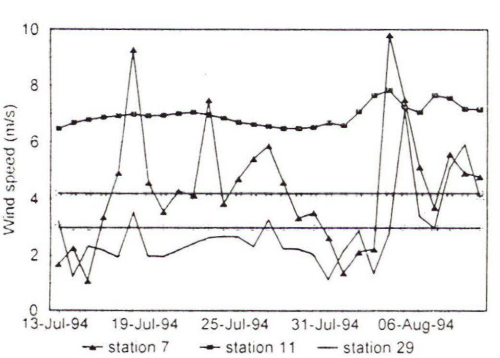

Fig. 2. Daily mean windspeed variations from 13 July to 11 August, 1994.

THE GENERAL CLIMATOLOGY

Preliminary results from this summer show some destinct characteristic features in the distribution of wind velocities on the glacier. The highest velocities are associated with a combination of high slopes and remoteness from the terminus. At the highest station (11) the wind is observed to be most steady and intense, as seen in fig 2 (station 8A and 6 are mean values over the whole period). Through the daily cycle, in turn, the variability is most pronounced at stake 11 (fig 3). A maximum occurs around 6 AM, which is in line with observations of katabatic winds close to the equilibrium line near Kangerlussuaq in Westgreenland (van der Broeke et al, 1994). The diurnal variations of air temperatures are also greatest at station 11 (Fig. 4). This apparently is associated with the longwave radiative cooling at night.

Conditions are rather different near the horisontal grounding line close to the terminus (station 29). Here the wind pattern is most transient (fig 2) with litttle or no diurnal amplitude in both wind (fig 3) and in air-temperatures (fig 4). This indicates little or no influence from the strong katabatic winds which are prevailing in the upper part of the ablation zone, and most pronounced at inclined slopes.

The observed distribution of wind velocities on the glacier may well explain the lack of snow accumulation as observed on satellite images from wintertime. The prevailing katabatic winds will most probably remove the deposited winter-snow on slopes, and thus highly disturbs the general massbalance-elevation gradient of the glacier and possibly also in other parts of the Northeast-Greenland icemargin.

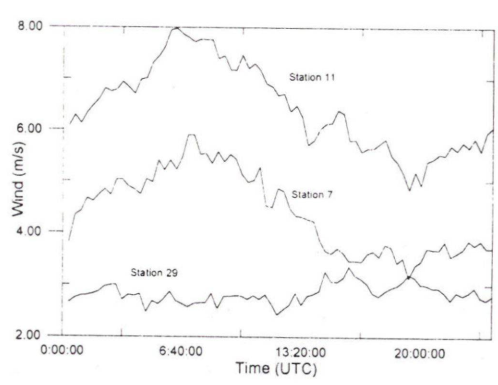

Fig. 3. Daily mean cycle of windspeed in the period 13 July - 11 August, 1994.

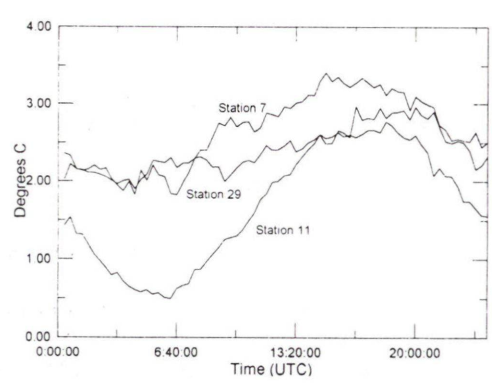

Fig. 4. Daily mean cycle of air temperature in the period 13 July - 11 August, 1994.

ENERGY BALANCE AT STATION 7

Evolution of each component in the energy balance is shown in fig 5 (positive downwards). The calculations are based on a model described in Bøggild (1991). As input to the model, the components of wind, humidity, air temperature and shortwave radiation balance are needed. The model setup is based on the assumption that melting only occurs at positive air temperatures which causes isothermal snow/ice surface conditions. Following these conditions all the vertical flux components in the energy balance, can be obtained needing only one level of measurements. From the model calculations the melt has been estimated to be 71 cm of snow, whereas the observed snowmelt from 13 July until 10 August was 58 cm. Many hypothesis can be addressed on the overestimated ablation e.g. densification of the snow, refreezing of melt water etc. A striking feature is that the observed albedo (fig 6) shows an increase of surface reflectance during a 5 day period from end July to beginning of August. This rise in albedo may originate from a snowfall event, by means of which mass was added to the surface and followed by reduced ablation as a consequence of a rise in albedo with new snow on the ice surface.

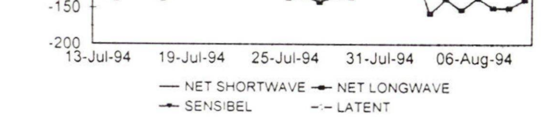

Fig. 5. Daily mean of the components in the energy balance in the period 13 July - 11 August, 1994.

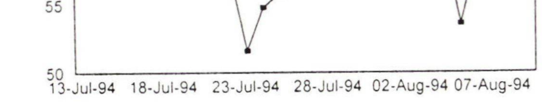

Fig. 6. Daily mean albedo from 13 July to 11 August, 1994.

ACKNOWLEDGEMENTS

Besides the Alfred Wegener Institutes involvement in the Northeast Greenland research, additional funding was provided by the Danish National Science Foundation. The Commision for Scientific Research in Greenland provided funding for the climate stations. The EU ENVIRONMENT programme also provided funding.

LITERATURE

Bøggild, C. E.(1991): En smeltende snepakkes masse og energifluxe - belyst ved beregningsmetoder. Thesis. Københavns Universitet. 94 pp.

Bøggild, C.E., N. Reeh and H. Oerter. 1994a. Past and present energy-balance studies of North-East Greenland. in: GGU Open File Series, Copenhagen., *Report from the 4th Workshop on Mass Balance and Related Topics of the Greenland Ice Sheet, Amsterdam 22.11 - 24.11. 94*, 18-23.

Bøggild, C.E., N. Reeh, H. Oerter. 1994b. Modelling ablation and mass-balance sensitivity to climate change of Storstrømmen, North-east Greenland. Global and Planetary Change. 9. 79 - 90.

Oerter, H., F. Jung-Rotenhausler, C.E. Bøggild and N. Reeh. 1994. Glaciological investigations in Kronprins Christian Land eastern North Greenland. Express Report. Eastern North Greenland and North-East Greenland, 1994. p 97 - 105.

van der Broeke, M.R, P.G. Duynkerke, J. Oerlemans. The observed katabatic flow at the edge of the Greenland ice sheet during GIMEx-91.. Global and Planetary Change. 9. 3 - 16.

ON A PRELIMINARY EVALUATION OF THE ENERGY BUDGET AT THE SUMMIT OF THE GREENLAND ICE CAP

Friedrich Obleitner
Institut für Meteorologie und Geophysik der Universität Innsbruck

1. Introduction

Within the framework of the Greenland Ice Core Project (GRIP) an associated study on the energy budget of the snow surface was carried out during a 4 week´s field season between June 24 and July 19, 1992. This report focusses mainly on documentation and discussion of measurement experiences especially concerning radiational fluxes, but presents a preliminary evaluation of turbulent fluxes as well.

2. The measurement period and site

During the measurement period the mean atmospheric conditions were characterized by:

Temperature (1.5m): -17.3°C (max.: -7.5 , min.: -29.5 °C)
Dewpoint: -18.5 °C
Wind speed: 3.6 m/s (max. : 11.5m/s)
Wind direction: W - SW
Accumulation: < 5cm

A succession of distinct arctic atmospheric conditions was observed, covering 4 clear days, 5 overcast days and 13 days with snowfall and drifting snow. Due to abnormal synoptic activity influencing the GRIP-site this summer period was experienced as a comparatively ´cool´ one.

The instruments were set up some 500m south of the main camp where major disturbances of the natural snow surface and of micrometeorological fetch by camp activities may be safely excluded.

The following instruments were maintained:

Temperature:	shielded and ventilated Pt -100	(50 / 150cm / 300cm height)
Humidity:	shielded and ventilated dewpoint-mirror	(50 / 150cm)
	shielded and ventilated Pt -100 psychrometer	(50 / 150 / 300cm)
Wind speed:	Aanderaa cup anemometers	(50 / 150 / 300cm)
Solar radiation:	Swiss-Teco pyranometers (ST- 2)	(150cm)
Terrestrial radiation:	Swiss-Teco pyrradiometers (SW- 2)	(150cm)
Snow temperatures:	Pt -100	(-5 / -11/ -25 / -50cm)

10min mean values calculated from 10sec scans were stored, the further evaluation is based on hourly mean values.

Attempts to measure evaporation directly by means of a weighted lysimeter failed mainly due to drifting snow. Glaciological information is provided by several stakes and a snow pit.

3. The Radiation Budget

3.1. Calibration and Accuracy

Before, during and after the field work, the shortwave sensitivities of all radiometers were determined by the shading method, the longwave sensitivities of the pyrradiometers are known from nighttime radiance above melting snow. By the use of pyrradiometers the longwave radiation fluxes cannot be separated independently of corresponding short wave components which must be remembered when judging the accuracy of measurements as follows:

- According to Ambach (1963), the use of isotropic sensitivities independently of solar height and cloudiness might introduce a maximum error in hourly shortwave fluxes of $40 Wm^{-2}$ which would correspond to about 5% of noon global radiation intensities observed during GRIP. Therefore in the evaluation presented here, the shortwave sensitivities of the upfacing sensors were fully kept dependend on solar height, but any variation of sensitivities with the degree of isotropy of the incoming radiation was not taken into account as hourly cloudiness observations were not available continuously. Reflected intensities monitored by the downfacing sensors were calibrated by use of isotropic shortwave sensitivities which were determined according an integrating procedure proposed e.g. by Ambach (1963).

- A serious problem concerning the measurement of shortwave fluxes occured due to intense riming which preferably touched the upper glass hemispheres. The following Fig.1 illustrates the typical effects on the recorded signals as well as an example of a correction applied by means of a graphical editor.

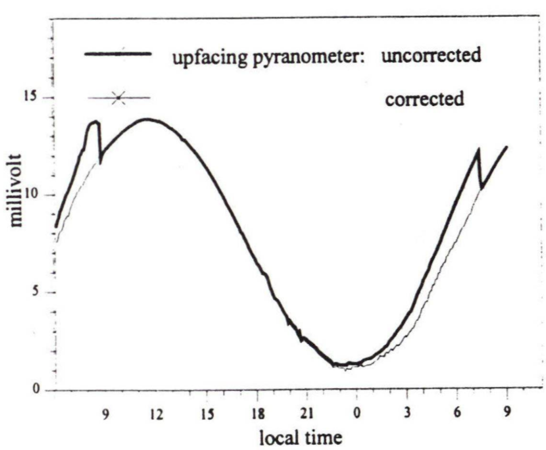

Fig.1: Example of the effect of rime forming at the hemispheres of radiation sensors and ist correction

If uncorrected, a maximum error of 12% would pierce the evaluation of all radiation components which is hopefully avoided by the procedure applied.

- The maximum difference of shortwave sensitivities from calibrations before and during the field work was about 3%. As in polar atmospheres the occurence of atmospheric ice needles can never be safely excluded, the field calibrations were less weighted.

- Due to the evaluation procedure applied, the individual longwave fluxes can never be more accurate than the shortwave components. However, the deposition of rime at the polyethylene domes was noticeable less than for the glass domes which in this regard improves the quality of longwave data.

- Unfortunately, the artificial ventilation of the pyrradiometers failed due to intense riming within the inflation system. Due to sufficient natural ventilation, no significant effect on the shortwave sensitivities is revealed by the field calibrations. However, Ohmura and Gilgen (1993) pointed out the general effect of lacking ventilation of pyrradiometers which even might be exceeded by effects of their exposure against direct solar radiation. Both was the case for the presented measurements too. As the calibrations were made under the same conditions / exposure as in the field, no correction was to be applied on the upfacing instrument, whereas intensities measured by the downfacing instrument generally tend to overestimate the corresponding longwave fluxes and have to be corrected. This was done in context of evaluation of turbulent fluxes and is described later on.

- A real quantitative extimation of the final accuracy of the individual radiational components is difficult, mainly due to the varying effects of rime. But assuming effective correction of rime disturbance by the procedure applied as well as sufficient natural ventilation the worst case estimation of the overall accuracy is surely within the common range of 5% for the shortwave resp. 15-20% for the atmospheric longwave component.

All radiation fluxes refer to the World Radiometric Reference.

During the 4 week´s measurement season from June 24 to July 19, 1992 the sun was continuously above the horizon, the minimum solar elevation was 6°, maximum 41°.

3.2. Global radiation

Based on a solar constant of 1367 Wm^{-2}, the calculated daily sums of extraterrestrial insolation were generally about 42 $MJm^{-2}d^{-1}$ and were subjected to a decreasing trend because of the season beyond the summer solstice. This naturally impinges on all shortwave radiational components. As an average for the whole summer period, 73% of extraterrestrial insolation succeded to penetrate the atmosphere down to the snow surface, on a daily basis a span of 76% for clear days and 57% for overcast days with precipitation was observed. As the ratio of measured global radiation against the extraterrestrial values eliminates latitudinal effects, it is a useful basis for a first climatological discussion of incident solar radiation resp. atmospheric turbidity. The following Fig.2 summarises some comparable information on this parameter as far as may be judged from corresponding publications which each refer to individual seasonal peculiarities and varying lengths of measurement periods:

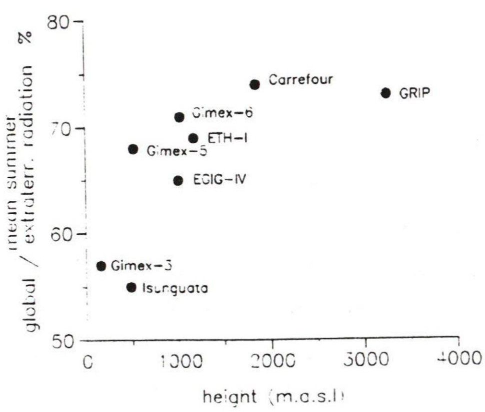

Fig.2. : Mean summer global radiation in % of extraterr. insolation versus heigth above sea level.
(Greenland region, data sources are cited in the references)

Within the Greenland region, the GRIP figures match the expectation of high atmospheric transparancy due to the remoteness and high elevation of this site.

During the GRIP field season the day of maximum brightness yielded a global radiation of 33 $MJm^{-2}d^{-1}$, the darkest day still 74% of the former.Typically, the day of maximum brightness did not occur with cloudless conditions, but with a layered and broken altocumulus prevailing throughout the day (July 15, 1992). As known especially for polar regions, the latter may effectively increase the diffuse component of global radiation by multiple reflections between the cloud base and the snow surface of equally high albedo. Minimum global radiation was observed during a day with a dense, low based overcast, snowfall and the heaviest snowdrift observed during the measurement period (July 5, 1992). This was the only day when the location of the sun was invisible.

For clear days, the occasional pyranometer calibrations by shading offered an estimation of the share of the diffuse component on incident global radiation which for air masses between 1 and 2 was found to be about 25%.

3.3. Albedo

Variation of mean daily albedo covered a range between 0.82 and 0.71, the mean value for the whole measurement period was 0.79. These figures are quite typical for polar inland stations (Ambach 1963, 1983, Kuhn 1977, van de Wal & Oerlemans 1993). As pointed out in Fig. 3, the lowest daily mean values were observed at the end of a period of calm weather with neglibible precipitaion or drifting snow.

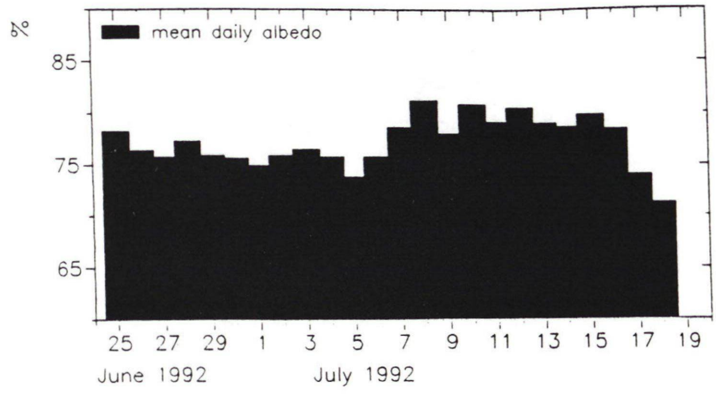

Fig.3: Mean daily variation of albedo

Snow metamorphosis and furtive pollution of the snow surface by remote camp activities are likely to be responsible for the more or less continuous decrease of albedo during this period. With the onset of bad weather the mean daily albedo recovered up to the maximum of 0.82.

Theoretical expectation and observations concerning the diurnal variation of the albedo above horizontally and physically homogeneous surfaces favour a single minimum during solar noon hours of clear days. This was not observed at GRIP where clear days were characterized by a maximum during noon hours. Similar as noted for other sites (e.g. Diamond &Gerdel 1957, Kuhn 1977), this is most probably due to the combined effects of naturally present sastrugis and additional disturbance of the horizontal homogeneity of the snow surface by mounting rods of the sensors resp. their maintainance. In that context it is to be mentioned that a flat and hill-shaped disturbance seems to have developed at the GRIP measurement site.

3.4. Atmospheric longwave radiation

Though corrected, the problems concerning rime are to be remembered again and -as pointed out earlier- no correction concerning non-shading and natural ventilation of the sensor was to be applied.
During the GRIP-92 season the daily sums of atmospheric longwave radiation varied slightly (17-22 Mjm $^{-2}$ d $^{-1}$), but followed clearly the sucession of synoptic scale weather systems passing the site. A 20% increase of atmospheric longwave radiation occured during the storm period which was due to continuous advection of maritime warm air masses and a low cloud cover with southwesterly upper air winds prevailing. With the passage of a cold front on July 15, a sharp decrease of atmospheric longwave radiation occured. This might be understood by prevailing clear sky and northeasterly winds advecting cold and dry air masses towards the summit of Greenland.
The diurnal variation of atmospheric longwave radiation was generally weak, the most striking variation occured in context with fog formation resp. ist dissolution. As typical for stormless days, a 20Wm^{-2} decrease of atmospheric longwave radiation occured within the 2 hours of fog dissolution in the early morning hours. Usually radiation fog formed again within an elevated layer at about 22 local time.

3.4. Surface emitted longwave radiation

As pointed out earlier serious constraints with pyrradiometric must be expected in case of operating the instrument in a downfacing mode. Thorough investigations (Ohmura & Schroff 1983, Dehne et al. 1993) demonstrated that in the inverted mode convection within the polyethylene cover will be inhibited due to a stable stratification. Thus during sunshine hours a general overestimation of longwave radiational fluxes must be expected when applying the sensitivities deduced from calibrations in the upfacing mode. This must be assumed to be most effective in case of high solar radiation intensities reflected by surfaces of high albedo. There is no way of a straightforward correction of such errors.
It was decided to estimate the surface emitted longwave radiation resp. radiometric surface temperatures by a numerical procedure in context of an evaluation of turbulent fluxes which is described as follows.

4. Turbulent fluxes

4.1. Measurement experiences

A thorough measurement of vertical temperature profiles above snow surfaces is still a challenge on experimental micrometeorology. This is mostly due to radiational heating/cooling of the temperature sensors resp. their supports which in case of strong insolation cannot be totally overcome by artificial ventilation. Unfortunately such conditions are likely to occur above high polar snow surfaces during summer.
The vertical temperature and humidity profiles above the snow surface were measured by 2 different devices, both were artificially ventilated and shielded against direct solar radiation. The corresponding mean profiles are documented in Fig.4.

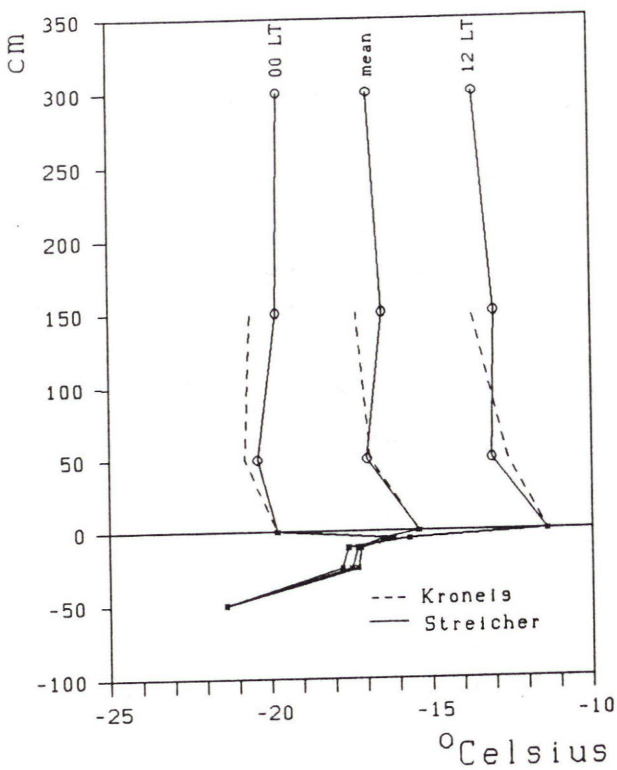

Fig.4: Mean resp. day/nigth temperature profiles as measured with 2 different devices

A considerable uncertainty in temperature measurements is to be admitted, between different levels and day/night respectively. Inspite of careful sensor laboratory calibrations before and after the field season it is unfortunately still impossible to interprete the observed deviations. A complex interaction of the Pt-100 sensors with their surrounding (i.e. radiation shield) must be assumed, most probably by longwave radiation too. All this inhibits a straightforward correction as the involved effects are obviously dependent on the design of the system support, measurement height, the amount of incident solar radiation and might be even on the orientation of the sensors relative to the position of the sun.

Some of these effects may falsify the temperature readings of sensors buried into the snow too, above all a depth-dependend error due to the absorption of penetrating solar radiation must be assumed.

Concerning a decision on the method used for evaluation of turbulent fluxes these measurement constraints have to be taken into account anyway, but the availability of proper humidity measurements as well. During the GRIP-92 field season wet bulb temperature profiles could not be maintained successfully -mainly because of quickly drying up. Thus the evaluation of turbulent latent heat transfer had to rely on the dewpoint measurements with the so called „Kroneis" device which have worked well within their experienced accuracy of $\pm$ 0.2°C.

Summarizing all these mentioned experiences it was decided to begin with an evaluation of the turbulent fluxes on the basis of temperature and dewpoint measurements at the 150cm level and by means of the „Kroneis" device (Θ,q). Having only one reliable level available, a bulk transfer parametrization of the turbulent fluxes is favoured which in turn involves measurement or calculation of surface temperatures (Θ_s,q_s)., wind speed (u) and bulk transfer coefficients for sensible resp. latent heat (C_i). The latter are to be calculated from near neutral wind profiles and kept dependend on stability:

$$F = (E_{h0} + \rho c_p C_{hu})(\Theta - \Theta_s)$$
$$L = (E_{v0} + \rho L_v C_{vu})(q - q_s)$$

$$C_i = k^2 \Phi_i^{-2} \left(\ln \frac{z}{z_0}\right)^{-2} \qquad \Phi_i = f(Ri) \text{ ... Businger}$$

E_{io} ... windless convection coefficients, constantly $2Wm^{-2}K^{-1}$ (resp. $2Wm^{-2}hPa^{-1}$)

The additional demand on correction resp. calculation of surface temperature/humidity was met by the use of a mass- and energy balance model for predicting temperature profiles within the snow cover (Sntherm.89, USA-CRREL, R. Jordan, 1991). This is a research grade, one-dimensional model which is adaptable to a full range of meteorological conditions and handles freeze-thaw cycles, accumulation, ablation, densification and metamorphosis as well as their impact on the optical and thermal properties of the snow cover. In depth absorption of solar radiation is treated as well. The governing equations for heat and mass balance are subject to meteorologically determined boundary conditions at the air interface, linearized with respect to the unknown variables and solved by a tridiagonal-matrix algorithm. Surface fluxes are calculated from user-supplied meteorological observations and have to match the above mentioned parametrization and iterated surface characteristics as well. The model is initialized with profiles of the physical characteristics of the various strata within the snow cover which are the main output of the model at the other hand.
Remembering the experienced constraints on measuring temperature and humidity profiles within the atmospheric boundary layer, the following was the philosophy of a preliminary evaluation of turbulent fluxes at GRIP: the model calculates turbulent fluxes and profiles of snow temperatures (including surface temperature), the input for the used model can be supplied. Furtheron, if calculated snow temperature profiles can be positively validated by corresponding measurements, the turbulent fluxes may not be out of order too.
Thus a kind of indirect validation of the model results resp. of the evaluation of turbulent fluxes was done by comparison of modelled and observed snow temperatures. This is demonstrated by the following 2 figures.

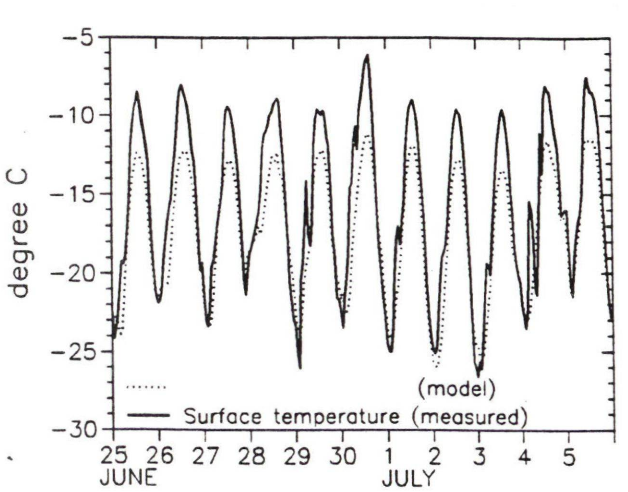

Fig.5a : Comparison of measured /modelled surface temperatures

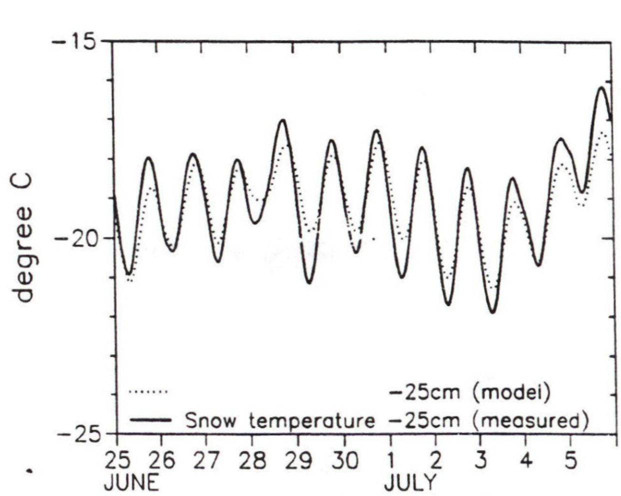

Fig.5b: Comparison of measured /modelled -25cm snow temperatures

Concerning measured surface temperatures (Fig. 5a) it is to be remembered that the pyrradiometric measurements are likely to overestimate surface temperatures during bright sunshine thus the lower simulated noon surface temperatures would be quite welcome with this respect. During these hours the measured -25cm snow temperatures (Fig.5b) may be somewhat falsified by absorption of penetrating solar radiation too. But as a first step the overall agreement is satisfactory as there is still some room for improvement left. During the GRIP-92 measurement season melting of the snow surface can be safely excluded.

4.2. Sensible heat flux

Measurements and simulation indicate frequent unstable temperature stratifications within the lowest 1.5m above the snow surface. Being somewhat unexpected and easily falsified by instrumental problems the qualitative occurence of unstable temperature conditions during summer was proved by thorough investigations at other high polar sites too (e.g. Carroll 1982, Dalrymple et.al. 1966, Riordan 1977).
With these suppositions for the GRIP-92 season a mean sensible heat flux of -31W m^{-2} off the surface results. Mean daily variations are characterized by 2 maxima at about 6LT and 16LT where maximum temperature gradients seemed to develop by differential solar warming and fog formation/dissolution respectively (Fig.6). The latter processes has to be investigated in more detail yet.

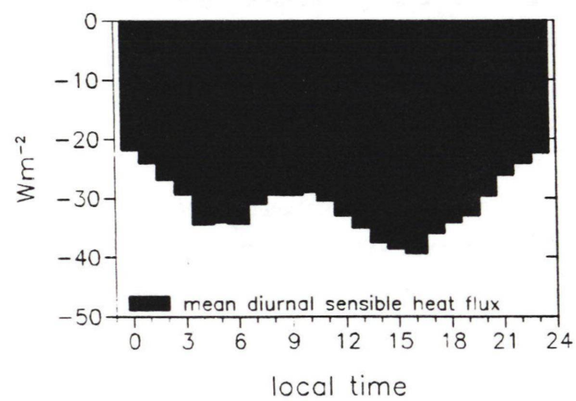

Fig.6: Mean diurnal variation of sensible heat flux

4.3. Latent heat flux

As expected for a high polar snow surface the mean latent heat flux is neglibible small. The evaluation result of -4Wm^{-2} indicates evaporation prevailing esp. during hours of abundant sunshine (Fig.7). Unfortunately this result cannot be verified by direct measurements.

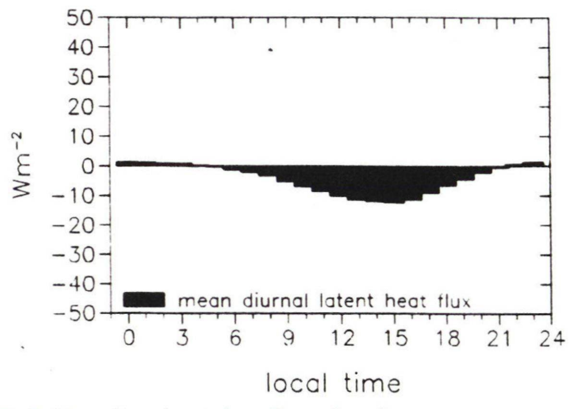

Fig.7: Mean diurnal variation of latent heat flux

4.4. Change of energy stored within the upper 1m of the snow pack

The preliminary evaluation presented here indicates a net storage of energy (+9Wm^{-2}) during the GRIP-92 field season which is qualitatively proved by an observed net warming of the snow cover throughout the period (Fig. 8). As demostrated by Fig.9 most of it occured during the hours of highly positive radiation budgets.

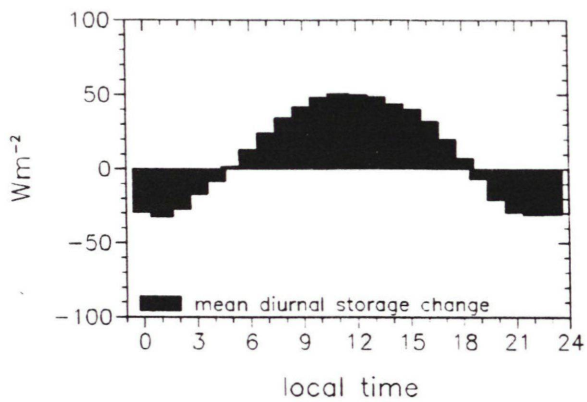

Fig.8: Mean diurnal variation of energy stored within the snow pack

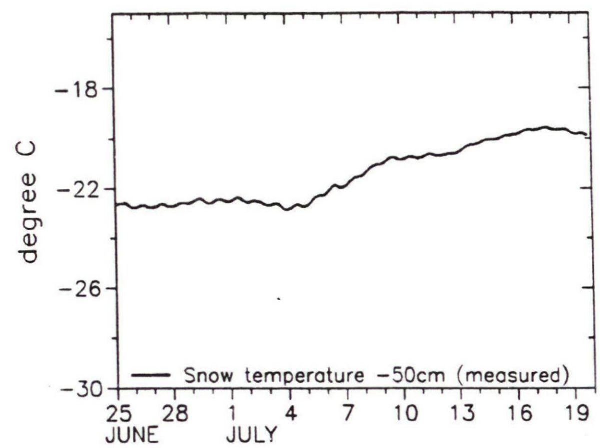

Fig.9: -50cm snow temperature as observed during GRIP-92

5. Synthesis of the GRIP-92 field season energy budget (June 24 - July 19, 1992)

By the calculation of surface emitted longwave radiation from modelled surface temperatures the radiation and energy budget could finally be closed as follows:

extraterr. insolation:	481 Wm^{-2}
global radiation:	354 Wm^{-2}
reflected global radiation:	278 Wm^{-2}
albedo:	78%
shortwave budget:	76 Wm^{-2}

atmospheric longwave:	218 Wm^{-2}
surface emitted:	- 249 Wm^{-2}
longwave budget:	- 31 Wm^{-2}

net radiation:	45 Wm^{-2}
sensible heat flux:	- 31 Wm^{-2}
latent heat flux:	- 4 Wm^{-2}
change in energy stored:	9 Wm^{-2}
no melting	

6. Final remarks

A number of serious constraints concerning radiational and micrometeorological measurements were experienced during the GRIP-92 field season. As seen now, some could have been avoided if more information on corresponding experiences made by other groups would have been available at the time of preparing. Therefore my emphasize on their detailed documentation within that report now, which hopefully mets the scope of the workshop though not all of it is true science. At the other hand some principal experimental problems with high polar experimental work came up once more which still call for substantial improvements. In that sense I clearly feel that a kind of evaluation as presented here still depends too much on model results which cannot be proved in the desired extent. Thus future effort will firstly concentrate on one of the most sensitive parameters i.e. a model-independent correction of measured surface emitted longwave radiation . If successful that would provide an independent estimation of surface temperatures which have a major impact on the estimation of turbulent fluxes too. Then sensitivity studies on the specific effect of uncertainties in temperature profiles on the resulting fluxes resp. their estimation by use of alternative parametrizations could be informative too. Concerning future field work, more cooperative experimental studies would be most desireable.

Acknowledgements

This work is a contribution to the Greenland Ice Core Project (GRIP) organized by the European Science Foundation. Thus Austrian field work was generous made possible by the GRIP steering comittee , practical work was mainly supported by the Alfred Wegener Institut for Polar and Marine Research, Bremerhaven. Especially the friendship and assistance by the GRIP-92 participants is gratefully acknowledged as well.
To some participants of the workshop thanks are to be given for valuable comments on the presented evaluation of field work.

References

Ambach W. 1963: Untersuchungen zum Energiehaushalt in der Ablationszone des Grönländischen Inlandeises (Camp IV-EGIG). Meddelelser om Gronland, Bd. 174, Nr.4 , 312pp.

Carroll, J., 1982: Long term means and short term variability of the surface energy balance components at the South Pole. J. Geophys. Res. 87 (C6), 4277-4286.

Dalrymple P., Lettau H., Wollaston S. 1966: South Pole micrometeorological program: data analysis, Antarct. Res. Ser., 9, 13-57.

Dehne K., Bergholter U., Kasten F., 1993: IEA Comparison of longwave Radiometers, IEA Technical Report of task 9, 71pp.

Diamond M., Gerdel R.W., 1957: Radiation measurements on the Greenland Ice Cap, IASH/ICSI General Assembly of Toronto, Volume IV, 403-422.

Kuhn M., Kundla L.S., Stroschein L.A. 1977: The Radiation Budget at Plateau Station, Antarctica, 1966-1967, American Geophysical Union, Antarctic Research Series Volume 25, 41-73.

Jordan R. 1990: One -Dimensional Temperature Model for a Snowcover: Technical Documentation for Sntherm.89. USA-CRREL Special Report 657, 136pp

Ohmura A., Gilgen H. 1993: Re-Evaluation of the Global Energy Balance. Geophys. Monogr. 75, IUGG Volume 15 , 93-110.

Ohmura A., Schroff K., 1983: Physical Characteristics of the Davos-type Pyrradiometer for Short- and Long-wave Radiation, Arch. Met. Geoph.Biokl., Ser.B, 33,57-76.

Riordan A.J., 1977: Varaitions of temperature and air motion in the 0 - to 32 meter layer at Plateau Station, Antarctica, American Geophysical Union, Antarctic Research Series Volume 25, 113-127.

Literature cited in Fig. 2:

Ambach W. 1963: Untersuchungen zum Energiehaushalt in der Ablationszone des Grönländischen Inlandeises (Camp IV-EGIG). Meddelelser om Gronland, Bd. 174, Nr.4 , 312pp.

Ambach W. , Markl G. ,1983: Untersuchungen zum Energiehaushalt in der Akkumulationszone des Grönländischen Inlandeises (Station Carrefour), Meddelelser om Gronland, Bd. 187, Nr.6, 61pp.

Holmgren B., 1971: Climate and Energy Exchange on a Sub-Polar Ice Cap in Summer, Meddelande Nr.111, Meteorologiska Institutionen, Uppsla Universitet, 111pp.

Maykut G., Church P., 1973: Radiation Climate of Barrow, Alaska, 1962-66, Journal of Appl. Meteorology, Vol. 12, 620-628.

Ohmura A. 1982: Climate and Energy Balance on the Arctic Tundra, Journ. of Climatol., Vol 2, 65-84.

Ohmura A. et al. 1992: Energy and Mass Balance during the melt season at the equilibrium line altitude, Paakitsoq, Greenland Ice Sheet. Department of Geography, ETH, Zürich, Progress Report No.2,94pp.

Oerlemans J., Vugts H.F. 1993: A Meteorological Experiment in the Melting Zone of the Greenland Ice Sheet, Bulletin of the AMS, Vol.74, No.3, 355-365.

Rott H., Obleitner F. 1992: The Energy Balance of Dry Tundra in West Greenland, Arctic and Alpine Research, Vol. 24, No. 4, 352-362.

Page intentionally left empty in printed version

BOUNDARY LAYER CHARACTERISTICS AT THE VU-CAMP
PROFILE RELATIONS ON A SLOPING ICE SURFACE

Edwin A.C. **Henneken**
Faculty of Earth Sciences, Vrije Universiteit Amsterdam, the Netherlands

Suppose you want to have estimates for the turbulent heat fluxes, but eddy correlation equipment is not available for some reason; how to proceed? At best you have observations of e.g. average wind speeds and temperatures at a number of levels above the surface. These observations, together with a theoretical tool called "flux–profile relations" enable you to give the required estimates.

These (emperical) relations are based on a number of assumptions concerning the character of turbulent motion in the atmospheric surface layer (ASL). One important ingredient is called "Monin–Obokhov Similarity" (MOS); it tells you that if some quantity is transported (vertically) by turbulent motion and can be represented by some observable, $C(z)$, then the vertical gradient of this quantity, when made dimensionless in a sensible way, depends only on the stability of the ASL thru some universal function (see also the contribution to the previous workshop (Henneken, 1994)). Note that MOS only tells you that such a function exists, it does not give its shape. This means that

$$\frac{\kappa z}{c_*}\frac{\partial}{\partial z}C = \phi_c(\zeta) \qquad (1)$$

where c_* is a characteristic scale for C and ζ ($\equiv z/L$) is a dimensionless parameter expressing atmospheric stability (with $\zeta > 0$ for stable conditions). Here C is either the horizontal wind speed, U, or the potential temperature, Θ; this means that only the turbulent transport of momentum and sensible heat are discussed.

Experience has on the one hand shown the flux–profile relations to be a powerful tool and on the other hand it has provided us with a number of expressions for the ϕ–function in expression 1. Especially observations in stable conditions have proven to be difficult. Since at the VU–camp both profile and eddy correlation observations are available, the shape of the ϕ–functions can be calculated; the ASL at this position was most of the time stably stratified, so the following question can be addressed: are the ϕ–functions, determined in experiments over land–surfaces for stable conditions, also applicable over (sloping) ice surfaces? In this light it is important to make a comparison with similar experiments on ice sheets at positions with the same terrain slope (like the ETH–expedition) and no (or very small) terrain slope (like the STABLE–expedition on the Brunt ice shelf, Antarctica (see King, 1990)). For the analysis of the VU–data a subset of observations obtained in the time interval of 11:00 till 17:00 has been used.

Before looking at the relation between turbulent transport and mean profiles, it is useful to first look at some properties of the turbulent motion itself. A number of scaling laws apply to turbulent motion; the standard deviations of horizontal and vertical wind speed, σ_U and σ_W, when made dimensionless with the friction velocity, u_*, are functions of stability, ζ, only; this also applies to the standard deviation of the potential temperature, σ_Θ, when made dimensionless with the turbulent temperature scale, θ_*. For stable conditions the relations are simple: the forementioned quantities are constants, i.e. not depending on stability. Figure 1 shows these relations for the VU–observations. The relations in this figure can be compared directly to those listed in the King–paper (1990); this comparison indicates that the scaling relations are not influenced by the presence of a terrain slope.

For the calculation of the ϕ–relations vertical gradients of profile quantities are required (see relation 1). These are obtained by fitting the relation

$$C(z) = c_1 + c_2 z + c_3 \ln z \tag{2}$$

to the profiles, using the measurements at 5 levels. It appeared that most profiles were well–represented by this relation.

Besides looking at the ϕ–functions, one can also look at the socalled ψ–functions, which are defined thru

$$\psi_c \equiv \int_{\zeta_o}^{\zeta} d\zeta' \{1 - \phi_c(\zeta')\}\zeta'^{-1} \tag{3}$$

where one usually can take ζ_o equal to zero. With this definition we have

$$\frac{\kappa}{c_*} C = \ln \frac{z}{z_o} - \psi_c(\zeta). \tag{4}$$

Figure 2 shows ϕ_M and $-\psi_M$ as calculated with the VU-data (taking a value of 10^{-3} m for z_o). The results in this figure are obtained by dividing the range of ζ–values into a number of 'bins'; the values shown in the diagrams are the medians calculated for these bins. The lines drawn are based on the ϕ_M–functions

$$\phi_M = 1 + \alpha_M \zeta \tag{5}$$

with α_M equal to 7.6, and

$$\phi_M = 1 + \alpha_M \zeta (1 + \alpha_M \zeta / a)^{(a-1)} \tag{6}$$

(see Högström, 1988), with α_M equal to 5 and a equal to 0.8. Taking the scatter into account we get results for ϕ_M in good agreement with the ETH–observations (Forrer and Rotach, 1994). The results for $-\psi_M$, on the other hand, pose a problem. If the linear relation 5 holds, then $-\psi_M$ must have the same slope as ϕ_M. It clearly has not. At present this result is not understood and is being looked into.

The results for ϕ_H and $-\psi_H$ are presently not shown because the results are too noisy to reach any meaningful conclusions at this stage.

REFERENCES

1. Forrer, J. and Rotach, M., 1994: *Comparison between measured and calculated turbulent fluxes*. Mass balance and related topics of the Greenland ice sheet, Report of the 4th workshop. J.J.M. van der Meer and R.J. Braithwaite (editors), 122pp.

2. Henneken, E.A.C., 1994: *on the use of the profile method on the Greenland ice sheet*. Mass balance and related topics of the Greenland ice sheet, Report of the 4th workshop. J.J.M. van der Meer and R.J. Braithwaite (editors), 122pp.

3. Högström, U., 1988: *Non–dimensional wind and temperature profiles in the atmospheric surface layer*. Boundary–Layer Meteorol., **42**: 55–78

4. King, J.C., 1990: *Some measurements of turbulence on an antarctic ice shelf*. Q. J. R. Meteorol. Soc., **116**: 379–400.

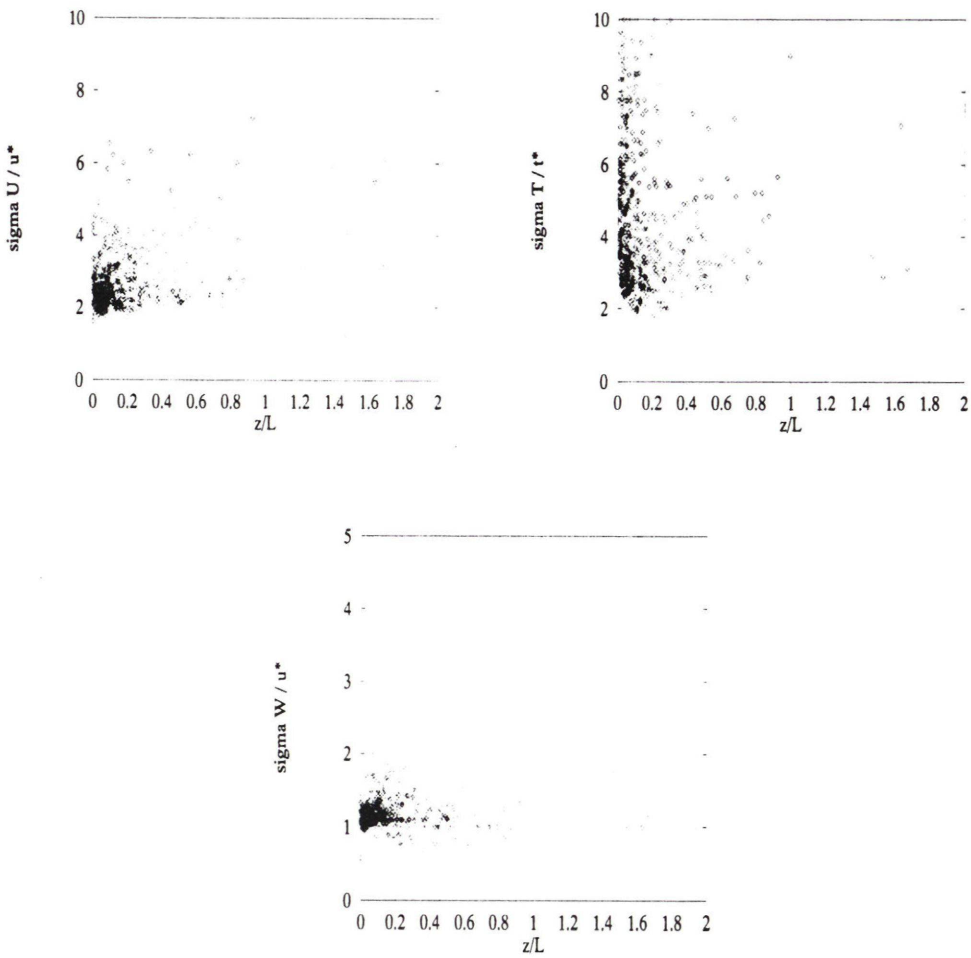

Figure 1: *Upper left panel:* σ_U/u_* *as function of stability. Upper right panel: same for* σ_W/u_*. *Lower panel: same for* σ_Θ/θ_*. *All relations are for the eddy correlation system at the nominal height of 4 meters above the surface*

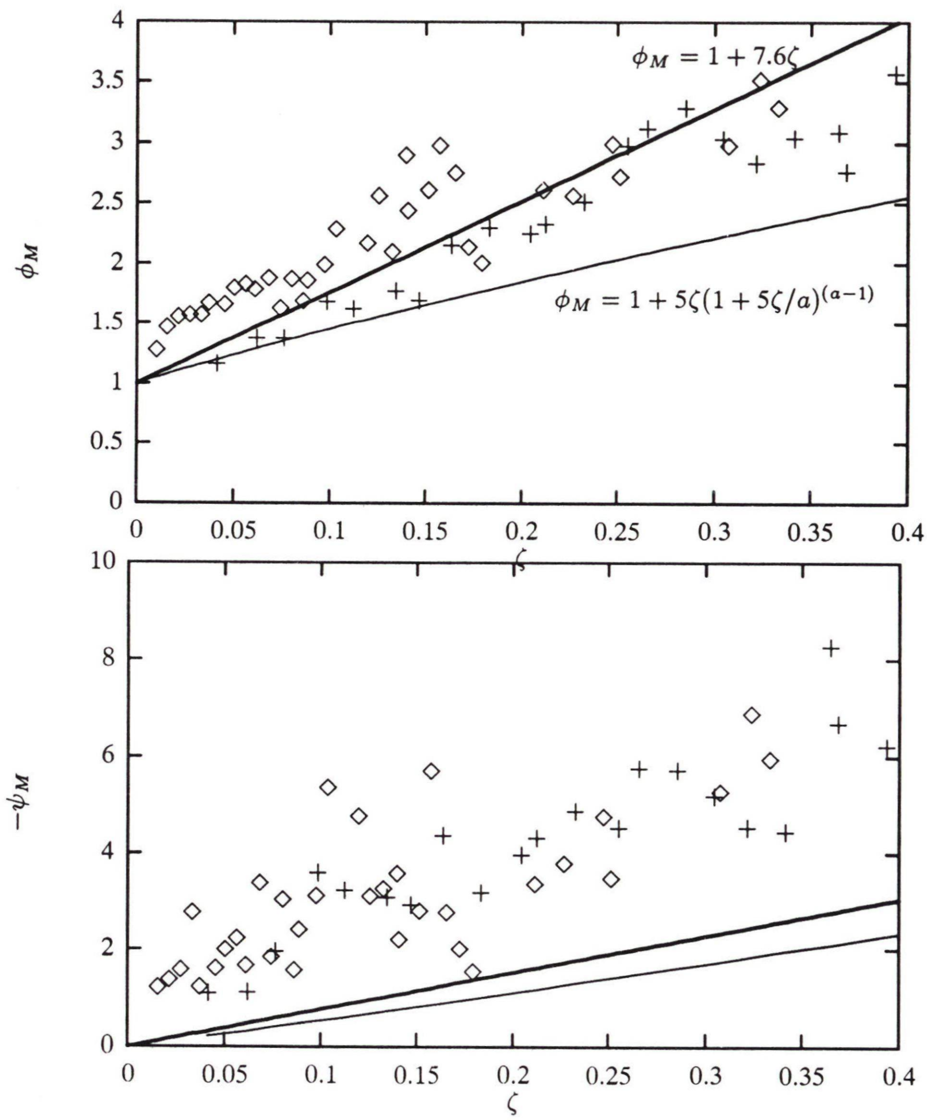

Figure 2: *Upper panel: ϕ_M as function of stability. Lower panel: $-\psi_M$ as function of stability. The ◇–symbol refers to the eddy correlation system at the nominal height of 4 meters, the +–symbol to the system at 13 meters. The drawn lines refer to ϕ-relations indicated in the top panel*

Page intentionally left empty in printed version

CALCULATING EXCHANGE COEFFICIENTS FROM ENERGY BALANCE CONSIDERATIONS

J. Oerlemans

Institute for Marine and Atmospheric Research
Utrecht University
Princetonplein 5, 3584 CC UTRECHT, The Netherlands

Extended abstract

Energy balance models used to simulate glacier mass balance (e.g. Van de Wal and Oerlemans, 1994) require a reliable parameterization of the turbulent fluxes of heat and water vapour. So far, direct observations of turbulent fluxes on glaciers (by eddy correlation techniques) have been very limited and data sets are not yet adequate to verify thoroughly existing theoretical schemes (the profile method, in particular). While better results on this matter are expected in the coming years, it seems worthwhile to use alternative methods to estimate exchange coefficients.

One such method is to calculate the total turbulent exchange as a residual in the energy balance. This requires accurate measurements of the radiation balance, the subsurface energy flux and the amount of energy used for melting. In practice, sufficient accuracy can only be obtained over longer periods of time, during which the melt proces is simple (negligible subsurface heat flux, no internal accumulation, air temperature above the melting point most of the time).

For three sites (4, 5 and 6, see Figure 1) along the GIMEX-transect these conditions are met, and an attempt has been made to estimate the turbulent exchange by closing the energy budget. The period considered is Julian days 161 - 205 1991 (see Oerlemans and Vugts, 1992 for an overview of the experiment). Available are measured ablation, air temperature, wind speed, absorbed solar radiation, humidity at site 4. Some other quantities were not used because the measurement errors were considered too large.

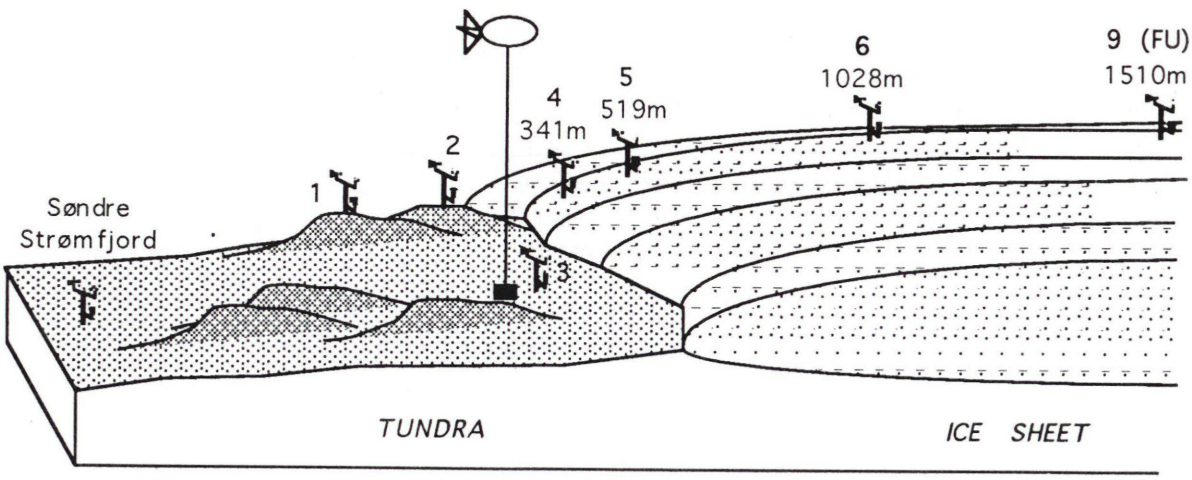

Figure 1. Set-up of the GIMEX-91 transect.

To calculate the longwave radiation balance, the parameterization of Konzelmann et al. (1994) has been used. First of all, cloudiness is estimated from the difference between theoretical clear-sky global radiation and the actually observed global radiation (the result for site 5 is shown in Figure 2).Estimated cloudiness, measured air temperature and vapour pressure is than used to calculate the long wave balance. Vapour pressure was only measured at sites 4 and 9. Values for sites 5 and 6 were obtained by interpolation on the relative humidity.

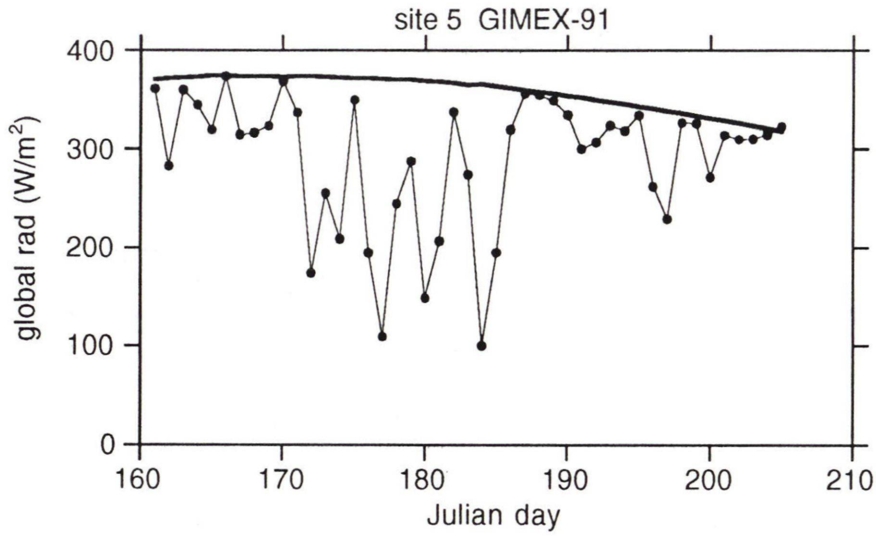

Figure 2. Theoretical clear-sky global radiation (including the effect of water vapour and variations in surface albedo through multiple reflection between surface and atmosphere) and measured global radiation at site 5.

Now the exchange coefficient K is defined in:

$$E = R + K\,v\,(T - T_m) + K\,\frac{L_v}{c_p}\,v\,(q - q_{sat})$$

Here E is the energy balance, R the net radiation, and the last two terms the turbulent flux of enthalpy and latent heat, respectively. K is the exchange coefficient (taken equal for sensible and latent heat !), v wind speed, T air temperature, T_m surface temperature (melting point), L_v latent heat of melt, c_p specific heat, and q specific humidity. The energy balance can be equated to the measured melt, including a correction for the vapour transport. The resulting equation can be averaged over the entire period and then be solved for K. The procedure is straightforward and will not be discussed here.

One can either solve for <Kv> or for <v>, depending on how one wants to define the exchange coefficient (< > represent a mean value over the entire period). Figure 3 shows the results. In spite of the large error bars, the data suggest that the exchange coefficient decreases significantly when going up the ice sheet.

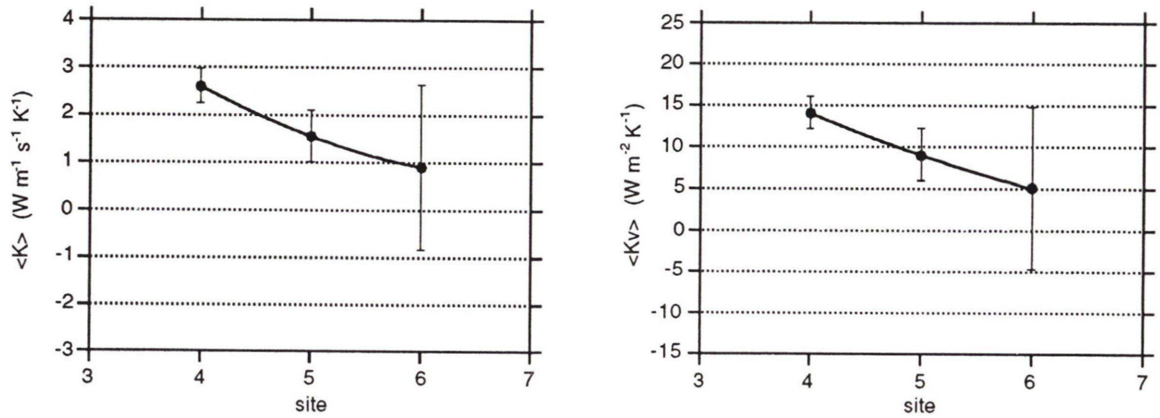

Figure 3. Exchange coefficients calculated by closing the energy balance for sites 4, 5 and 6. The error bars result when the uncertainty in the energy balance is assumed to be 6 %. This gives a very large error for site 6, because the turbulent fluxes are small here.

References

J Oerlemans and H F Vugts (1992): A meteorological experiment in the melting zone of the Greenland ice sheet. *Bulletin of the American Meteorological Society* **74**, 355-365.

R S W van de Wal and J Oerlemans (1994): An energy balance model for the Greenland ice sheet. *Global and Planetary Change* **9**, 115-131.

T Konzelmann, R S W van de Wal, W Greuell, R Bintanja, E A C Henneken and A Abe-Ouchi (1994): Parameterization of global and longwave incoming radiation for the Greenland ice sheet. *Global and Planetary Change* **9**, 69-78.

Page intentionally left empty in printed version

RESPONSE OF THE LONGWAVE RADIATION TO CLIMATE CHANGE

Antoon Meesters
Institute of Earth Sciences
Vrije Universiteit
Amsterdam, Netherlands

Parameterization of the incoming longwave radiation L↓ is important in models to study the response of the Greenland ice sheet to global warming. It is well known that the clear sky radiation can be calculated fairly accurately from the profiles of temperature and moisture. However, in current models it is often assumed that L↓ can be parameterized as

$$L \downarrow = \varepsilon_{eff}\, \sigma\, T_h^4 \qquad (1),$$

in which T_h is the absolute temperature at reference height, σ is the Stefan-Boltzmann constant and ε_{eff} is an effective emissivity. This emissivity is expected to depend on location and altitude, as well as on the moisture content. However, even for a given place, measured values for $L\downarrow/\sigma T_h^4$ are scattered around some average, so that (1) will yield only an expectation value or a climatic mean. This scatter is mainly caused by the fact that the T-profile cannot be determined uniquely from T_h.

Due to this scatter, the empirical validation of (1) is difficult, though some effort has been spent on this in the past. Hence, the acceptance of (1) for use in models is essentially based on theoretical expectations. The main point is that if the air flowing over the ice sheet is adapted to the surface up to a sufficiently great height, there should be a narrow relation between T_h and the whole profile.

The present research is intended to test the validity of (1). This is done by considering the validity of this relation for the results of two runs with the two-dimensional atmospheric/ice surface model that was developed for the Greenland ice sheet margin (Meesters et al. 1994, Meesters 1994). The first run (run A) is a simulation of the conditions for a clear day in summer. The second run (run B) differs from the former one in that the *initial* air temperatures are everywhere 5 K higher. As the simulations proceed, the air adapts to the ice surface, which cannot become warmer than 0 °C. Hence, in the surface layer, profiles of great static stability are generated, especially for the warm run B. Figure 1 shows the T-profiles, averaged over the second day of the simulations, for the top of the ice sheet (H), a location near the margin (L), and a location for which the surface altitude is halfway (M).

It is seen that the rise of T_h, from A to B, is considerably smaller than the rise of the temperatures at higher levels. Moreover, the profiles are very stable, and their stability increases from run A to run B. L↓ will rise according to some weighted average of T_h^4 and T^4 at higher levels, so that its rise will be stronger than the rise of T_h^4. In figure 2, the relative rise (A → B) of T_h^4 and L↓ is depicted. Especially in the vicinity of the ice margin, where the inhibition of the rise of the mean surface temperature is strongest, the discrepancy appears to be quite large. Equation (1) underestimates the growth of L↓ by a factor of 2-3 there.

Though only two runs have been considered, it is clear from the discussion that the rise of L↓

in response to warming is *systematically* underestimated by (1). The error in L$\downarrow$ has important consequences in practice, since the net longwave radiation tends to cancel the net shortwave radiation during the melting season, so that large errors in the net allwave radiation are likely to result. It is concluded that the use of (1) is better avoided, and that a multi-level calculation of L$\downarrow$ should be used in models to determine the response of the ice sheet to climate change.

references

Meesters, A.G.C.A. (1994): Dependence of the energy balance of the Greenland ice sheet on climate change: Influence of katabatic wind and tundra. Quarterly Journal of the Royal Meteorological Society 120, 491-517.

Meesters, A.G.C.A., E.A.C. Henneken, N.J. Bink, H.F. Vugts and F. Cannemeijer (1994): Simulation of the atmospheric circulation near the Greenland ice sheet margin. Global and Planetary Change 9, 53-67.

figure captions

1) Daily-averaged temperature profiles, for low (L), middle (M) and high (H) surface altitude, for run A (solid) and B (dashed).

2) Relative increase of longwave radiation (LW) and relative increase of the fourth power of the reference height temperature (T_h^4), from run A to run B.

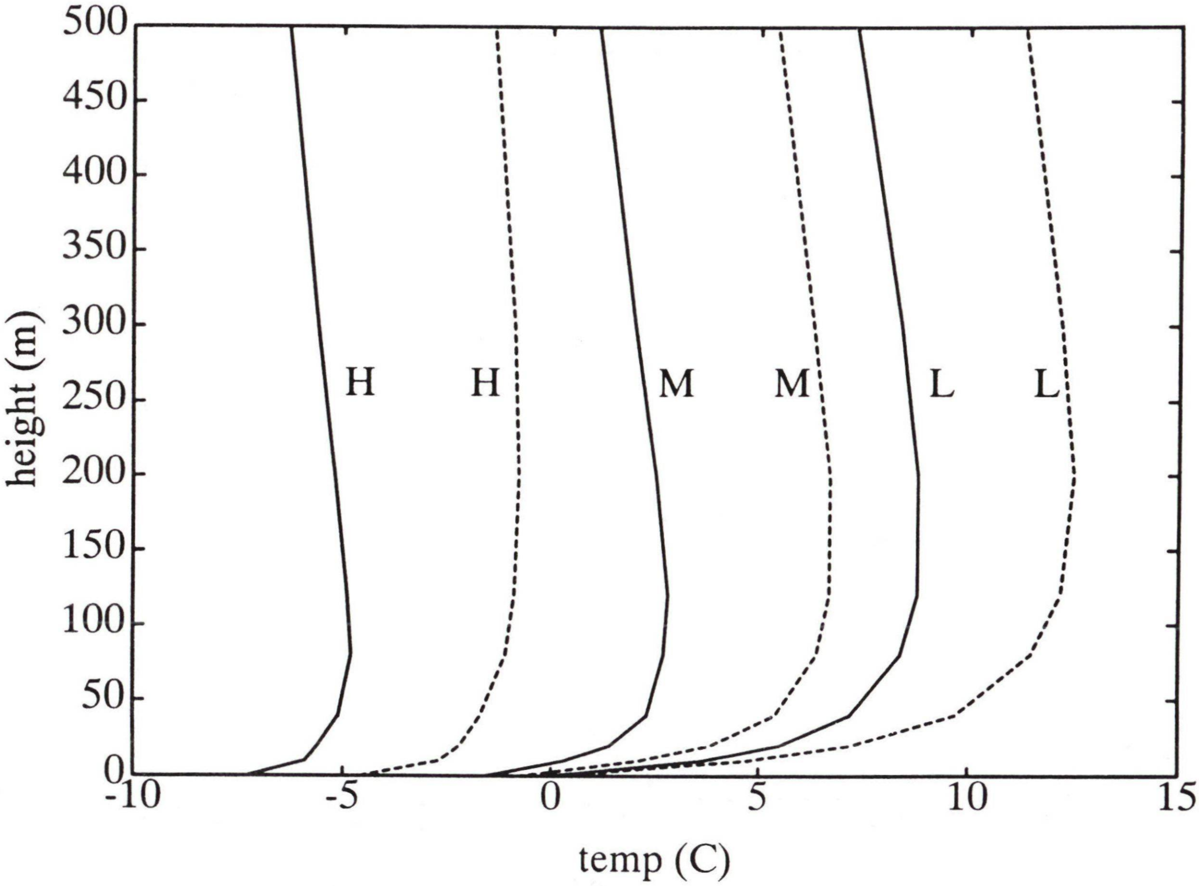

fig. 1: Daily-averaged temperature profiles, for low (L), middle (M) and high (H) surface altitude, for run A (solid) and B (dashed).

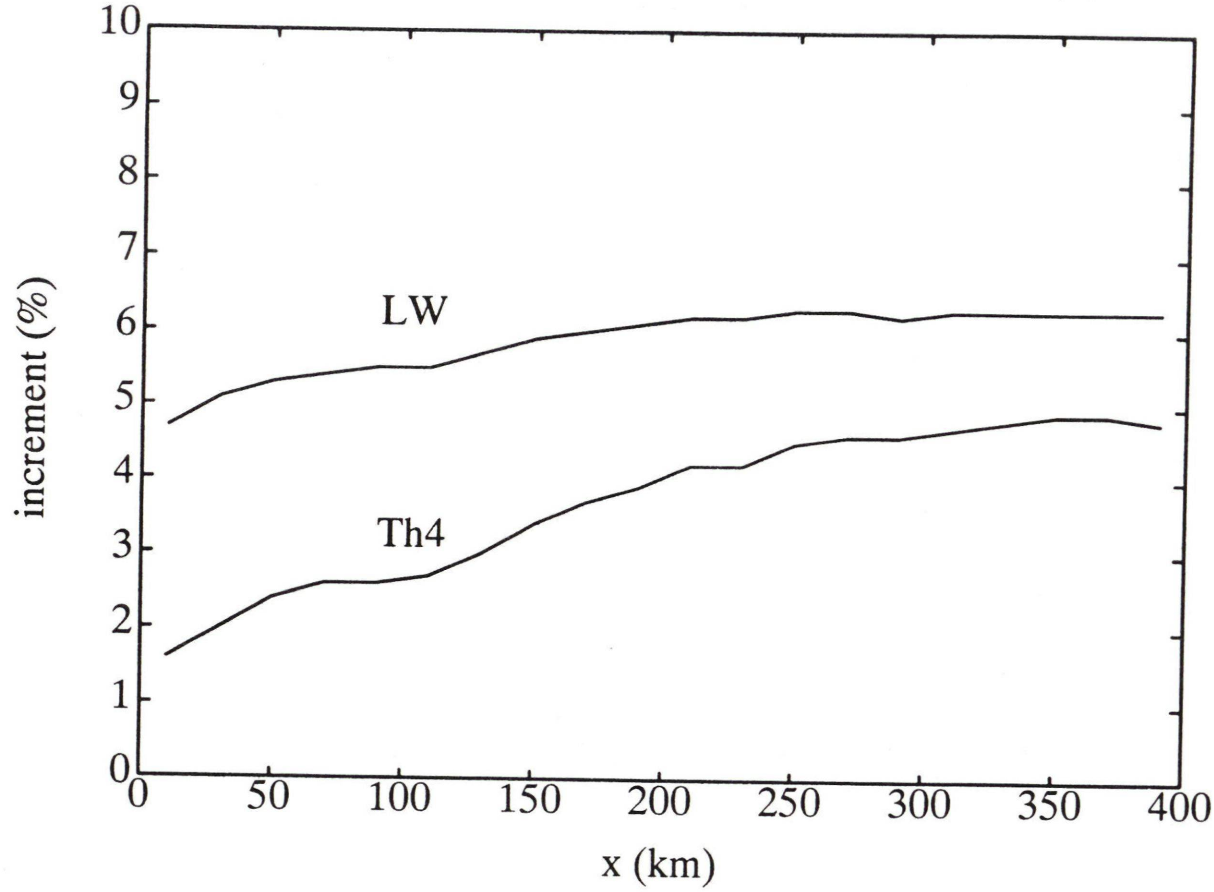

fig. 2: Relative increase of longwave radiation (LW) and relative increase of the fourth power of the reference height temperature (T_h^4), from run A to run B.

A POSSIBLE CHANGE IN MASS BALANCE OF GREENLAND AND ANTARCTIC ICE SHEETS IN THE COMING CENTURY

Atsumu Ohmura and Martin Wild
Department of Geography
Swiss Federal Institute of Technology
Zurich, Switzerland

Abstract

A high resolution GCM is found to simulate precipitation and surface energy balance of high latitudes with so far unprecedented accuracy. This opens new possibilities to investigate the future mass balance of polar glaciers and its effect on sea-level. The surface mass balance of the Greenland and the Antarctic ice sheets is simulated using the ECHAM 3/T-106 GCM experiment. The experiment is based on the five year equilibrium test based on the ECHAM 1/T-21 transient experiment which provided the boundary conditions for the present and the year 2050 when carbon dioxide is expected to be doubled. A comparison of the two experiments over Greenland and Antarctica shows to what extent the reactions of the mass balance on the two largest glaciers of the world can differ. On Greenland one sees a slight decrease in accumulation and a substantial increase in melt, while on Antarctica a large increase in accumulation without melt is projected. The change in the combined mass balance of the two continents is almost zero. The sea level change of the next century can be affected more effectively by the thermal expansion of the sea water and the mass balance of smaller glaciers outside of Greenland and Antarctica.

Introduction

The glacier mass balance is considered to play a significant role in influencing global sea-level, besides other potential mechanisms such as the thermal expansion of sea water and the earth's crustal movements. The ice sheets on Greenland and Antarctica are considered especially important because of their large surface areas and ice volumes. In the short term, glacier total mass balance is influenced more by the surface area than the volume. The Greenland and the Antarctic ice sheets occupy 1.75 and 13.92 x 10^6 km^2, respectively, corresponding to 10.9 and 85.7 % of the total global glacier surface (Haeberli et al., 1989). Under the concept of an ice sheet, in the context of this work, small glaciers on Greenland and Antarctica are also included. In the long term, ice volume becomes important. Greenland (2.65 x 10^6 km^3) and Antarctica (30.11 x 10^6 km^3, Drewry, D.J. ,1983) make up 99.7 % of the total global glacier ice volume (Ohmura, 1987). These ice volumes are equivalent to the sea level changes of 6.7 m and 67.9 m, respectively, without considering the effect of hydro-isostasy. The combined contribution of all other glaciers to the sea level increase is only about 27 cm. This consideration places both ice sheets at the front of importance in evaluating the causes of the sea-level change. Simulation of the mass balance change of the ice sheets under the near future climate has so far been hampered by the difficulty in estimating future precipitation on glaciers. In the past, the future mass balance of the ice sheets was calculated by either assuming certain scenarios or keeping the precipitation constant. In recent years, however, it has become possible to simulate future precipitation because of the transient experiments with GCMs. The problem of coarse grids, a necessary characteristic for a long range transient experiment, can be overcome by driving a high resolution GCM for a limited duration of time, using the boundary conditions provided by the transient experiment. This method is considered to be superior to a mere nesting of a meso-scale model, because the high resolution GCM captures smaller scale structures more effectively on the global scale.

GCM experiments

In the present investigation, the ECHAM 1/T-21 100 years experiment with the IPCC CO_2 Scenario-A, business as usual (Cubasch et al., 1992), was used to drive ECHAM 3/T-106 for 6 years for the present and the time when the doubled CO_2 is expected. The latter is hypothesised to be reached between year 2045 to 2050. The transient experiment was carried out fully coupled with the ocean. The statistics made from 5 years data from the second to the sixth year was then used to represent the climate. The present climate was simulated with the observed boundary conditions of the mid-1980s. The simulation of the present climate was used to test the capability of the high resolution GCM against the observed climate and also to compare the future climate (Arpe et al., in press). In view of the high degree of accuracy of this experiment in simulating the precipitation distribution, it is judged appropriate to used this method to compute the future mass balance of Greenland and Antarctica and to assess their contributions for the sea-level change. At this stage the time domain considered is one century. This rather short time domain allows us to consider the mass balance problem purely as the surface exchange phenomenon, without involving dynamic aspects such as the changes in geometry and calving. The dynamic effects become important, when the ice sheet is coupled with the climate model for durations longer than 1000 years(Abe-Ouchi, 1993).

Present and future precipitation

The capability of ECHAM 3/T-106 to simulate the present precipitation can be seen in Figs. 1, 2 and 3. The observed annual precipitation distributions are based on accumulation studies and long-term meteorological observations (Giovinetto et al., 1990; Ohmura and Reeh, 1991). The model-computed precipitation maps reveal a high degree of success in simulating the major geographical patterns of precipitation and also the absolute values. For Greenland, the occurrence of the largest precipitation on the southeast coast, the sharp latitudinal gradient on the southwest coast, the zone of high precipitation on the west slope culminating in the maximum north of Melville Bay and the driest area north of Summit are well represented.

On Antarctica the main features are well captured (Fig. 3); they are generally drier East Antarctica, wetter West Antarctica with a sharp gradient near the coasts, lower precipitation on Ross and Filchener ice shelves and a distinctive contrast between the east and west coasts of the Antarctic Peninsula On a much more regional scale, the ECHAM 3/T-106 experiment captures such fine features as larger precipitation gradients from the coast to the interior as observed in Princess Martha Coast and Enderby Land. A smaller gradient between these two regions around Prince Harald Coast is also clearly represented. It is also remarkable to see that the zone of maximum precipitation in East Antarctica around Wilkes Land is successfully simulated. Both for Greenland and Antarctica, the model computations give on an average 15 and 5 cm W.E. more precipitation than the observations, respectively. Regarding this small difference one can not simply conclude an overestimation in the computation, as the observed distributions are more likely underestimated. The conventional precipitation measurements are prone to underestimation (Sevruk, 1993). Further underestimations are caused through the mass loss by drifting snow off the coastal line and the evaporative loss from the snow cover, both of which are not included in the pit and core observations. A comparison of the T-106 with the other coarser grid experiments based also on the same ECHAM 3 indicates that by increasing the horizontal resolution, the precipitation is probably the most improved element. Globally seen even the T-106 presents a serious underestimation of the summer precipitation for the mid-latitudes. The cause of this underestimation is known to be the difficulty to produce precipitation from convective clouds. The success of the precipitation simulation for the polar regions is mainly owing to the fact that the precipitation on Greenland and Antarctica is not derived from convective clouds.

Under the doubled CO_2 climate, annual total precipitation (Fig. 4) over Greenland increases by about 30 mm/y in most regions, except for the coastal zone in the southeast and on the northwestern slope around Melville Bay. The significant decrease in the southeast Greenland where presently the largest accumulation is observed, occurs throughout the year owing to the weakening of the icelandic low.

Somewhat weak decrease on the west slope is observed only during warmer months and owing to the weakening of the eastward migrating cyclones from the Canadian Arctic. The regions with a large increase in precipitation are expected in the southwest and northeastern region of the ice sheet. Averaged for the entire ice sheet the change is a decrease by 2mm/y, mainly owing to the drastic decrease in the southeast coast. The solid precipitation (Fig. 5), however, decreases by 12 mm/y owing to the temperature increase. This is an important difference of the change in precipitation for Greenland in comparison with that for Antarctica.

For Antarctica all precipitation is accounted for as solid both for the control and the doubled CO_2 cases. In Antarctica an increase exceeding 100 mm/y appears in Victoria Land, Ellsworth Land, Marie Byrd Land and Enderby Land (Fig. 6). These are generally the regions where annual precipitation is larger in the present climate. Other regions with large precipitation under the present climate such as Princess Martha Coast and Adélie Coast, however, receive a modest increase of about 50 mm/y. The increase in the interior region of East Antarctica remains small with 5 mm/y. Ross Ice Shelf receives a moderate increase of 40 mm/y, while the increase on Filchner Ice shelf remains small at 10 mm/y. Generally the increase in West Antarctica is larger, receiving 45 mm/y, than in East Antarctica where the regional average increase is only 20 mm/y. Averaged for entire Antarctica, the increase is substantially large at 25 mm/y.

Present and future air temperature

As Figs. 7 and 8 show, the simulation capability of the present experiment for air temperature is extremely good. In detail, it can be said that for Greenland there is a small tendency of overestimation for the interior and underestimation for marginal zones throughout the year. The degree of these over- and underestimations is about 1 ^{o}C. The error is the smallest for altitudes of about 2'000 m a.s.l.. For Antarctica, small overestimations are seen for the Antarctic Peninsula and Ross and Filchiner Ice shelves. Generally the agreement with the observation is slightly better for East Antarctica. The simulation of the annual mean temperature of the top of Dome A comes within 1 ^{o}C of the observation.

After the doubling of CO_2, both for Greenland and Antarctica, the annual mean temperature increases by 2 ^{o}C near the margin and by 4 ^{o}C near the top of the ice sheets. An interesting aspect of the seasonal features is the altitude dependent variations in temperature. It turns out that the often mentioned larger temperature increase is a characteristics of winter for the lower elevation. The temperature increase in the interior of both ice sheet seems to be similar in all seasons. The most important feature of the temperature increase on the ice sheets is the movement of -2 °C isothermal line for the three summer months. The summer temperature of -2 °C is the minimum temperature where the mass loss due to the melt can be expected as is presented in Fig. 9. On the Greenland ice sheet -2 °C isothermal line for JJA appears presently at 1'500 and 750 m a.s.l. in southern and northern Greenland, respectively. The vertical shift of the line is 500 m in northern Greenland, while it is only 250 m in the south (Fig. 10). Because the surface gradient of the ice sheet is smaller in Mid- and North Greenland where the surface area is larger, this regional trend contributes to a substantial increase in the melt. On the Antarctic ice sheet, the -2 °C isothermal line still remains outside of the ice sheet margin, even after the CO_2 is doubled. This temperature distribution is interpreted that the Antarctic ice sheet will not experience significant melt before the mid-21st century.

Computation of the melt

The computation of the melt on the Greenland ice sheet was done by two method. The first is based on the surface energy balance. Since ECHAM 3 does not compute the melt of snow and ice on glaciers, the sum of net radiation, sensible and latent heat fluxes is first computed. This is the quantity which can be equated to the sum of the subsurface heat conduction and the latent heat of fusion. The comparison of the computed fluxes and those observed is presented in Fig.11. The comparison was made for ETH Camp using the 1991 summer observations. Details of the observational procedures are presented in Ohmura et al.(1992). The simulation capability of the present numerical experiment can be judged as practically good enough for the computation of the melt. The annual melt is assumed to be equal to the sum of the three components mentioned above, as the annual total subsurface heat flux can safely be assumed as zero.

The second method for the melt computation is based on the observed relationship between the annual loss of mass due to the melt and the mean air temperature for the summer three months of June, July and August as is presented in Fig. 9. Based on this relationship, the increase in the ablation was estimated, using the computed temperature distributions for the present and the year 2050.

Present and future mass balance

For Greenland the increase in the mass loss due to the melt was calculated for the region in lower altitudes than the JJA mean isothermal line of -2 °C for the year 2050 stage. The components of the mass balance for Greenland are presented in Table 1 with respect to the present observation, and this numerical experiment for the control and the doubled CO_2 cases. The energy balance method gives an annual increase in melt of 197 mm/y, while the temperature-based approximation yields 208 mm/y. It is remarkable that the two very different methods give an almost identical increase in the melt. The change in the mass balance on Greenland is characterised by a small decrease in mean annual specific accumulation (12 mm/y) and by a substantial increase in the mean specific melt (197 - 208 mm/y). This calculation gives an annual total increase in the ablation of 365 - 384 km^3. The new mass balance for the Antarctic ice sheet is solely based on the increase in solid precipitation which projects an annual increase in accumulation of 348 km^3 . It is important to note that the reaction of the two existing ice sheet towards the climate warming is extremely different. As Greenland discharges water to the oceans, Antarctica takes it up. The difference of the mass balance for Greenland and Antarctica is between 17 and 36 km^3 which becomes an annual increase of the ocean water, corresponding to the sea-level rise of 0.05 to 0.10 mm/y. The most important result of the present investigation is the prospect that the net contribution of glaciers in Greenland and Antarctica to the sea-level change in the mid-21st century is practically zero.

Conclusion

The mass balance of the Greenland and Antarctic ice sheets for the period of the IPCC Scenario-A doubled CO_2 was simulated in the ECHAM 3/T-106 which was driven by the results of the atmosphere/ocean coupled ECHAM 1/T-21 100 year transient experiment. It was found that Greenland showed a mean specific balance of -209 to -219 mm W.E., while Antarctica gave +25 mm W.E., resulting in the annual sea-level rise of 0.05 to 0.10 mm/y. For some time in the future the mass balances of the two largest glaciers may compensate for each other. This result demonstrates that the role of thermal expansion and mass balance of glaciers not in Greenland and Antarctica may play a significant role in controlling the future sea-level. A possible significance of small glaciers for the global sea-level change was advocated by Meier (1984).

Acknowledgement

The authors express deep feelings of thanks to colleagues at Max-Planck-Institut für Meteorologie in Hamburg for introducing us into the area of GCM experiences. In particular thanks are due to Prof. L. Bengtsson, Dr. E. Reckner and Dr. K. Arpe. The present work was financed by the Swiss National Science Foundation, through Grant No. 4031-032250 and No.5001-35179 for climate modelling. The Greenland field experiment was financed by the Swiss National Science Foundation, through Grant No. 20-29822690 and 20-3264991 and an ETH research fund for ETH Greenland Expedition.

References

Abe-Ouchi, A.,1993. Ice Sheet Response to Climate Changes - A Modelling Approach. Zürcher Geographische Schriften No. 54, ETH, Zurich, 134pp.

Arpe, K., Bengtsson, L., Dümenil, L., and Röckner, E., in press. The hydrological cycle in the ECHAM 3 simulations of the atmospheric circulation. in Desbois, N. and Desalnand (Eds.), Global Precipitations and Climate Change, NATO ASI Series, Vol.I26, 361-377.

Cubasch, U., Hasselmann, K., Höck, H., Maier-Reimer, E., Mikolajewicz, U., Santer, B., and Sausen, R., 1992. Time-dependent greenhouse warming computations with a coupled ocean-atmosphere model. Climate Dynamics, Vol. 8, 55-69.

Drewry, D.J.(Ed.), 1983. Antarctica: Glaciological and Geophysical Folio. Scott Polar Research Institute, Cambridge.

Giovinetto, M.,Waters, N.M., and Bentley, C.R., 1990. Dependence of Antarctic surface mass balance on temperature, elevation, and distance to open ocean. Jour.Geophys.Res., Vol.95, No.D4, 3517-3531.

Haeberli, W., Bösch, H., Scherler, K., Ostrem, G.,and Wallén, C.C., 1989. World Glacier Inventory Status 1988. IAHS(ICSI), UNEP, UNESCO, ETH, Zurich.

Meier, M.F., 1984: Contribution of small glaciers to global sea level. Science, Vol.226, No.4681, 1418-1421.

Ohmura, A., 1987: New temperature distribution maps for Greenland. Z.Gletscherkd.Glazialgeol., Vol.23, No.1, 1-45.

Ohmura, A., 1987. Heat budget of the climate system between the Last Glacial Maximum and the Present. Bull.Dept.Geogr. Univ. Tokyo, No.19, 21-28.

Ohmura, A., and Reeh, N., 1991, New precipitation and accumulation distribution maps for Greenland. Jour.Glaiol., Vol.37, No.125, 140-148.

Ohmura, A., Steffen, K., Blatter, H., Greuell, W., Rotach, M., Stober, M., Konzelmann, T., Forrer, J., Abe-Ouchi, A., Steiger, D., and Niederbäumer, G., 1992. Energy and Mass Balance During the Melt Season at the Equilibrium Line Altitude, Paakitsoq, Greenland Ice Sheet. Progress Report 2, ETH, Zurich., 94pp.

Ohmura, A., Konzelmann, T., Rotach, M., Forrer, J., Abe-Ouchi, A., and Toritani, H., 1994. Energy balance for the Greenland ice sheet by observations and model computation. IAHS Publication.

Sevruk, B., 1993. Checking precipitation gauge performance. In Couling, S.(Ed.). Measurement of airborne pollutants. Butterworth Heinemann, Oxford, 85-107.

Caption for figures

Fig. 1: Comparison of the computed(right) and observed(left) annual total precipitation for Greenland. Source for the observed is Ohmura and Reeh(1991).

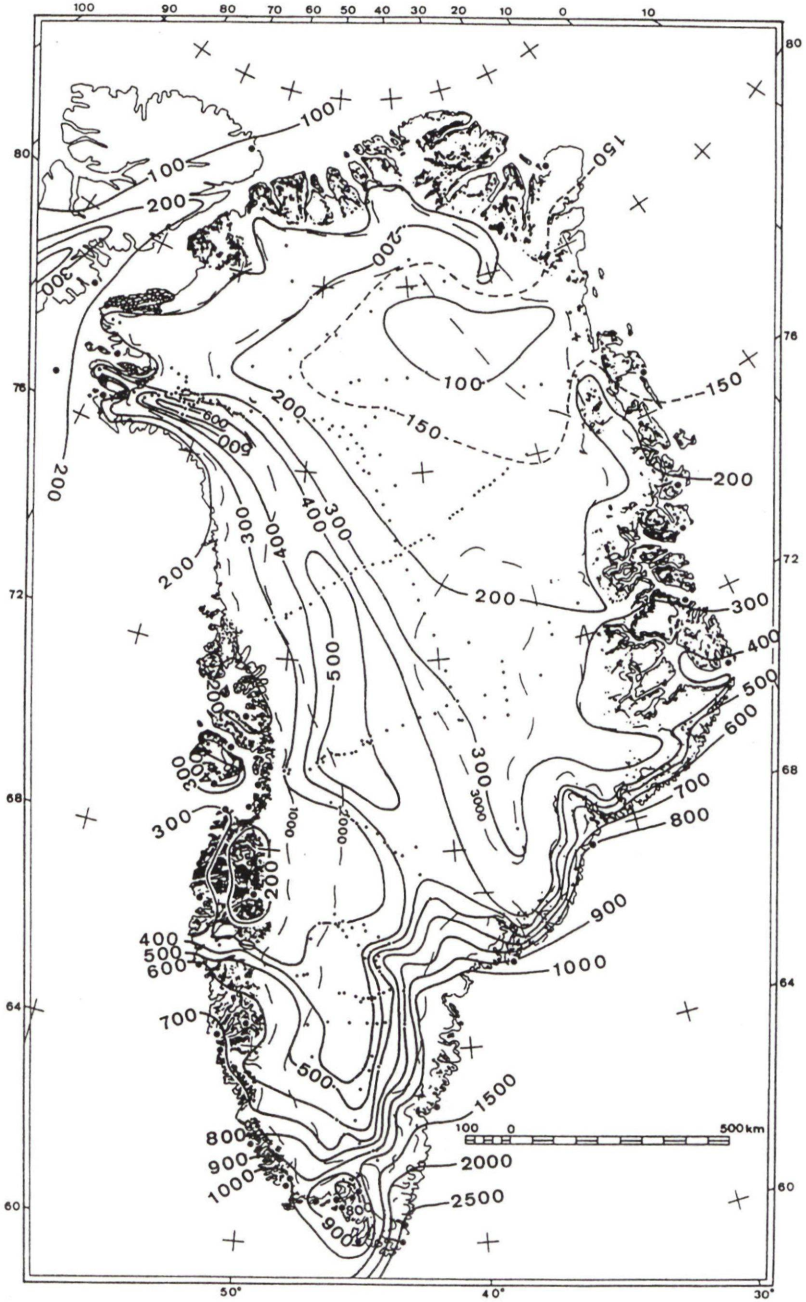

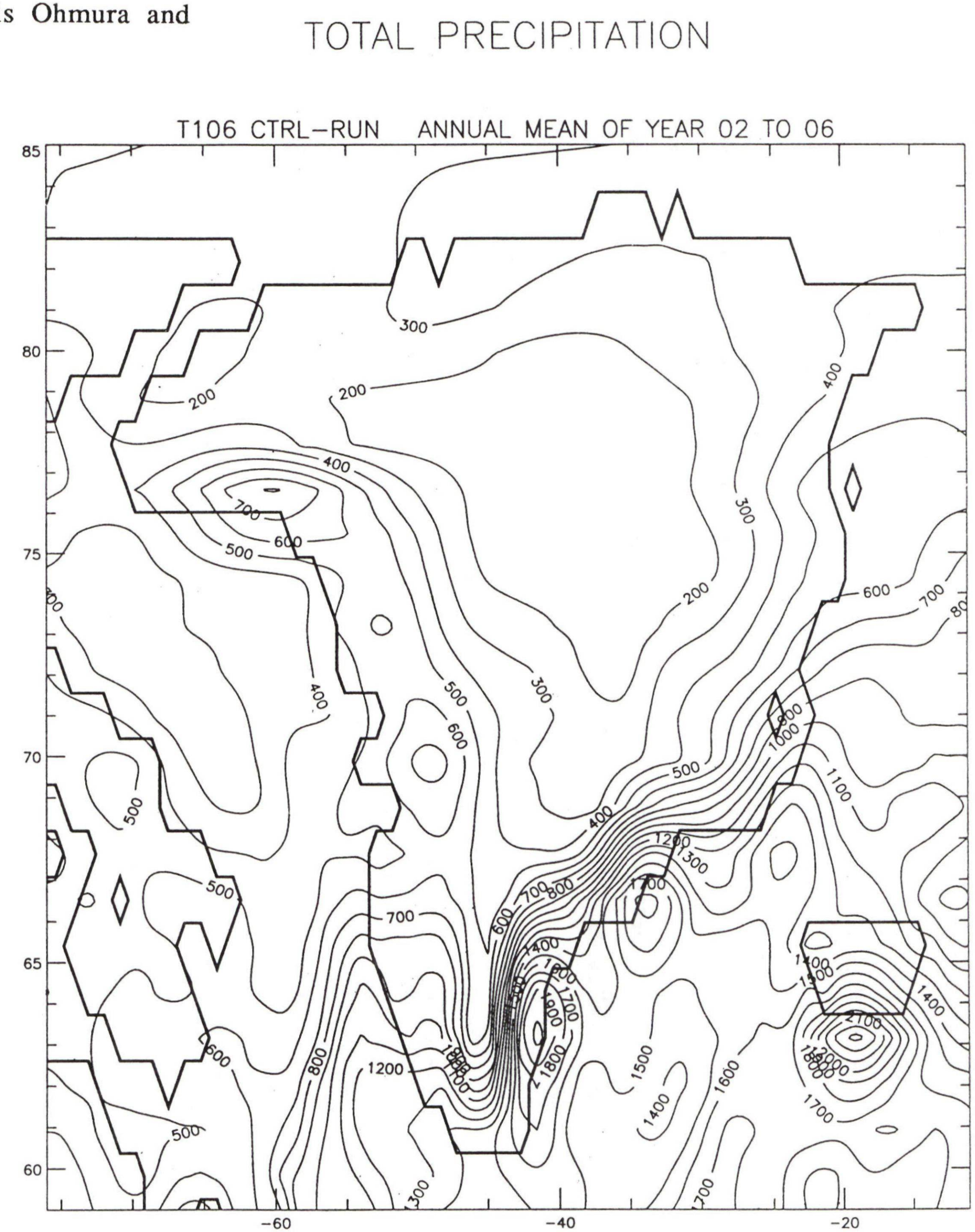

Fig. 2: Comparison of the computed (right) and observed (left) annual solid precipitation or accumulation. Source for the observed is Ohmura and Reeh (1991).

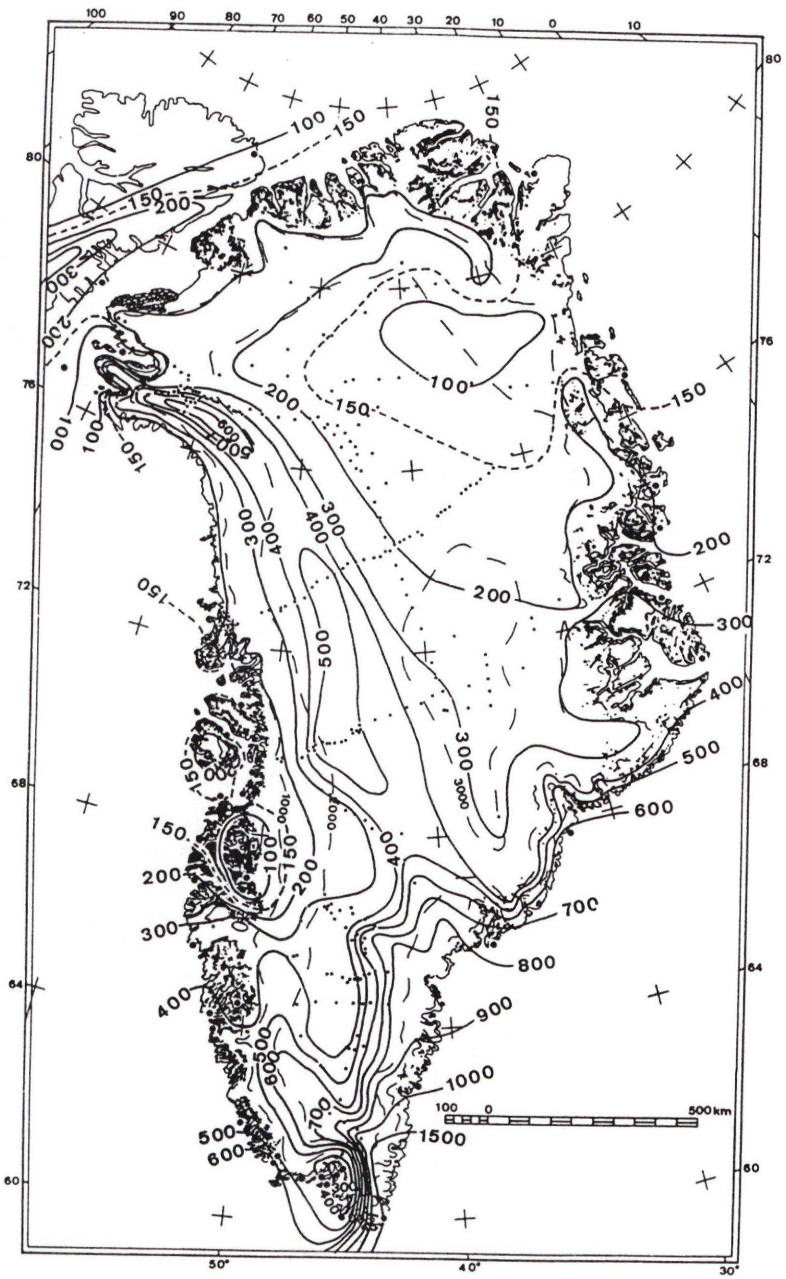

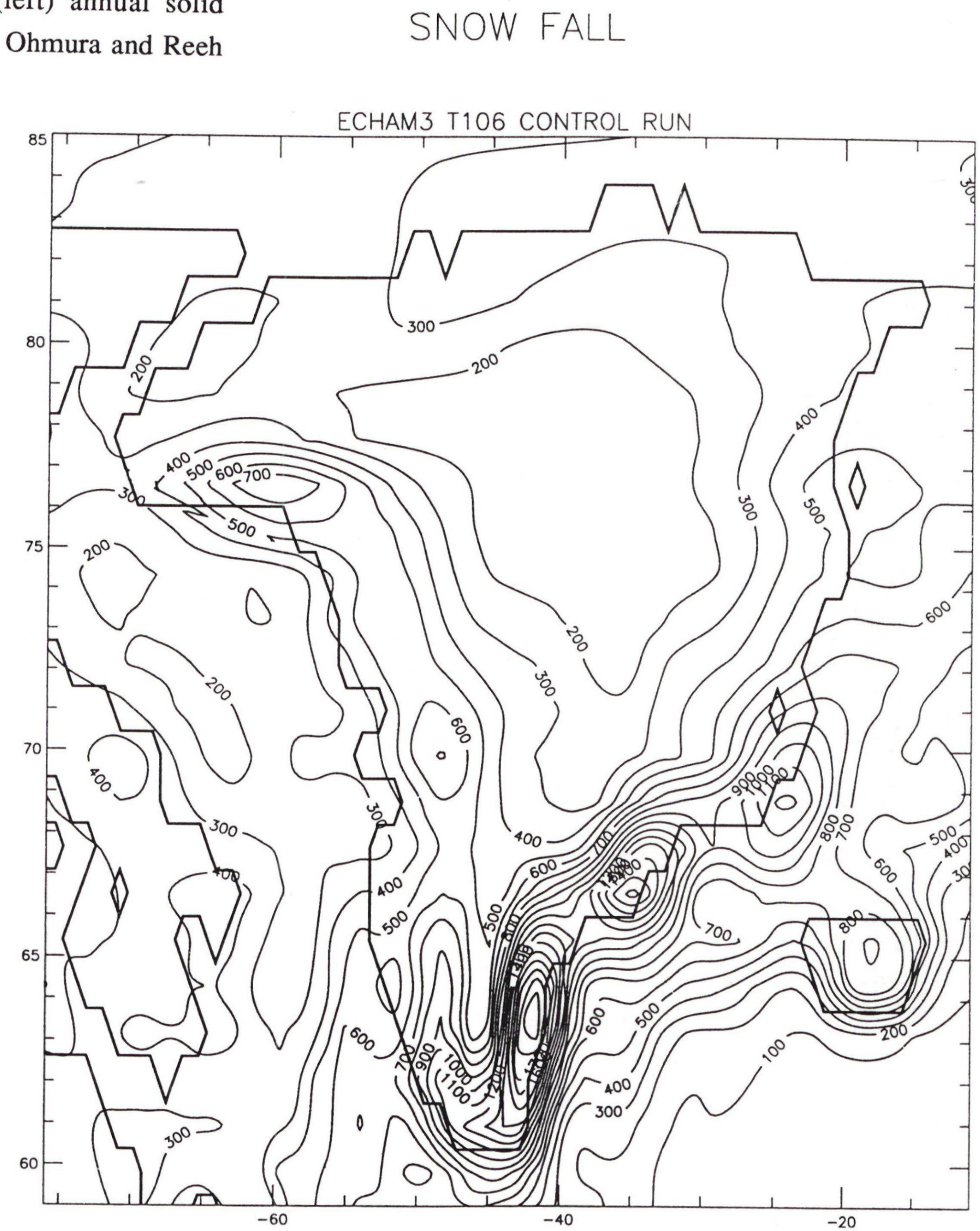

GIOVINETTO ET AL.: DEPENDENCE OF ANTARCTIC SURFACE MASS BALANCE 3519

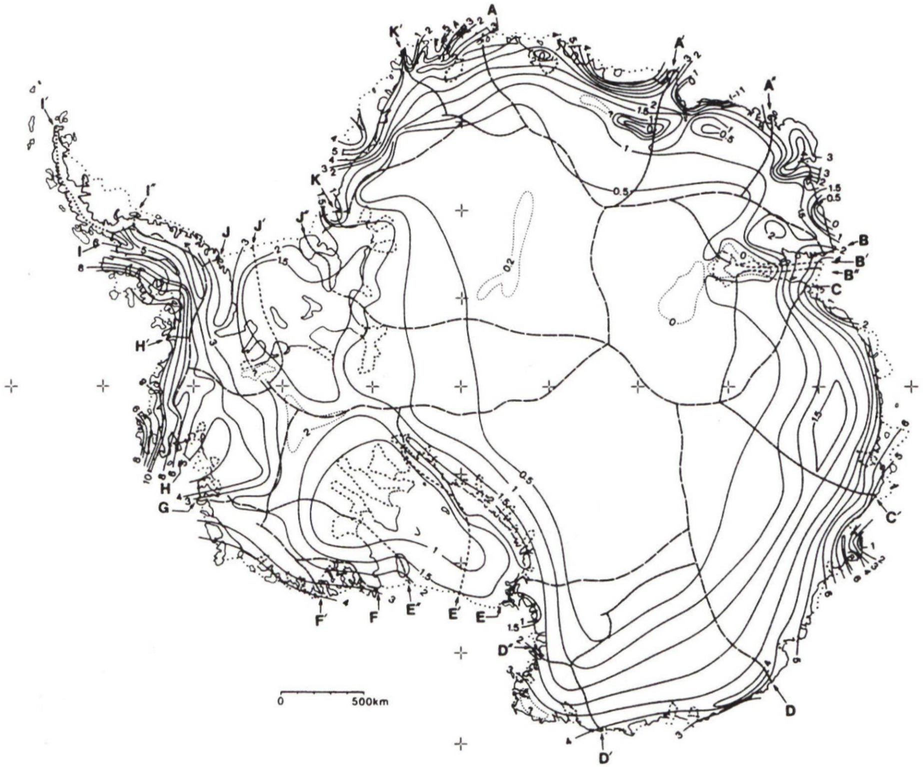

Surface mass balance rates (solid lines) and drainage divides (dashed lines) [after *Giovinetto and Bentley*, 1985]. Numbers on isopleths are in units of 100 kg m^{-2} a^{-1}. A discussion of how the drainage divides were positioned and designated (eg. A, A', A", etc) is given by *Giovinetto and Bentley* [1985].

Annual Total Precipitation [mm y^{-1}]

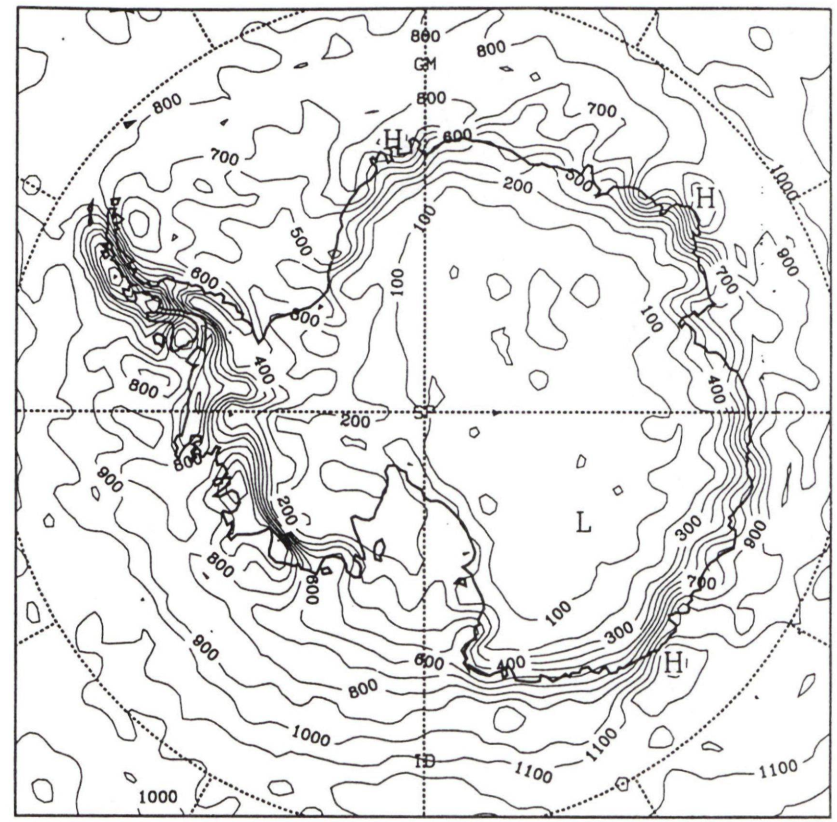

Fig. 3: Comparison of the computed(right) and observed(left) annual total precipitation for Antarctica. Source for the observed is Giovinetto et al.(1990).

TOTAL PRECIPITATION

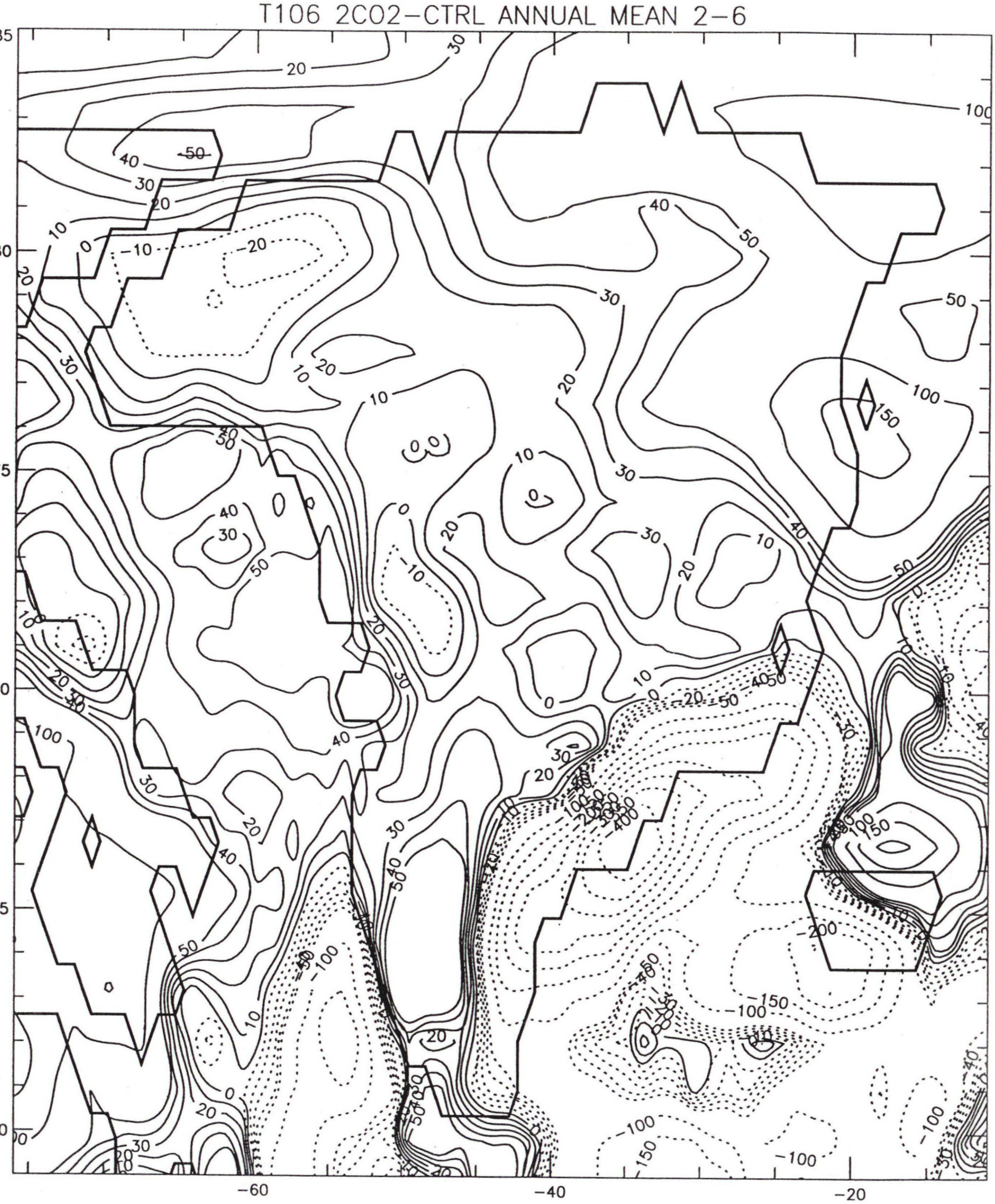

Fig. 4: Difference in annual total precipitation, x2 CO_2 minus x1 CO_2 for Greenland unit in mm

SNOW FALL

Fig. 5: Difference in auual solid precipitation or accumulation, x2 CO_2 minus x1 CO_2 for Greenland unit in mm.

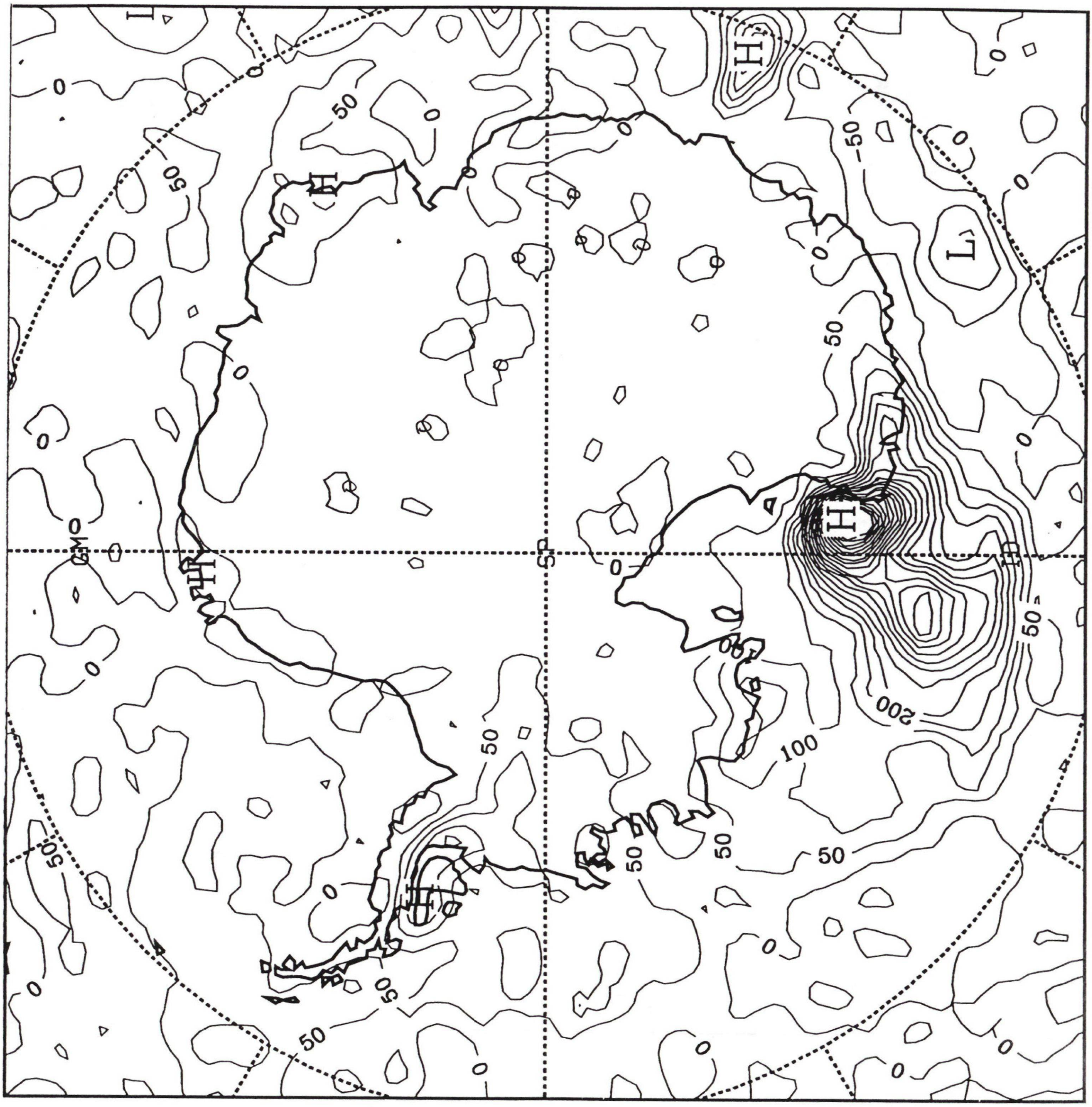

Fig. 6: Difference in annual total precipitation, x2 CO_2 minus x1 CO_2 for Antarctica unit in mm.

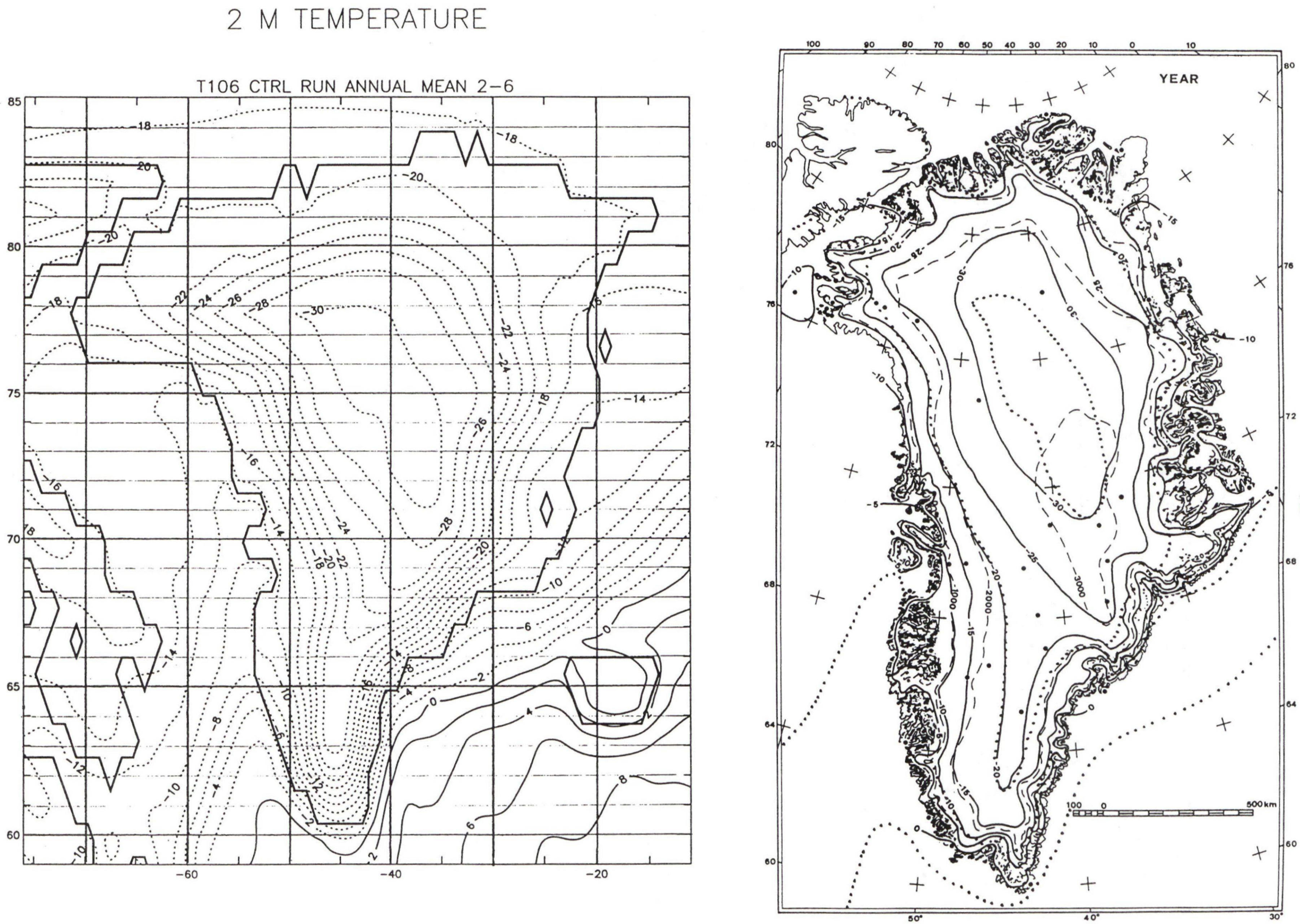

Fig. 7: Comparison of the computed(left) and observed(right) annual mean air temperature for Greenland. Source for the observed is Ohmura(1987).

3520 Giovinetto et al.: Dependence of Antarctic Surface Mass Balance

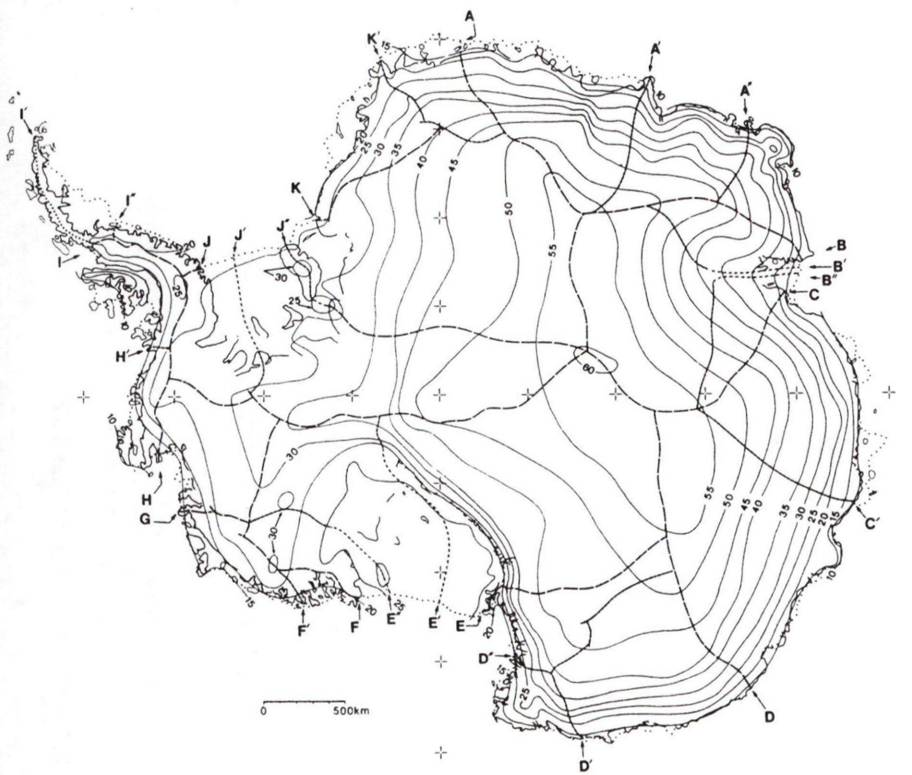

Mean annual surface temperature, which is approximately that of the air temperature measured at

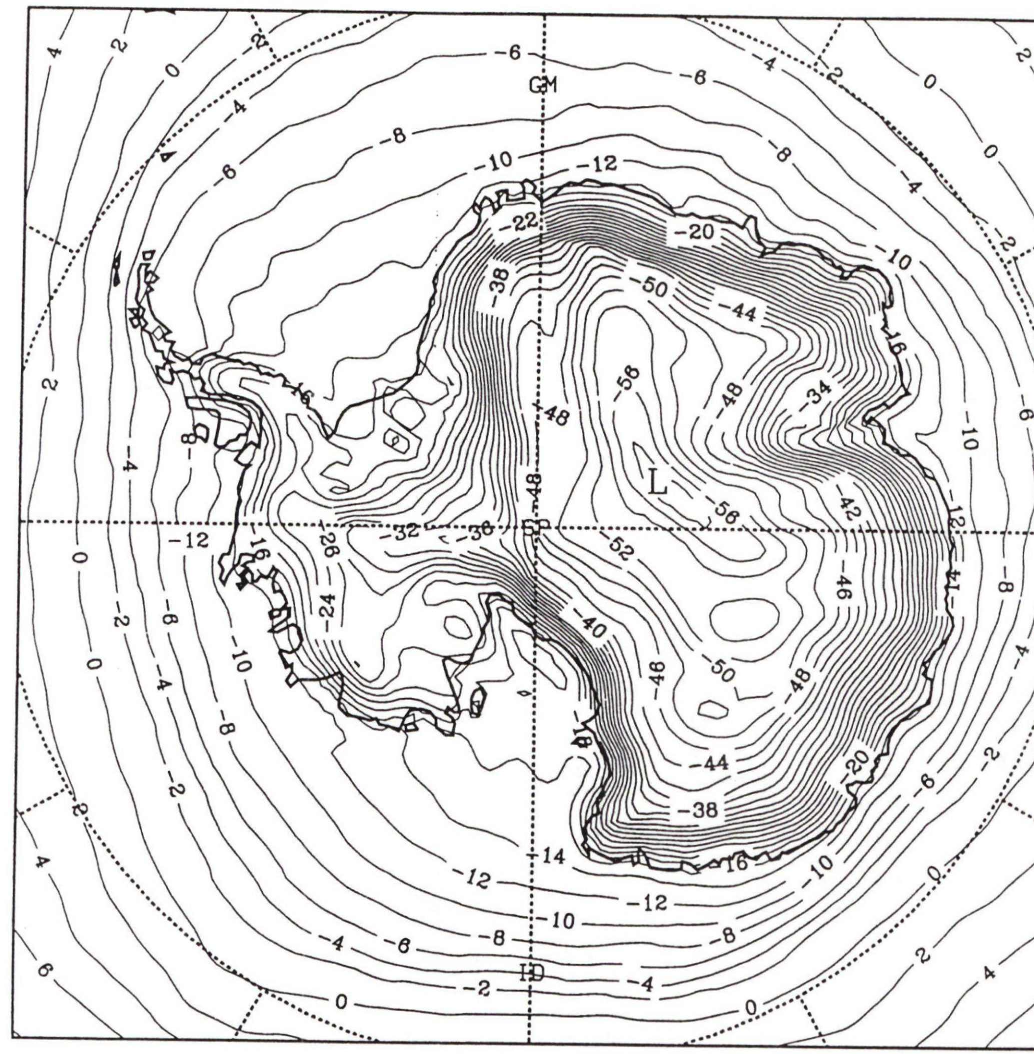

Fig. 8: Comparison of the computed(right) and observed(left) annual mean air temperature for Antarctica. Source for the observed is Giovinetto et al.(1990).

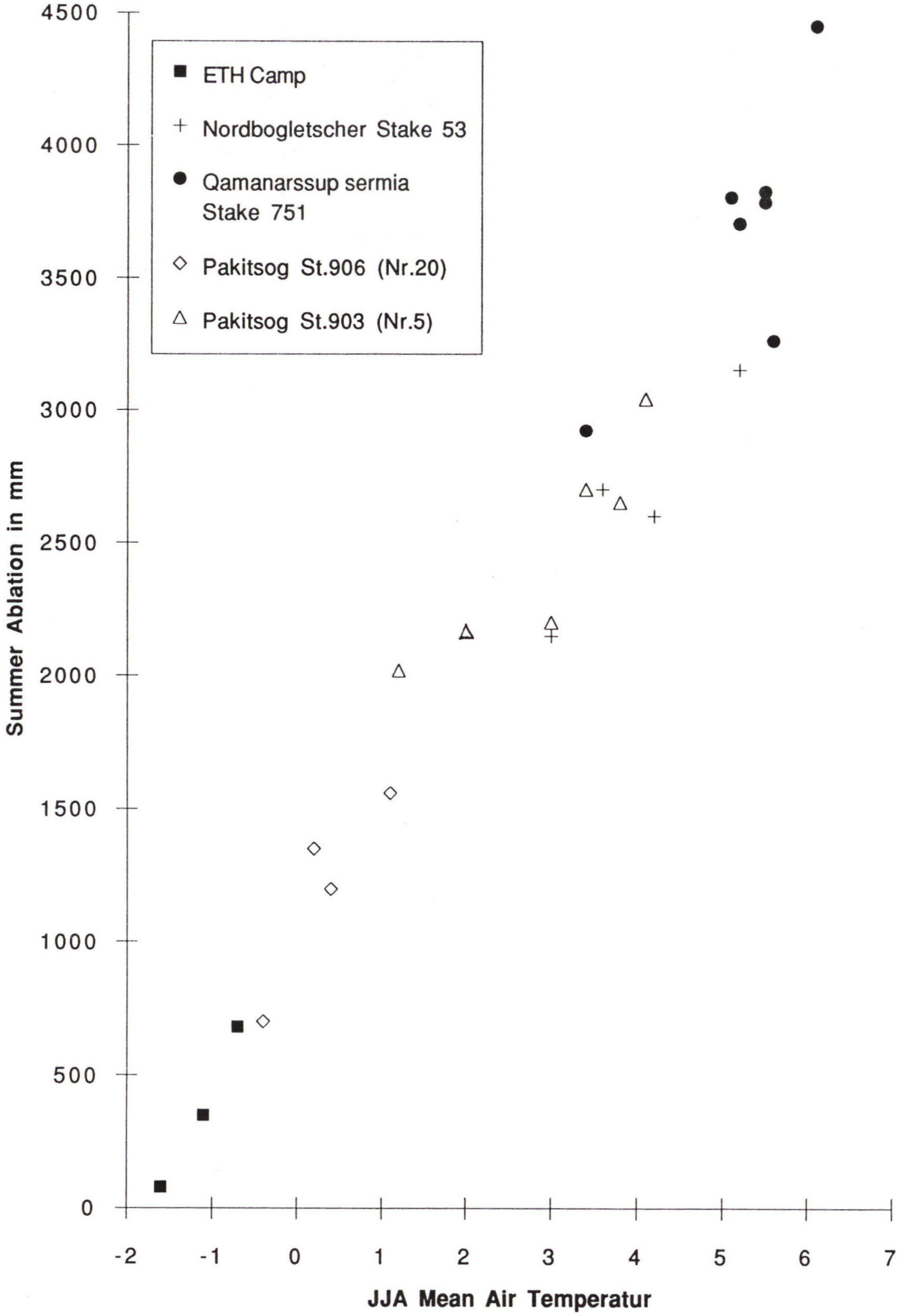

Fig. 9: Relationship between the annual total mass loss due to melt and mean air temperature for June, July and August for Greenland. Note that -2 ^{o}C is the minimum required temperature for the mass loss.

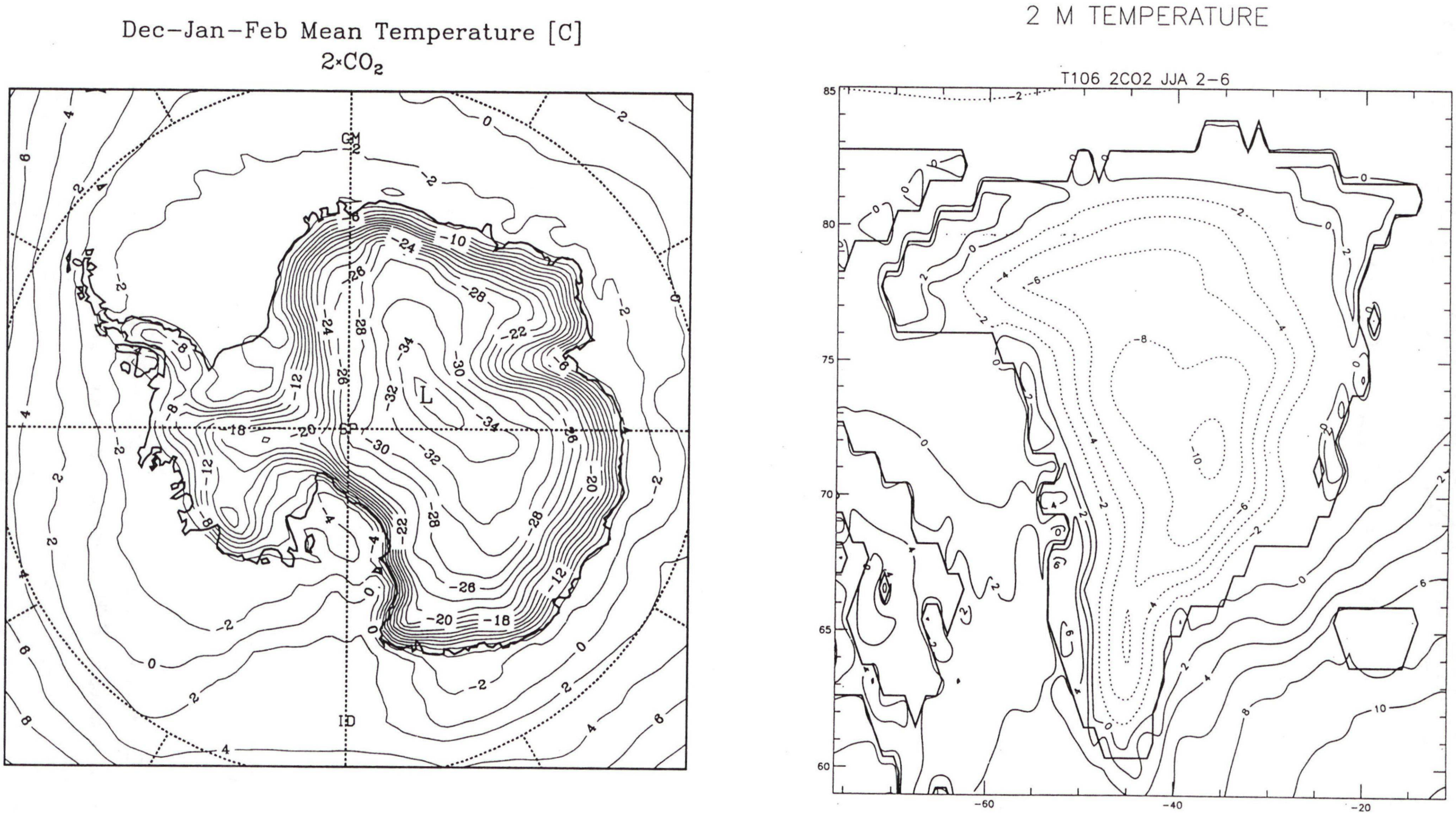

Fig. 10: Mean summer air temperature for Antarctica(Dec., Jan., and Feb.) and Greenland(Jun., Jul., and Aug.) expected under the doubled CO_2 condition.

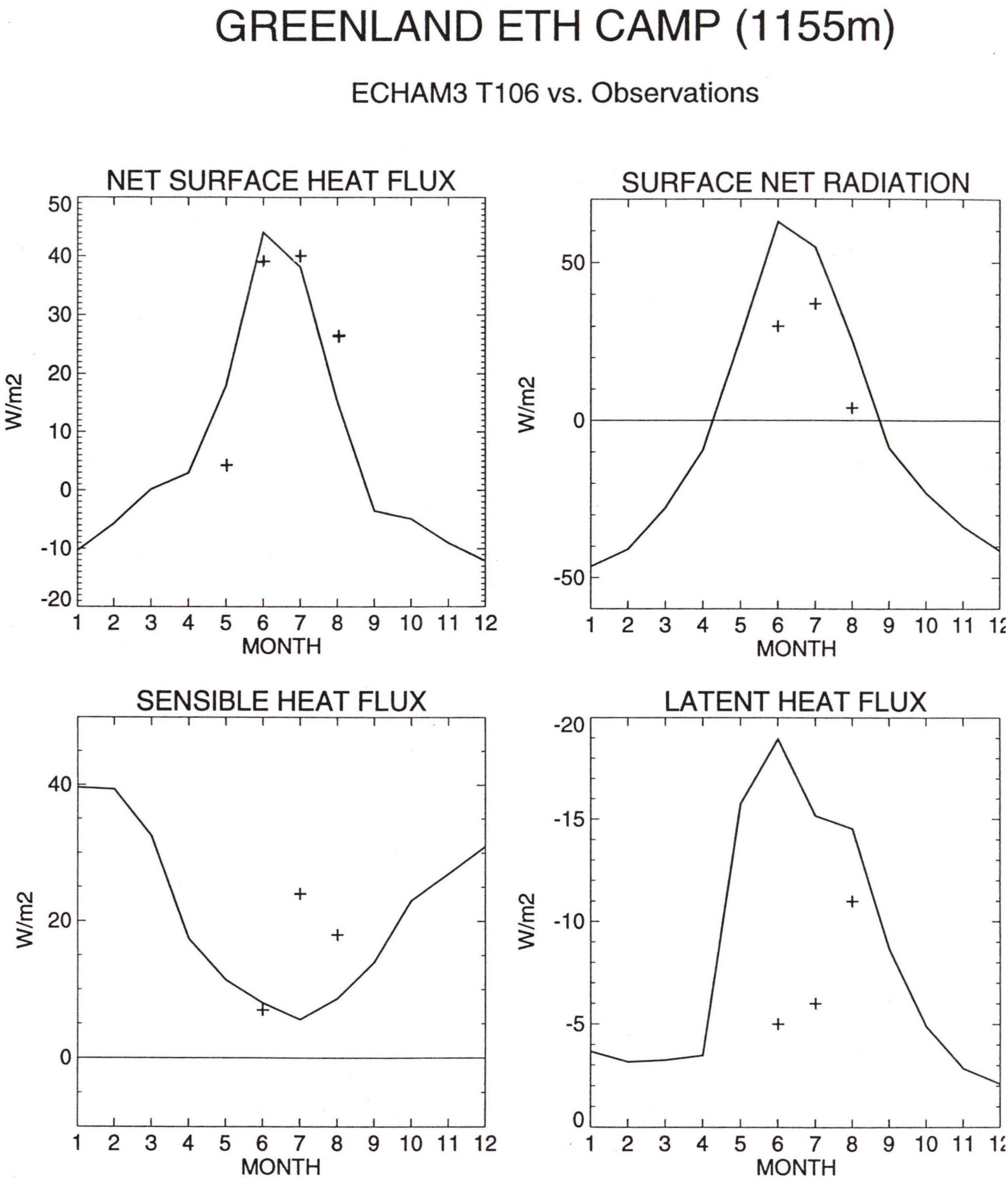

Fig. 11: Comparison of the computed(solid line) and observed(cross) monthly mean heat fluxes for ETH Camp. Source is Ohmura et al(1994).

Components related to the annual mass balance for Greenland

unit in mm/y

		Observations	Model Experiments		
			Contorl	x2 CO_2	x2CO_2 - Control
1 Annual precipitation		340	494	492	-2
2 Annual accumulation or solid precipitation		317	475	463	-12
3 Annual ablation based on energy balance			228	425	197
4 Annual ablatio based on summer temperature		200	146	353	208
5 Storage change and	2 - 3		247	38	-209
calving	2 - 4	117	329	110	-219
Sources		Ohmura & Reeh(1991)	This study		

Tab. 1: Mass balance for the present and for the time of the doubled CO_2 for Greenland.

GLACIOLOGICAL FIELDWORK ON STORSTRØMMEN GLACIER: RESULTS 1994

F. Jung-Rothenhäusler[1], H. Oerter[1], C. Bøggild[2] & N. Reeh[3]

1 Alfred Wegener Institute for Polar and Marine Research, Germany
2 Geologic Survey of Greenland, Danmark
3 Danish Polar Center, Danmark

Introduction:

The glacier Storstrømmen is believed to be a surge type glacier, which has surged most recently in the period 1978 to 1984. The surge was identified by means of Landsat satellite imagery which showed a large advance of the glacier front, distortion of supraglacial morainic material etc. The front advance came to a stop in 1988, as described earlier by [Reeh, 1993]. At present the glacier is in the recovery phase, transporting ice from the accumulation area into the ablation area, which results in an apparent thickening of the glacier within the ablation area.

Fieldwork:

Fieldwork started 1989 in the Storstrømmen region in Northeast Greenland. The objectives of the ongoing study are:

- Glacier mass balance
- Glacier dynamic
- Glacier climate relationships

Work on Storstrømmen was carried out in collaboration with the GGU Eastern North Greenland expedition. The glacier was visited twice in 1994. First from July 11^{th} – July 14^{th}, second from Aug. 11^{th} – Aug 13^{th}. The fieldwork in 1994 consisted of five main tasks:

- Measurement of climate parameters at various locations during the summer melt period. (For details see Bøggild elsewhere in this report.)
- Replacement and readjustment of the automatic 'all-year' weather station.
- Ablation stake reading and maintenance of the stake network.
- Stake positioning with differential GPS measurements.
- Setup and positioning of AIRSAR corner reflectors.

Results:

Fig. 1 is an overview of the ablation area of Storstrømmen Glacier, for which a detailed Digital Elevation Model is available. The Digital Terrain Model covers the whole area shown, the apparent 'misfit' of the satellite image is caused by the satellite's orbit. Contour lines, with an interval of 100 m are drawn over the entire area. The stake positions are shown as small black-white squares. Note the cluster of stakes near the ice margin and the two strain figures near the glacier snout. The four white squares denote the AIRSAR corner reflectors. The white line west of the semi-nunatak is the estimated position of the grounding line for Storstrømmen Glacier. The white lines, originating at stake locations, are velocity vectors showing the direction and magitude of the glacier movement from 1993 - 1994. The lenght of the velocity vectors are magnified by a factor of 100 for better interpretability.

The results of the ablation stake readings, carried out during the period 1989 – 1994 are shown in Fig. 2. As expected, there is an increase in ablation with decreasing elevation. The variations are mainly caused by local topographical influences. The highest ablation values are found in the lower tongue area, west of the semi-nunatak. The cluster of ablation values between 200 – 240 m a.s.l represents the stake cluster near the margin. The stakes 28 – 38 in the lowermost part of the glacier were not available before 1993.

The velocity measurements derived from the GPS positioning of the ablation stakes are shown in Fig. 1 and Fig. 3. It is clear that the glacier movement pattern is highly variable throughout the ablation area. The part with pratically no movement is located just north of the grounding line, whereas high ice velocity can be measured in the upper part of the ablation region and the terminus region south of the grounding line.

A second means of deriving glacier movement pattern and its associated mass transport is the analysis of satellite images. By analyzing four images of the Storstrømmen ablation area, covering the period 1978 – 1984, the velocity as well as the change in frontal position was determined. The change in glacier terminus area south of $77^o11'51"$ is shown in Table 1.

Table 1: Front Advance of Storstrømmen Glacier 1978 – 1988

Date of image acquisition	Area $[km^2]$	Change $[km^2]$	Change $[km^2yr^{-1}]$
Sept. 07, 1978	1073.43		
Aug. 10, 1980	1161.86	+88.43	+44.2
Aug. 07, 1984	1267.05	+193.62	+26.5
Aug. 18, 1988	1278.04	+204.61	+2.8

Also glacier velocity was derived at four different positions within the ablation area. Position A is a supraglacial channel at $77^o10'N$ and $22^o10'W$, position B is the Sælsøgletcher at $77^o5'N$ and $21^o55'W$, position C is the main glacier calving front and position D is the calving front east of the semi-nunatak. The change in glacier velocity at these positions is shown in Fig. 4. The highst velocities are those at the main calving front during 1978 – 1980, the lowest ones are those at Sælsøgletscher, which showed slight retreat until 1984. Since 1980 the velocities decreased at the calving front, but still increased at points C and D. A general decrease in glacier velocity can be seen past 1984 for points A, C and D.

Discussion:

As already indicated by [Reeh, 1993] Storstrømmen has experienced large scale fluctuations of its frontal positions during 1978 – 1988. The glacier velocities derived in this study, as well as the change in glacier thickness at the terminus region, allow to describe this event as a glacier surge.

The movement pattern for the whole period 1978 - 1994 as shown in Fig. 4 and Fig. 1 shows a typical surge post-surge situation. During the surge the glacier transported ice over the grounding line at speeds higher than the replacement from the accumulation area would normally allow. Now during the post-surge stadium the glacier replentishes the tongue area again. Thus a very interesting velocity pattern emerges.

The high velocity measured near the glacier terminus, stems from the fact that the glacier front is at present fast disintegrating, the terminus being pushed out into the bay by Bistrup Brae advancing from the South.
The zone of almost zero velocity is the area where the glacier gains mass, which is transported downslope from the accumulation area. Therefore thickening of the glacier is expected. This thickening was measured by GPS in 1993 and 1994 and was already reported by [1].
The ice velocity at position B, the Sælsøgletscher front sheds light to the situation at the ice margin. During the main advance between 1978 and 1984, ice mass was transported past the Sælsøgletscher, thus melting reduced the glacier's tongue. At the present build-up situation , Sælsøgletscher receives more material again, thus its terminus advanced again with 250 m per year until 1988.
At present the GPS measurements indicate that the glacier movement pattern as shown in Fig. 4 continues until today. Additional information will become available through the Danish AIRSAR experiment and through the use of further satellite imagery.

Acknowledgements:

The work was carried out with financial support by the EU contract EV5V-CT91-0051 and support from the Nordic Research Council.

References

Reeh N., C.E. Bøggild and H. Oerter. 1993. On the Dynamics of Storstrømmen, an outlet glacier from the Northeast Greenland Ice Sheet. In *Mass Balance and Related Topics of the Greenland Ice Sheet,* pages 54 – 59. GGU.

Figure 1: Storstrømmen Glacier Velocity Vectors

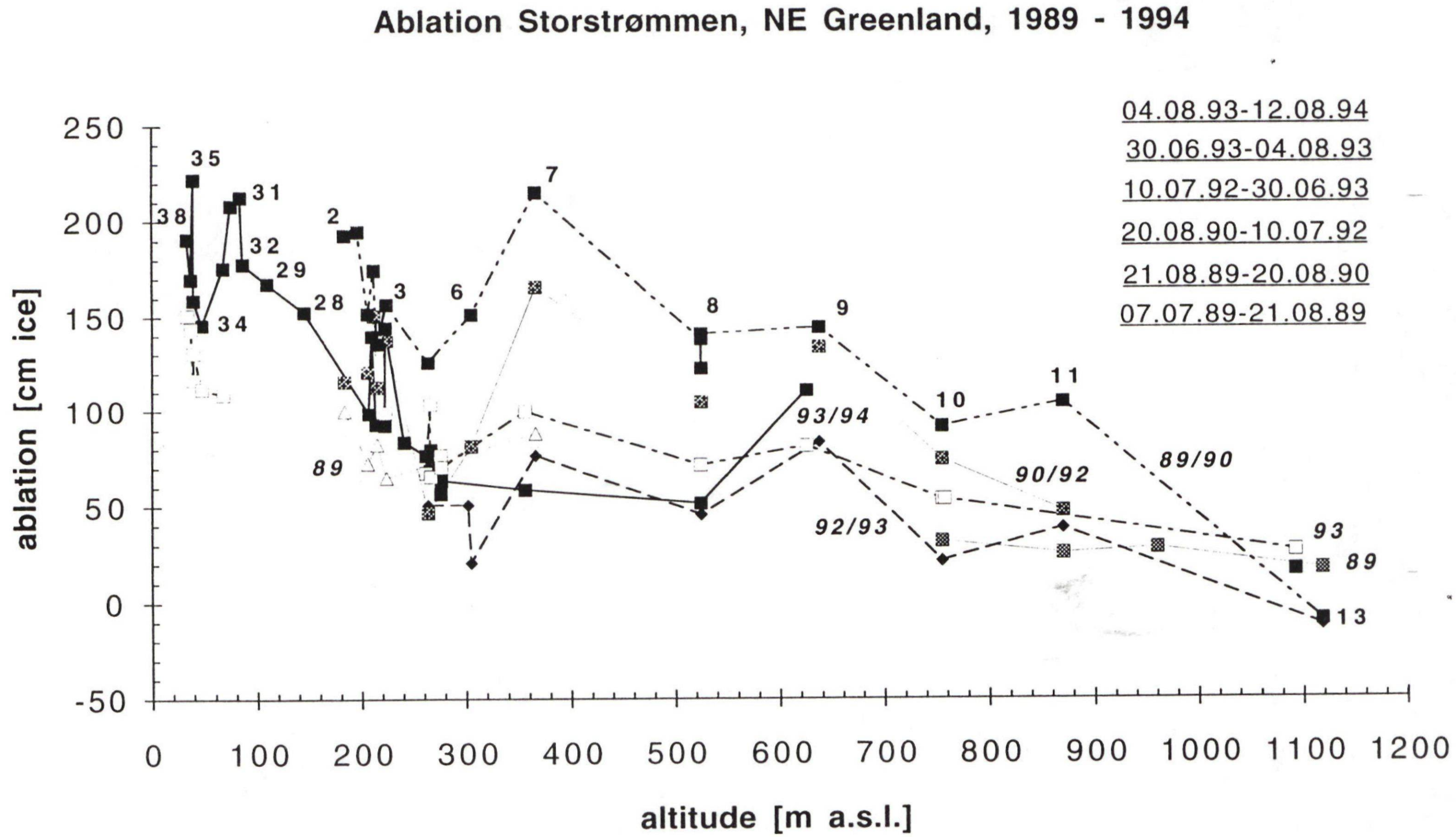

Figure 2: Ablation values between

Figure 3: Ice velocity as measured by GPS 1992 – 1994

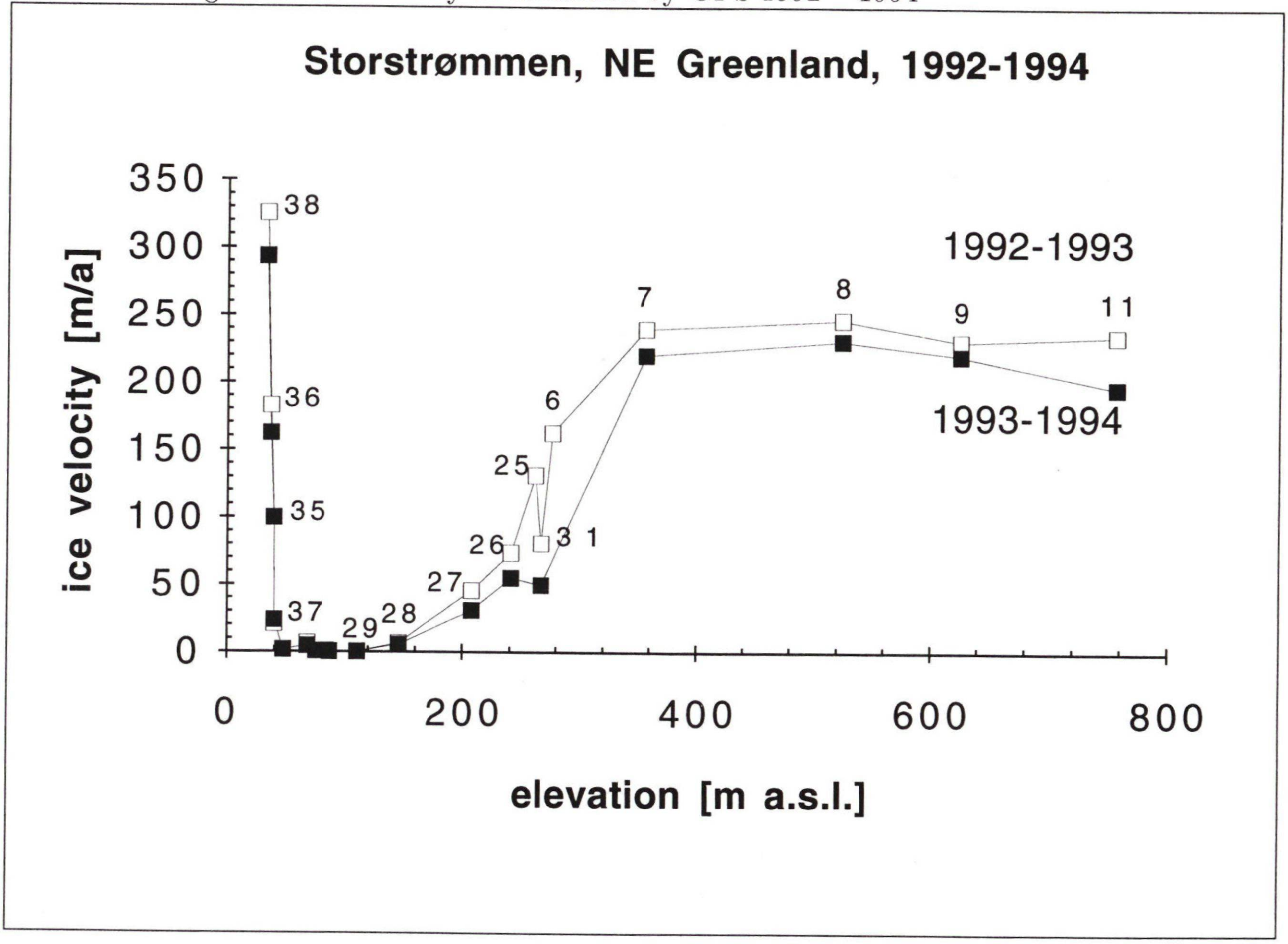

Figure 4: Glacier movement between 1978 – 1988

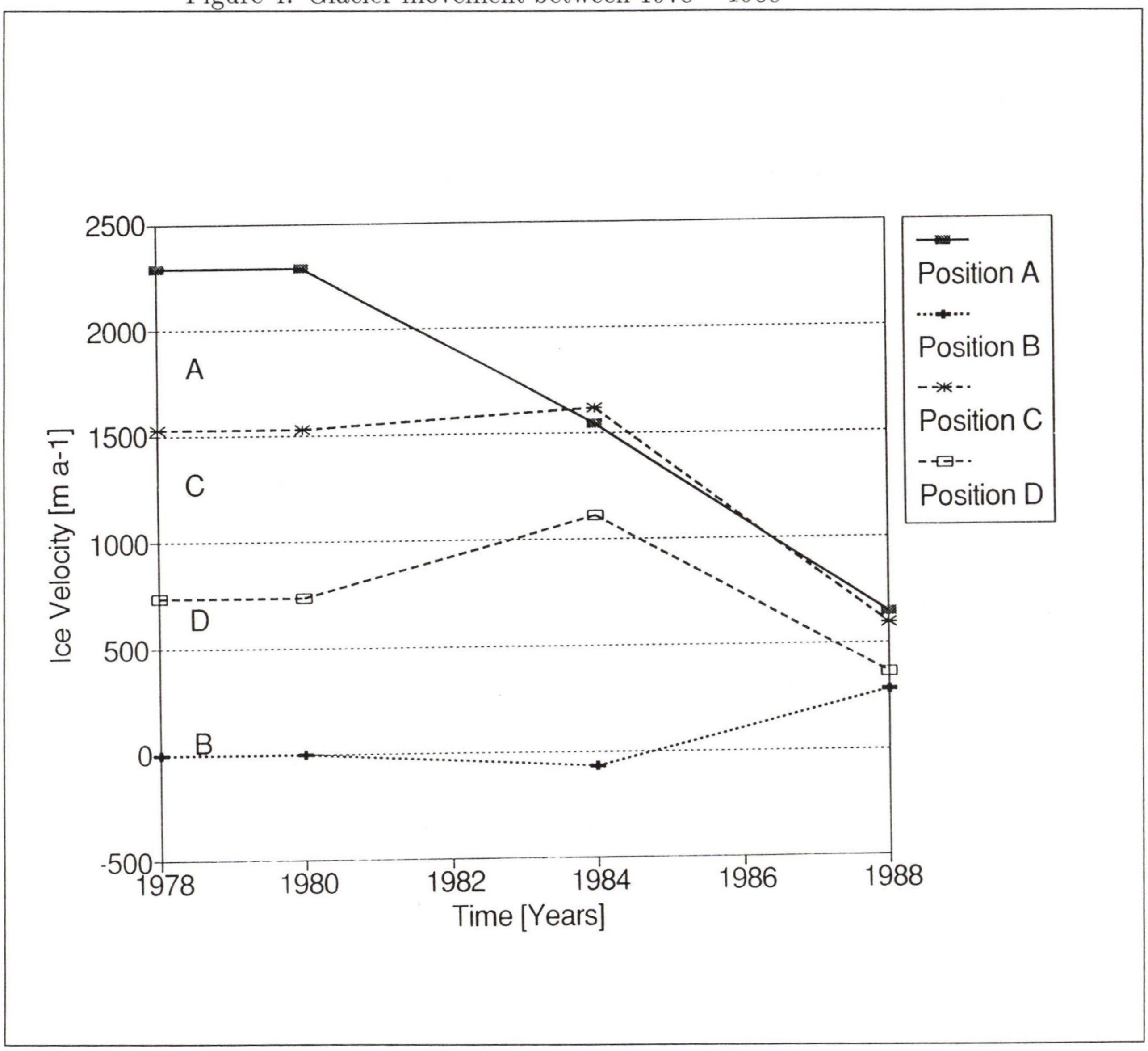

THE 1994 NORTH GREENLAND TRAVERSE

J. Kipfstuhl, L. Hempel, U. Nixdorf and Th. Thorsteinsson
Alfred-Wegener-Institut für Polar und Meeresforschung, Bremerhaven, FRG

H. Fischer, D. Wagenbach and M. Werner
Institut für Umweltphysik, Heidelberg, Germany

J.C. Moore
Arctic Centre, University of lLapland, Rovaniemi, Finland

In July of 1993 the North Greenland traverse left Summit and reached 78N/36W. In 1994, the traverse moved further north, crossed the ice divide at 80N/41W and returned to the present winter camp position at 78N/44W. We drilled four ice cores, 100 - 150 m in length to sample ice from the last 500 - 1000 years. To determine more recent precipitation rates and firn temperatures, additional firn cores were drilled. At each of the four major drilling sites, strain nets were set up. En route, ice radar sounding and gravity measurements were taken.

Bulk density and DEP (dielectric profiling) of all the cores was determined in the field. Three cores (B16, B18 and B21) underwent further processing in the lab. The first results from the 100 m deep B16 core show an average $\delta^{18}O$ value of -37.3 ‰ over the last 500 years, somewhat less than the mean Holocene value measured in the GRIP core(-35‰). Mean accumulation derived for the area 150 km north of Summit is 15 cm/a. After taking 2 - 3 year averages, measurements of the ice core's ion concentrations reveal a significant increase in sulfate at the end of the last century and in nitrate in the mid 1950s. Both increases clearly show anthropogenic influences. No trends during this period were observed in the calcium and sodium measurements.

Tab. 1 compares the depths of volcanic events recorded in 8 cores to the depths recorded in the GRIP ice core. The depths are derived from measurements of the electrical conductivity taken in the field (DEP) and in the lab (B16, B17 and B21). The main result is that north of Summit the decrease in accumulation is much faster and the area with very low accumulation is much larger than expected from the map of Ohmura & Reeh (1991).

In 1995, the traverse will follow the ice divide south to 74 30N, jog westward, and then turn north and follow a line parallel to the ice divide to Camp Century.

Literature

Ohmura, A., and N. Reeh, 1991: New precipitation and accumulation maps for Greenland. J. Glaciol., 37, 140-148.

Tab. 1: The depths in meters and dates of volcanic events observed in the North Greenland traverse cores

Core	**GRIP**	**B16**	**B17**	**B18**	**B19**	**B20**	**B21**	**B22**	**B23**	
Length	3028	100	100	150	150	150	100	120	150	m
Position	72 35	73 56	75 15	76 37	78 00	78 50	80 00	79 20	78 00	N
	37 38	37 38	37 37	36 24	36 24	36 30	41 08	41 08	44 00	W
1912AD	31.0	22.7	-	19.0	-	17.6	19.4	24.1	19.9	Katmai
1816AD	58.8	42.7	37.8	35.3	32.7	32.6	36.1	45.5	39.4	Tambora
1783AD	67.6	49.3	43.2	40.2	37.3	37.2	41.2	52.1	45.4	Laki
1601AD	111.4	81.1	71.7	64.5	-	60.9	66.6	-	78.2	Huaynaputina
1259AD	187.3	-	-	105.3	96.0	100.8	-	-	120.6	?
934AD	256.8	-	-	142.0	134.7	136.9	-	-	-	Eldgja

THE HANS TAVSEN GLACIOLOGICAL PROJECT

Ole B. Olesen[1], N. Reeh[2] & R. B. Braithwaite[3]

[1]*Geological Survey of Greenland, DK*
[2]*Danish Polar Center, DK*
[3]*University of Manchester, UK*

The Hans Tavsen glaciological project was initiated in 1993 and is planned to run through 1995 with a possible extension in 1996-1997. It is a joint Scandinavian operation involving participants from Denmark, Norway, Sweden and Iceland and is being funded by The Council of Nordic Ministers (NMR), EU and the participating institutions.

INSTITUTION	*COUNTRY*
Dansk Polarcenter (DPC)	*Denmark*
Niels Bohr Instituttet for Astronomi, Fysik og Geofysik (NBIfAFG)	*Denmark*
Grønlands Geologiske Undersøgelse (GGU)	*Denmark*
Norges Landbrugshøjskole, Institutt for Jordfag	*Norway*
Tekniska Högskolan, Universitetet i Lund	*Sverige*
Sciencε Institute, Universitetet i Reykjavik	*Iceland*

Table 1. Institutions participating in the Hans Tavsen Ice Cap Project

The objectives are: "To investigate the present and past climate and glacier dynamics of North Greenland by means of ice-core records, ice margin studies, ablation-climate studies, and glacial geological studies on and around Hans Tavsen Ice Cap, North Greenland" (N. Reeh, application to NMR, 1992).

The project is an attempt to integrate glaciological, climatological, geophysical and geological methods to achieve a thorough knowledge of the past and present climatic and dynamic behaviour of the ice cap. This will be attempted by investigations from surface to bedrock and from the highest point in the accumulation area out into the ice-free foreland which was covered by ice under earlier climates (Fig. 1).

The main reasons for choosing Hans Tavsen Ice Cap (Fig. 2) for this study is based on the following considerations:

1 There were no paleoclimatic ice core records covering 200 years or more from North-East Greenland at the time of planning.

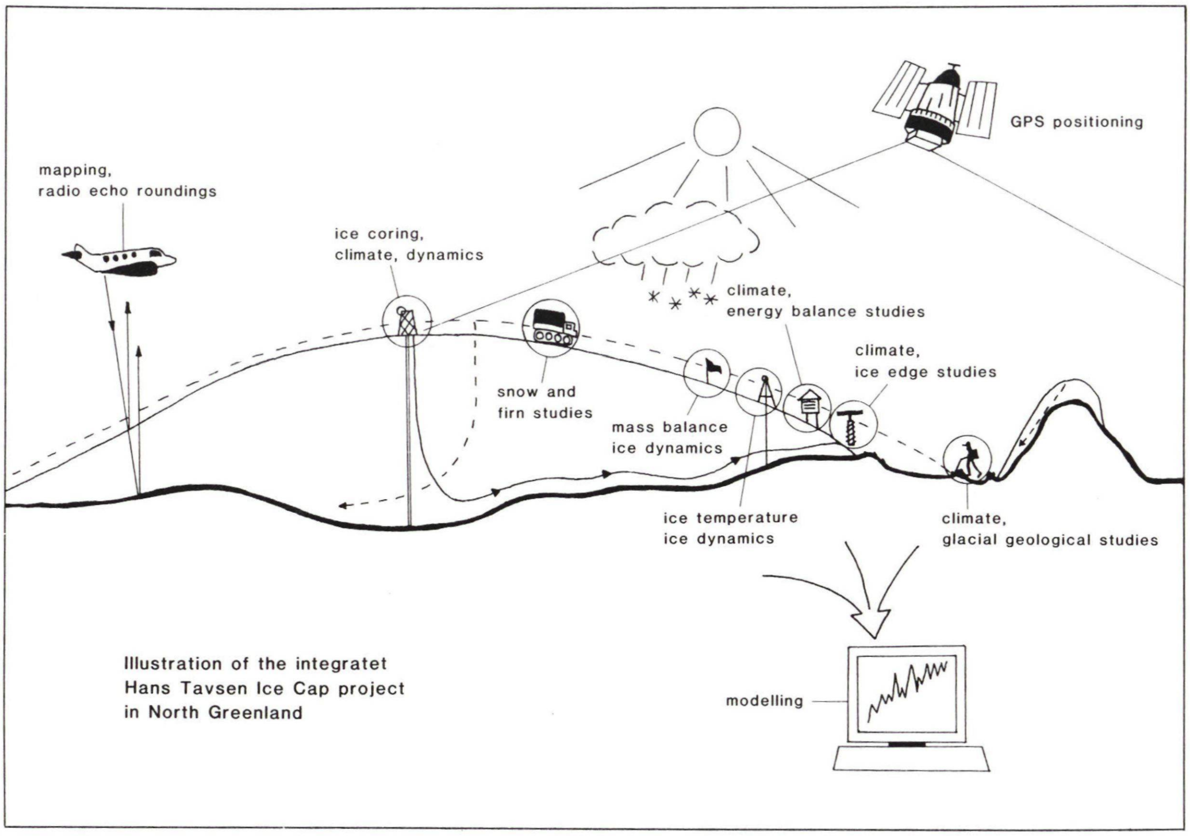

Figure 1 *Concept of the Hans Tavsen glaciological project. From surface to bedrock and from the centre out onto the foreland (ill. H. H. Thomsen, GGU).*

2 Quaternary geology information seems to indicate that the high north to northeast region is prone to high climatic variability and sensitivity.

3 The Hamburg GCM predicts extreme sensibility to climate change for North Greenland with a centre close to Hans Tavsen Ice Cap.

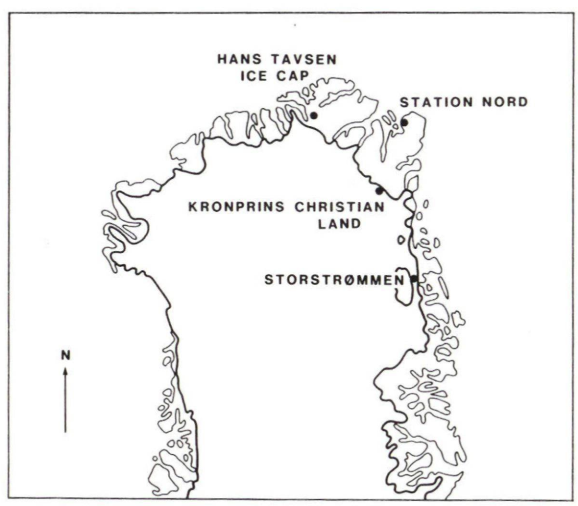

Figure 2 *Location of place names mentioned in the text.*

4 Parallel glacier-climate studies are carried out in Kronprins Christian Land and on Storstrømmen making it possible to compare conditions.

5 Drilling on the northern part of the Inland Ice would be much more costly.

Several shallow (30 m) ice cores and one core to bedrock (c. 350 m) will be drilled.

The cores will be analysed in order to establish annual and quarterly time series of precipitation and isotopic composition covering the last 200 years and to investigate the Holocene and glacial-time climate of North Greenland.

Ablation-climate studies of the margin will be performed as an understanding of the present climate-dynamics relationship as a necessary condition for modelling the past.

Ice samples from the margin will be collected for isotope-analysis for comparison with the isotope record from the deep drilling at the top to establish the Holocene and glacial-time climate and dynamic history of the ice cap.

Surface and bed profiles, ice flow velocity, ice temperature and mass balance will be measured along a flow line from the top of the ice cap to the margin to provide background data for ice-dynamic model studies.

Glacial-geological studies will be performed around the ice cap to provide controls on the modelling of the ice-cap response to climate variations and to supply data on the glacio-isostatic changes.

The information mentioned above will be combined by means of a "regional" GCM-model for Greenland, an ablation-climate model, and a local ice dynamic model synthesizing the recent and past history of climate, mass balance and ice dynamics in North Greenland.

	1993	1994	1995	1996
DRILLINGS				
Core shallow (30 m)		x	x	
Core deep (350 m)			x	
Hot water			x	
ABLATION-CLIMATE		x	x	
ICE MARGIN SAMPLING		x	x	
ICE DYNAMICS				
Profiles surface	x	x	x	
Profiles bed	x	x	x	
Velocity		x	x	?
Inclinometry			x	?
Temp. shallow		x	x	
Temp. deep			x	?
Mass balance		x	x	?
GLACIAL GEOLOGY		x		
MODELLING		x	x	x

Table 2. Time schedule for the Hans Tavsen Ice Cap Project's field work

1993

The main result of the 1993 field work was the relatively detailed measurement of surface and bedrock elevations by radio-echo sounding from a Twin-Otter aircraft the position of which was continuously registered by a special GPS system developed for this project. The results made it possible to identify a suitable general area for the deep drilling (Fig. 3).

Figur 3 *Contour map of Hans Tavsen Ice Cap based on information by Kort- og Matrikelstyrelsen, Danmark (KMS), the Geological Survey of Greenland (GGU) and the Geophysical Department of the University of Copenhagen. D: Site of deep ice core drilling. Climate, mass/energy balance and ice dynamics studies are accomplished at the extreme north-east sector of the ice cap.*

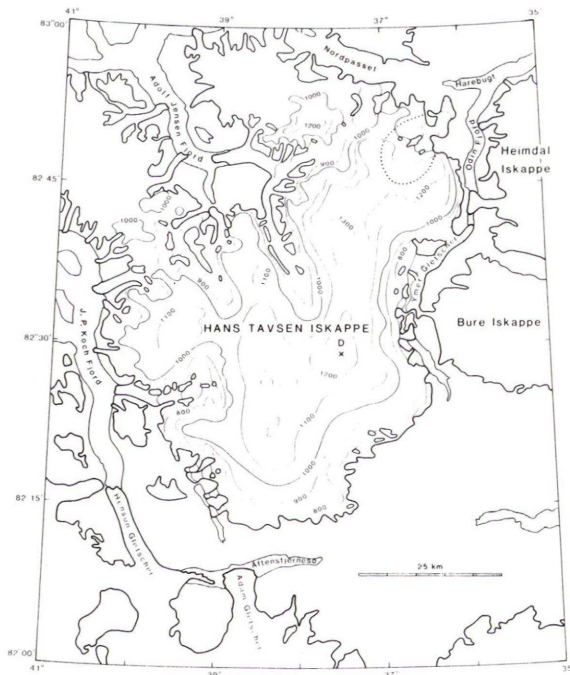

Reconnaissance flights for suitable locations for mass balance, ice dynamics and surface isotope studies were also carried out at the same time. Unfortunately the best location, an outlet glacier to the north-east, originates at the northern dome of the ice cap which is not an optimal deep-drilling site.

Also mass balance and dynamics of Storstrømmen and ablation/climate studies in Kronprins Christian Land were carried out.

The drill for the deep drilling, modified to operate in an only partly liquid filled hole, was successfully tested at the GRIP drill site at Summit.

1994

At the intended drill site detailed top and bottom profiles were measured within a 6 x 6 km area by radio-echo soundings and kinematic GPS-positioning. Additionally two surface and bottom profiles, 16 km to the south-west and 6 km to the north of the drill site, were measured.

A strain net consisting of 8 x 3 poles to a distance of 3 km from the reference point was measured using GPS. Also a 6 m ice core for a $\delta^{18}O$ measurements was obtained. Postprocessing of the data show that the location, chosen from the 1993 survey, is optimal for the deep drilling.

The equipment for the deep drilling has been moved to the drill site and is ready for an early start in 1995.

A stake network for mass balance studies was established between the northern dome at about 1320 m elevation and the terminus of the outlet glacier at about 220 m with approximately 100 m elevation intervals and measured several times during the field season (Fig. 4). At the uppermost stakes snow pits and firn cores were obtained for determination of stratification and densities.

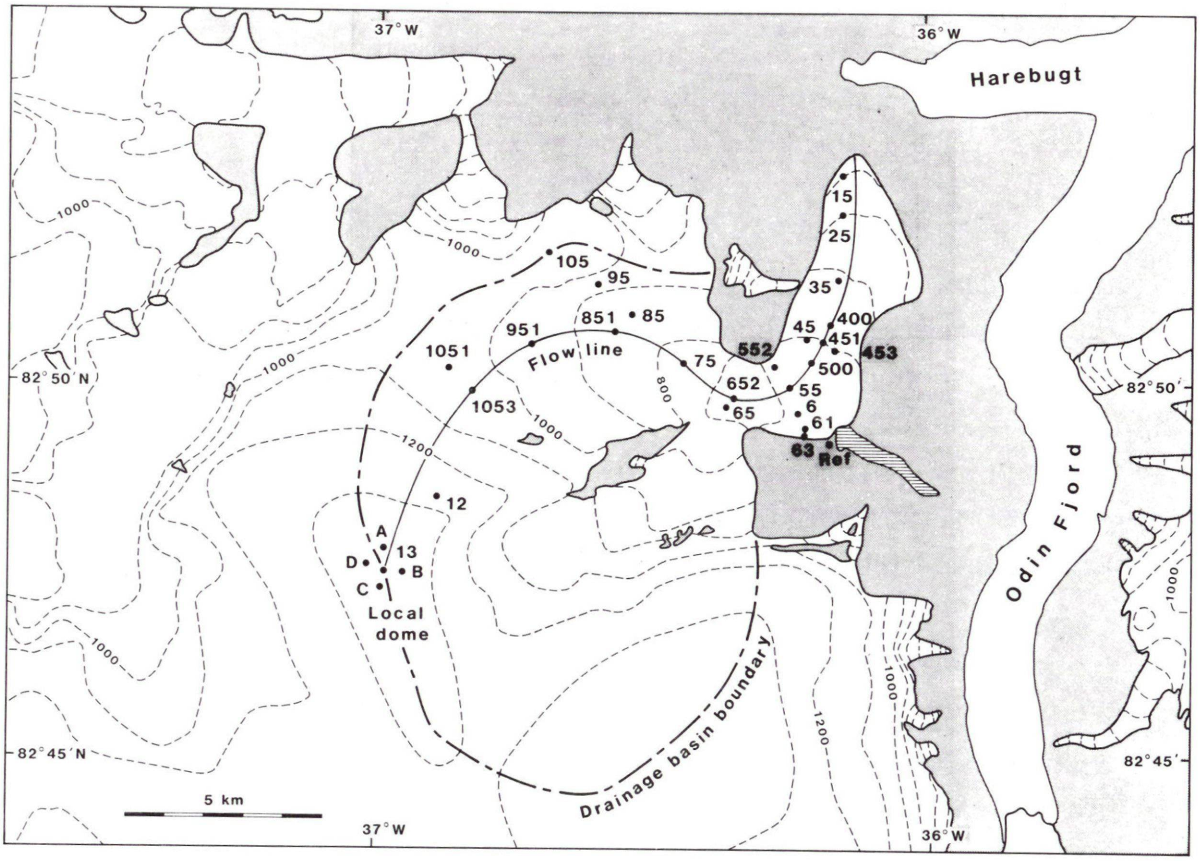

Figur 4 *Map of the north-east part of the Hans Tavsen Ice Cap. Numbers are stake positions for mass/energy balance and ice dynamics studies. Field camp near Ref.*

The programme also involved daily measurements of ablation in a 10-stake cluster at approx. 540 m elevation together with continuous logging of radiation components, ice albedo, air temperature, humidity, wind speed and englacial temperatures. Despite the short field season, 23 June to 11 August, the measurements appear to cover the major part of the melting period at this high latitude. Preliminary evaluation of the data shows that net radiation is the largest source of ablation energy but that heat conduction into the ice is a significant heat sink.

The mass balance stakes were supplemented by additional stakes for a more detailed study of surface-ice velocities and deformations. Both at the northern dome and at a location on the glacier tongue, with expected regular flow conditions, stake networks were set up for determination of strain rates. All stakes were positioned relative to a reference point on bedrock near the camp-site by means of GPS. Preliminary processing indicates that relative horizontal coordinates have millimetre accuracy whereas the relative vertical coordinates are determined within a few centimetres. At all stakes along the central flow line accurate levelling was carried out 100 m up and down from the stake along the flow line to provide local surface slopes to be used in ice flow model studies together with ice-thickness and englacial temperature data hopefully obtained next year.

To obtain an idea of the $\delta^{18}O$-distribution in the surface layers of the ice cap 10 surface-ice samples were collected at each of the stakes in the ablation section of the flow line from the northern dome to the glacier terminus. Samples were also collected from the snow pits and firn cores in the accumulation zone. Furthermore, near the terminus of the glacier, where the oldest ice is expected to be found, 34 surface-ice samples were collected over a distance of 115 m. Similar sampling was carried out on the glacier margin near the camp site and at the terminus of a glacier near the deep-drilling site.

The purpose of the sampling is to determine if pre-Holocene ice is present at the margin. If not it could indicate that the ice cap had retreated considerably during the Holocene climatic optimum. So far the ice samples have not been analysed.

Glacial geological studies were carried out along the northern margins of Hans Tavsen Ice Cap. The general area has a high relief with summits over 1000 m and has been subject to extensive solifluction which has destroyed much of the stratigraphic records.

Preliminary interpretations of the observations suggests a confluence of Hans Tavsen ice Cap with ice masses to the north during the late Weichselian. Corresponding heights of marine limits (Fig. 5) suggest an almost simultaneous deglaciation of Frederick Hyde Fjord to the east Nordpasset to the north and G. B. Bøggild Fjord to the north-west. Findings of driftwood up to an elevation of 26 m a.s.l. suggest that the fjords were seasonally ice free during the Holocene climatic optimum.

1995

After the present plans for the field work in 1995 operations start in late May when both deep and shallow ice core drillings on the south dome will commence.

Ice cores will be only partly processed in he field and then consecutively flown back to Copenhagen (in frozen state) for further laboratory analyses. At the same time the strain net established in 1994 will be remeasured with high precision GPS-receivers. The operation on the south dome should be accomplished by the end of June at which time the crew and equipment will return to Station Nord.

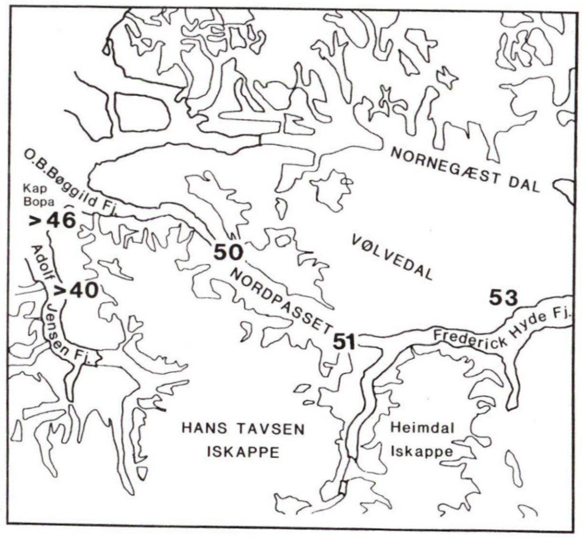

Figur 5 *Map of the glacial geology study area. Bold numbers are marine limits in metres above present sea level (after J. Y. Landvik & A. Hansen 1994).*

On the north dome and outlet glacier work will begin in early June and comprises GPS-remeasuring of all mass balance stakes and strain nets from 1994 for the ice-dynamics programme. Mass balance and ablation/climate measurements will be started with snow pits, shallow (10 m) firn cores and erection of three simple climate stations measuring temperatures, humidity and wind speed. No radiation measurements are planned.

Radio-echo soundings will be carried out on the north dome and outlet glacier with emphasis on the areas around the strain-nets as these areas were not covered by the radar flights in 1993. The equipment used will be identical to the 1994 equipment.

By the end of June the crew will be flown out but equipment and camp will remain.

In mid July field work will be commenced with hot-water drilling for emplacing thermistor strings down to bedrock at the strain-net sites. This will also give a reference depth for the radio-echo soundings. At the same sites inclinometers will be installed and left in place until 1996 when we hopefully will be able to return and remeasure them.

Sampling for $\delta^{18}O$ at the ice margin will be continued and intensified in areas which the 1994 sampling has shown to be of special interest. All stakes should be resurveyed and mass balance and ablation/climate measurements wound up by the first weeks of August when crew and part of the equipment will return to Station Nord.

So far funding for a continuation in 1996 has not been secured but we hope that it will be at least possible to return to remeasure stake positions, deep temperatures, inclinometers and the winter mass balance 1995/1996.

References

Landvik, J. Y and A. Hansen (1994): The glacial history along the northern margin of the Hans Tavsen ice cap, North Greenland. Express Report, Eastern North Greenland 1994, Grønlands Geologiske Undersøgelse.

Reeh, N (1992): Application to Nordic Environmental Research Programme, NMR Climate Change Research.

Reeh, N. (1994): Progress Report 1994 for Hans Tavsen ice cap project. - Glacier climate change research, North Greenland.

Reeh, N., R. J. Braithwaite and O. B. Olesen (1994): Glaciological Investigations on Hans Tavsen Ice Cap, North Greenland. Express report eastern North Greenland 1994, Grønlands Geologiske Undersøgelse.

GLACIOLOGICAL FIELDWORK IN KRONPRINS CHRISTIAN LAND: RESULTS FROM 1994

Hans **Oerter**[1], Carl E. **Bøggild**[2], Friedrich **Jung-Rothenhäusler**[1], Niels **Reeh**[3]

1 Alfred-Wegener-Institut für Polar- und Meeresforschung, Bremerhaven, Germany
2 Geological Survey of Greenland (GGU), Copenhagen, Denmark
3 Danish Polar Centre (DPC), Copenhagen, Denmark

Area under investigation

The area under investigation at the ice margin in Southwestern Kronprins Christian Land (KPCL) covers a latitudinal range from 79°33.6´ to 79°56.5´ N and a longitudinaly from 24°0.7´ to 26°17.6´ W. The investigations have been carried out since 1993 along a 60 km long stake line, starting 186 m a.s.l. and ending at 1065 m a.s.l. (see fig. 1). Figure 2 shows a view on the ice margin.

For climatic observations three stations (table 1) have been in operation.
The main stake net for the mass-balance and ice-dynamic investigations is displayed in figure 3 and compiled in annex table 5.

Table 1: Climatic stations run in Southwestern Kronprins Christian Land in the period 1993-1994

station	lat.	long.	altitude	period of operation	Parameters
name	[N]	[W]	[m a.s.l.]		
AWS 3315	79°54,883´	24°7,533´	415	since 7.7.93 8.7.-5.8.94	air temperature (appr. 2 m) wind speed wind direction barometric pressure global radiation
AWS 3316	79°54,741´	24°13,233´	495	since 18.7.94	air temperature in 2 levels (appr. 1 and 2 m) wind speed wind direction barometric pressure ice ablation/snow accumulation
NG9318	79°41,586´	25°36,465´	986	7.7.-3.8.94	air temperature (appr. 2 m) humidity wind speed

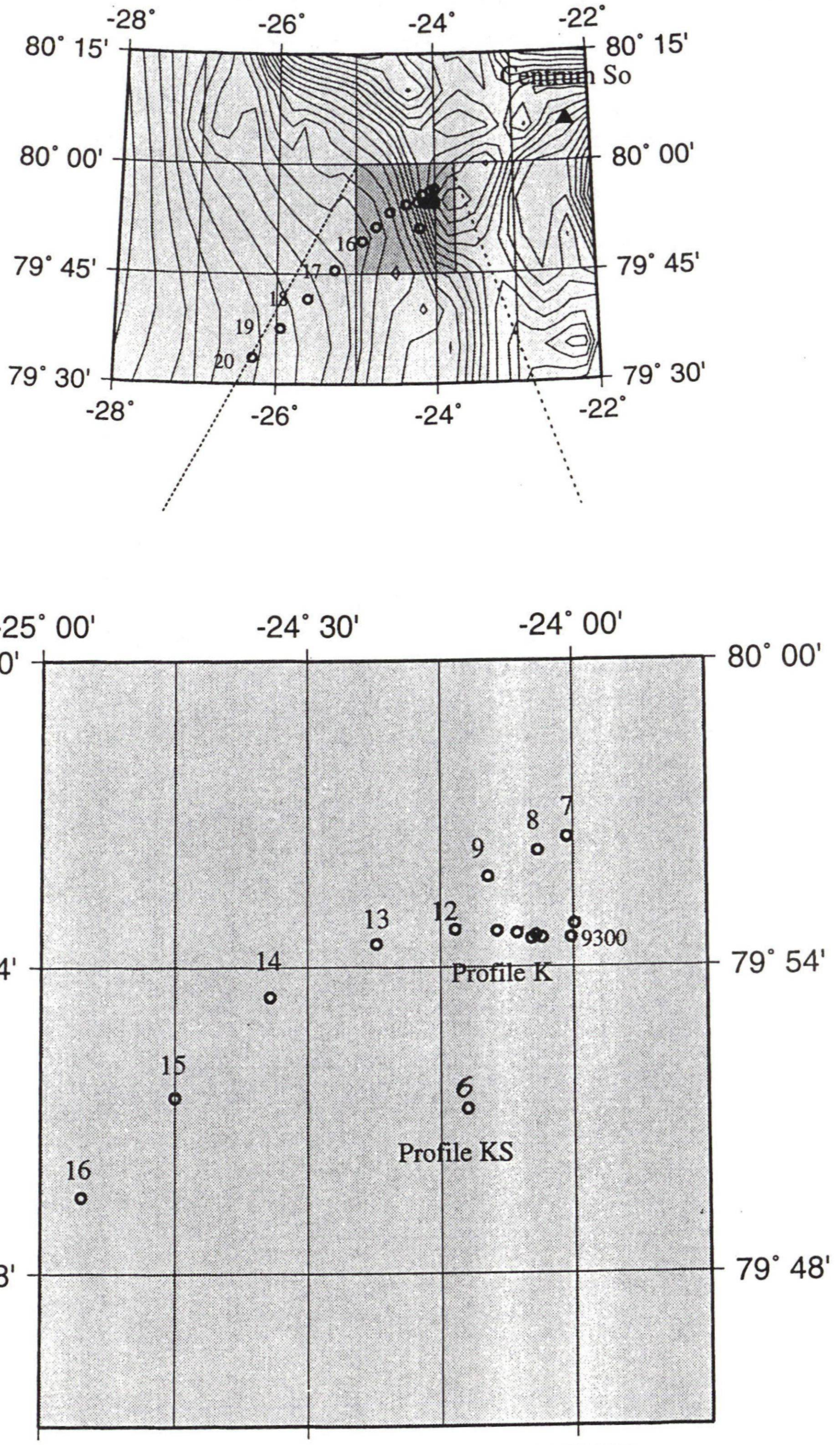

Fig. 1: Map of the ice margin area at Kronprins Christian Land showing the location of the stake net for ablation and ice-dynamic measurements as well as the two profiles K and KS along which surface ice samples were taken for $\delta^{18}O$ analyses.

Fig. 2: View of the ice margin at Southwestern Kronprins Christian Land. Profile K started appr. in the middle of the left margin. (Foto: H. Oerter, 30.7.1993)

Field work 1994

The field work was carried out in co-operation with GGUs Geological Eastern North Greenland Ecpedition. The field season iwas devided into two visits at Storstrømmen (11.07.94-17.07.94 and 08.08.94-16.08.94) and two visits at the ice margin in KPCL (06.07.94-10.07.94 and 17.07.94-07.08.94). For the Kronprins Christian Land work a camp was established at the very ice margin with support from GGUs base camp at Centrum Sø. The helicopter was working out of this base camp, too (Oerter et al., 1994b). The objectives were:

- mass balance studies comprising measurements of accumulation as well as ablation, albedo, climatic parameters, and near-surface ice temperatures,
- to down load the recording weather station built up in 1993 on the ice, and to install a second one with ARGOS transmission (AWS no 3316) at a higher elevation,
- surveying work to get positions and ice velocity of all stakes,
- ice sampling for paleoclimate isotope studies, and
- first attempt to do geoelectric work on the ice with a light weight 4-point measuring device for comparison of electric properties of the ice at the margin with deeper ice cores.

Results on mass-balance studies

Albedo

Albedo measurements were carried out with a Kipp & Zonen Albedometer CM 7 in the Storstrømmen and the KPCL area.

In the Kronprins Christian Land area the albedo measurements were performed as single spot measurements along the main stake line (fig. 3 and 4). Both figures demonstrate the high spatial variability due to the varying dust content on the ice surface. The changes in albedo with time can be recognized by comparing the 1993 and 1994 measurements. The elevation range from 430 to 500 m is characterized by extreme low albedo values of about 0,2 (see also discussion on isotope content). This wide range of albedo values within the ablation area makes it very difficult to define comparable regional degree-day factors.

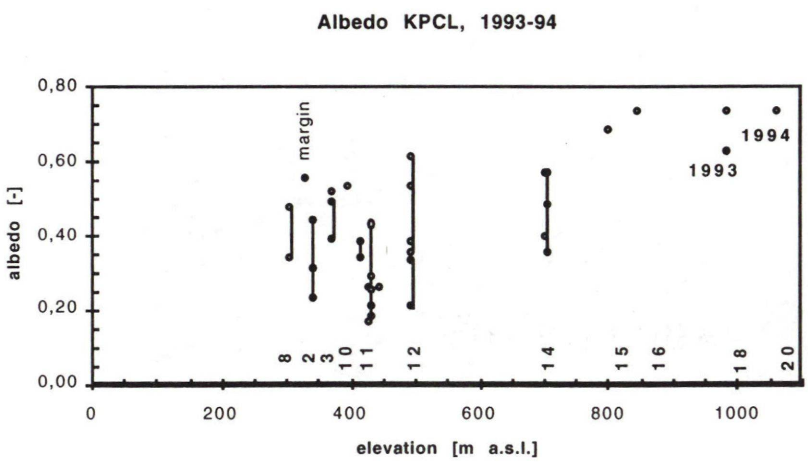

Fig. 3:
Ice margin Kronprins Christian Land: Results of albedo measurements in the summer seasons 1993 (•) and 1994 (o) along the main stake line. For more details in the elevation range 330-500 m see fig. 7.

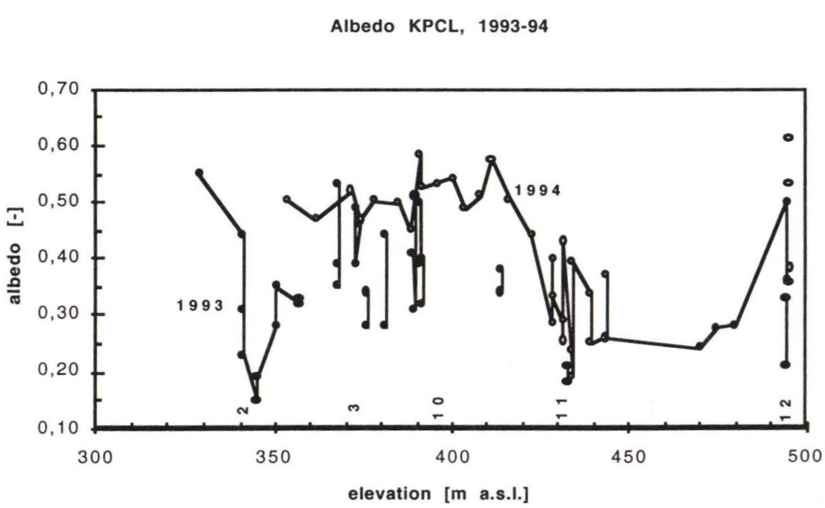

Fig. 4:
Ice margin Kronprins Christian Land: Results of albedo measurements in the summer seasons 1993 (•) and 1994 (o) along the main stake line in the elevation range 330-500 m.

Ablation

The mass balance studies in Kronprins Christian Land started in 1993 and will be continued until 1995. Fig. 5 shows three curves, first for the 1993 summer season (9.7.-25.7.93), second for the late summer 93, winter 93/94 as well as spring season 1994 (25.7.93-7.7.94) and third for the 1994 summer season (7.7.-3.8.94). The ablation in 1993 was considerably higher than in 1994.

Fig. 6 shows the net mass-balance for the period 7.7.93 to 7.7.94. For this period the elevation of the equilibrium line was at 800 m a.s.l. This may indicate an upper limit of the equilibrium line altitude, as at least above about 850 m a.s.l. it is very likely that all meltwater will completely refreeze again in the firn pack. The maximum of the ice velocity (fig. 7) indicates a lower mean equilibrium line altitude between 500 and 600 m a.s.l.

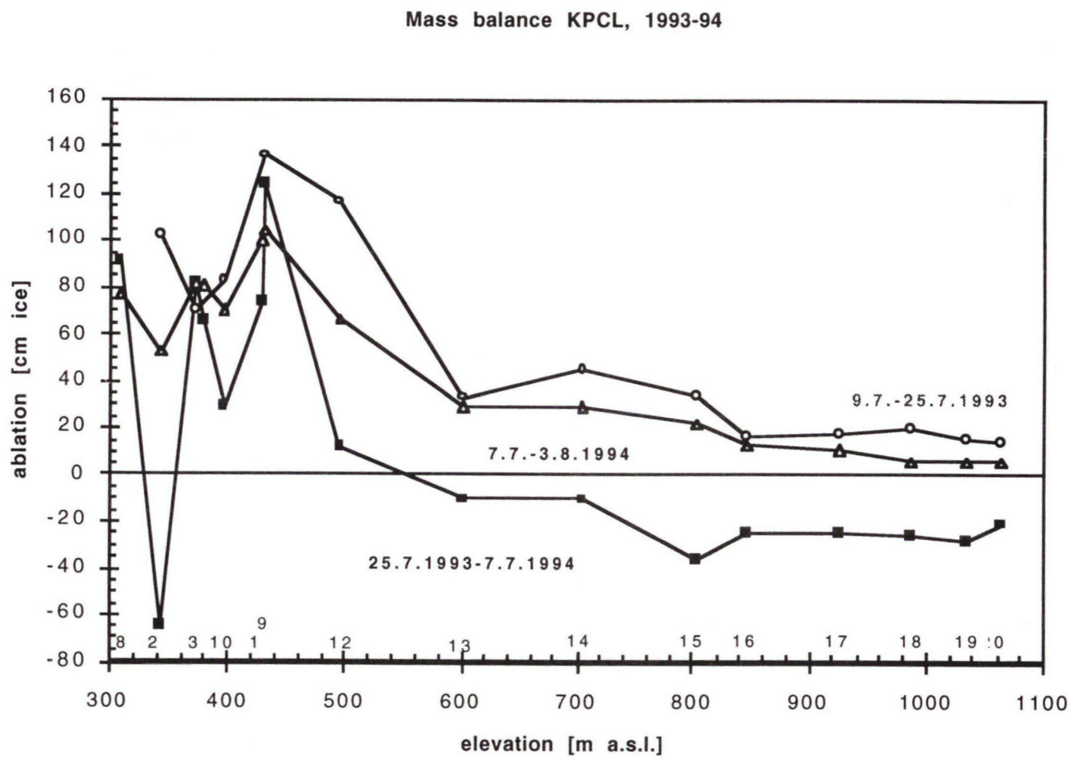

Fig.5: Kronprins Christian Land: Results of ablation measurements along the main stake line (fig. 2) from 1993 to 1994.

Degree-day factors

The work for calculating regional degree-day factors by using the ablation stake readings and the temperature record from the various climate stations is still in progress. As a first step degree-day values were calculated for the locations of the weather stations AWS 3314 and 3316 by using the record of the ultra-sonic snow-depth sensor and the temperature sensor at the 2-m level (table 2). In addition in table 2 some older values are included for the same location as AWS 3314 (NE8903). For KPCL some averaged values along the lower stake line are given as well, using the temperature record of AWS 3315 and applying an temperature gradient of -0.7K/100 m. The temperature records provided hourly and 3-hourly values.

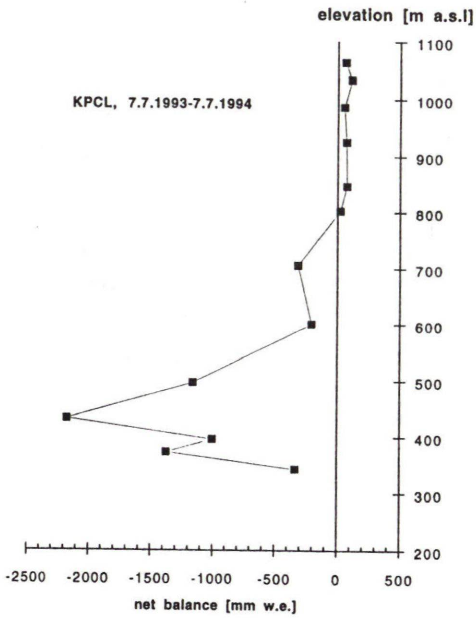

Fig. 6: Net mass balance along the main stake line in KPCL for the period 7.7.93-7.7.94.

Table 2: Degree day factors for selected locations and periods on Storstrømmen and in KPCL. *average over several stakes

Location	period	ablation [mm w.e.]	degree days [K d]	degree-day factor [mm K^{-1} d^{-1}]
Storstrømmen				
NE8903	07.07.-31.07.89	490	59.0	8.3
NE8903	01.08.-22.08.89	205	14.8	13.8
NE8903	09.07.-31.07.90	390	46.3	8.4
NE8903	01.08.-19.08.90	280	22.8	12.3
NE8908C	07.07.-28.07.90	459	49.2	9.3
AWS3314	01.07.-31.07.93	517	41.5	12.5
AWS3314	12.07.-31.07.94	384	43.7	8.8
AWS3314	01.08.-14.08.94	198	25.4	7.8
			mean:	**10.15** ±2.33
KPCL				
NG9303 - NG9310*	11.07.-27.07.93	758	67.2	11.2
NG9311	13.07.-29.07.93	958	57.8	16.6
NG9312	12.07.-26.07.93	792	42.7	18.5
AWS3316	19.07.-31.07.94	405	40.5	12.3
AWS3316	01.08.-15.08.94	307	22.3	13.8
NG9303 - NG9310*	19.07.-02.08.94	394	44.1	8.9
NG9310 - NG9311*	19.07.-02.08.94	453	38.9	11.6
NG9311 - 2000*	19.07.-02.08.94	586	38.9	15.1
			mean:	**13.5** ±3.14

On an average the degree-factors of 10.1 and 13.5 mm K^{-1} d^{-1} calculated for these two Northeast Greenland areas are higher than the values of 7.0 and 8.2 mm K^{-1} d^{-1} reported by Braithwaite and Olesen (1989) for Nordbogletscher and Qamanârssup sermia , West Greenland. These values were calculated as long term averages based on monthly ablation rates.

The variability of the degree-day factors is strongly influenced by albedo variations in the marginal area and by the wind speed conditions at various locations. This shows the limits of degree-day methods compared with energy-balance models.

The degree-day factors will be discussed together with ablation gradients in more detail elsewhere later.

Results on ice dynamics

In the Kronprins Christian Land area the main stakes of the stake line were positioned by GPS in the period 7.7.-9.7.1994. During this period four ASHTECH receivers, two from AWI and two borrowed from the National Survey and Cadastre (KMS) Copenhagen, Denmark, were in operation simultanously. The plastic poles drilled in within the first 2 km from the margin in 1994 were surveyed from a rock point (NG9300) by means of theodolite and distance meter on 27.7.94 as well as the main stakes NG9305, NG9310, NG9311, NG9304, NG9303, and NG9302.

The calculated ice velocities at the stake positions are given in figure 7. The flow direction indicate that the stakes up to stake NG9317 represent almost an ice flow line, originating in the northern part of the Greenland ice sheet. The higher stakes obviously belong to the catchment area of Nioghalvfjerdsbræ further South.

The maximum ice velocity occurs between at stake NG9313 and NG9312, which should be at the equilibrium line altidute under steady state conditions.

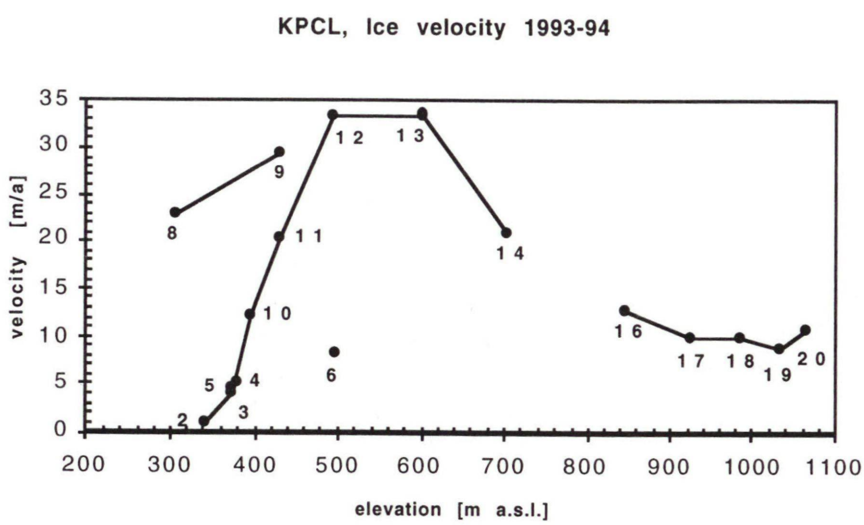

Fig. 7:
Ice flow velocity 1993-94 along the main stake in KPCL determined by GPS or ground survey.

Results on isotope studies

At the ice margin in Kronprins Christian Land ice sampling was carried out in 1993 and 1994 along the main stake line and along the two marginal profiles K and KS (fig. 3). The 1993 samples were analysed completely, whereas from the 1994 samples a major amount of profile KS (Oerter et al. 1994a), which was completely resampled with a higher spatial resolution of o.5 m, are still in progress.

Figure 8 shows the $\delta^{18}O$ content of surface ice samples along the main stake line. From our mass-balance studies 1993/94 one can conclude that the equilibrium line is at an elevation of appr. 800 m a.s.l. (fig. 6). With respect to ice velocity (fig. 7) the mean equilibrium line altitude should be between 500 and 600 m a.s.l. This would be in better accordance with the isotope results than the 1993/94 mass balance, as one normally would expect to find the maximum $\delta^{18}O$ value at the elevation of the mean equilibrium line (e.g. Reeh et al. 1987). At stake 12 exposed ice was sampled, which looks very dirty, also the crystal size there is much larger than further downhill. This kind of ice surface, which was already discussed with respect to the albedo measurements, was exposed appr. from stake 11 to stake 13 in 1993 and to stake 12 in 1994.

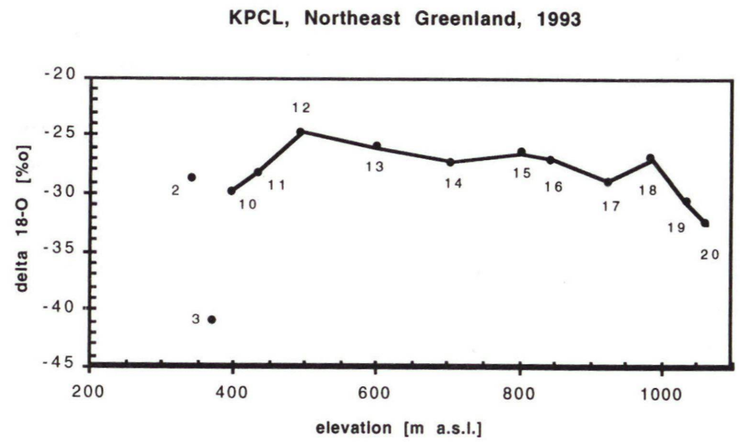

Fig. 8:
Distribution of $\delta^{18}O$ content of surface ice samples along the stake line in Kronprins Christian Land (see fig. 3) based on surface ice samples (stake 2-13) or snow pits (stake 14-20).

Geoelectric measurements

An important parameter to characterise glacial and interglacial ice is the electrical conductivity of the ice. Therefore in 1994 a pilot study with geoelectric measurements was performed, using a new designed, light weight 4-point measuring device. The electrodes were arranged symmetrically with a distance of 5 cm (Wenner arrangement). The measurements showed that the method can be used, but the electrodes still need some more development. Values determined for the apparent specific resistance range from 8 10^4 to 2.7 10^6 Ohmmeter, with a clear change at the transition from holocen (low resistance) to pleistocene ice (high resistance) (fig. 9a). These values will be compared with the isotope values (fig. 9b) to prove how the electrical properties of ice change under varying climatic conditions.

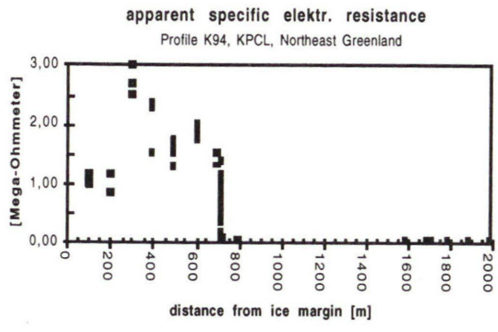

Fig. 9a:
Apparant specific electric resistance of ice measured at the ice surface along profile K.

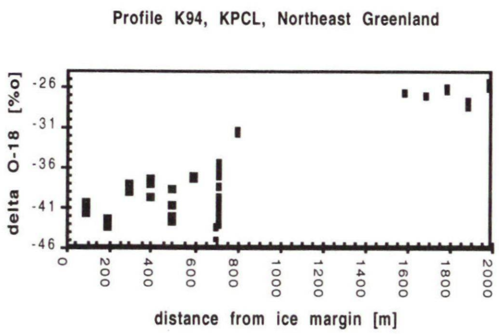

Fig. 9b:
$\delta^{18}O$ content of surface ice sampled along profile K at the same locations where the electrical resistance was measured.

References

Braithwaite, R. J. and Olesen, O. B.: Calculation of glacier ablation from air temperature, West Greenland. in: Oerlemanns (ed.) Glacier Fluctuations and Climate Change. Dordrecht: Kluwer Academic Publishers, 219-233 (1989)

Oerter, H., Reeh, N., Bøggild, C.E.: Glaciological fieldwork in 1993 at the ice margin in Kronprins Christian Land, NE Greenland. in: J.J.M.van der Meer & R.J. Braithwaite (eds.) Rep. 4thWorkshop on Mass Balance and Related Topics of the Greenland Ice Sheet. Open File Series Grønlands Geologiske Undersøgelse **94/13**, Copenhagen, 87-90 (1994a)

Oerter, H., Jung-Rothenhäusler, F., Bøggild, C.E., Reeh, N.: Glaciological Investigations in Kronprins Christian Land, Eastern Northgreenland. in: N. Henriksen (ed.), Express Report Eastern North Greenland and North-East Greenland 1994, GGU, Copenhagen, 97-105 (1994b)

Reeh, N., Thomsen, H. H., Clausen, H.B.: The Greenland ice-sheet margin - a mine of ice for paleo-environmental studies. Palaeogeogr., Palaeoclimatol., Palaeoecol., **58**, 229-234 (1987)

ISSN 0903-7322